1971

A step-wise gray approximation of the radiative absorption coefficient for an isothermal hydrogen plasma

Keith Harlan Browne

Department:

A STEP-WISE GRAY APPROXIMATION OF THE RADIATIVE ABSORPTION COEFFICIENT FOR AN ISOTHERMAL HYDROGEN PLASMA

By

KEITH HARLAN BROWNE, 1948-

A THESIS

Presented to the Faculty of the Graduate School of the

UNIVERSITY OF MISSOURI-ROLLA

In Partial Fulfillment of the Requirements for the Degree

MASTER OF SCIENCE IN MECHANICAL ENGINEERING

1971

Approved by

W. F. Nelson (Adviser) A. L. Crosbie

F B Pauls

ABSTRACT

The radiative absorption coefficient of an isothermal hydrogen plasma is calculated using a step-wise gray approximation. The approximation retains a high degree of accuracy while significantly reducing the numerical computer time. The accuracy of the approximation depends on the spacing of the steps taken in the frequency spectrum as well as the number of steps used; 135 steps are used in this study.

Plasma conditions of interest in this study are for temperatures between 5000 and 60,000°K, densities between 10^{-5} and 10^{-7} gm/cm^3, and thicknesses between 0.1 and 100 cm. Flux and intensity calculations are made for each case using the average absorption coefficient developed from the step-wise gray approximation.

The importance of the trade-off between the shift to higher frequencies in the maximum of the Planck function and the population increase of the high electronic states as temperature increases is discussed. The results are shown in graphical and tabular form for conditions pertinent to the Jovian atmospheric entry problem.

ACKNOWLEDGMENT

I would like to express my gratitude to my graduate advisor, Dr. H. F. Nelson, for his guidance, patience, and knowledgeable leadership throughout the course of this research.

Also, deserving thanks go to NASA and NSF for the financial backing in the way of research grants received from them. Lastly, the Department of Mechanical Engineering of the University of Missouri-Rolla deserves my thanks for the teaching assistantship provided during the spring semester of 1971. Without these funds, my completion of this research would have been impossible.

TABLE OF CONTENTS

Table of Contents (Con't) Page

LIST OF ILLUSTRATIONS

LIST OF TABLES

NOMENCLATURE

$B_\nu(T)$	Planck function (ergs cm^{-2} sr^{-1})
c	speed of light (2.99793 X 10^{10} cm sec^{-1})
E	electronic internal energy of atom (ergs)
F	flux (ergs cm^{-2} sec^{-1})
F_ν	spectral flux (ergs cm^{-2})
h	Planck's constant (6.62517 X 10^{-27} erg sec)
I	total intensity (ergs cm^{-2} sec^{-1} sr^{-1})
I_ν	spectral intensity (ergs cm^{-2} sr^{-1})
k	Boltzman's constant (1.38044 X 10^{-16} erg/^oK)
L	thickness of shock layer plasma (cm)
N	number density (cm^{-3})
n	electronic energy level
P_e	electron pressure (dyne cm^{-2})
S^*	atomic line strength (cm^{-1} sec^{-1})
T	temperature (^oK)
Z	electronic partition function (cm^{-3})
α	fraction of atomic hydrogen that exists as protons
γ	half width of atomic line (sec^{-1})
δ	fraction of atomic hydrogen that exists as the negative hydrogen ion
η	fraction of molecular hydrogen that exists as H_2^+
$\bar{\kappa}$	total average absorption coefficient (cm^{-1})
$\bar{\kappa}_c$	continuum average absorption coefficient (cm^{-1})
$\bar{\kappa}_l$	line average absorption coefficient (cm^{-1})
$\bar{\kappa}_\nu$	spectral absorption coefficient (cm^{-1})

Nomenclature (con't)

λ	wavelength ($\mathring{A}$)
ν	frequency (sec^{-1})
ρ	density ($gm\ cm^{-3}$)
σ	absorption cross section (cm^2)
τ	optical depth
Ψ	fraction of molecular hydrogen dissociated

Subscripts

c	continuum
e	electron
i	specie
l	line
o	line center
ν	frequency

I. INTRODUCTION

Radiation is an important mode of energy transfer in much of the current heat transfer analysis. Currently there is considerable interest in exploring the planets of the solar system. This requires high speed entry into their atmospheres. Radiation is the most important form of heat transfer in the maximum decelleration portion of most planetary entry trajectories. The exact calculation of the radiative heating, which must be known to design the entry vehicles, is a costly numerical process. Because of the excessive computer time required to calculate the nongray radiation from the shock layer plasma, it is desirable to develop accurate approximate methods. This analysis investigates the possibility of using a step-wise gray approximation for the radiation absorption coefficient.

In the shock layer region around a body entering a planetary atmosphere, the temperature changes from very hot near the shock to a much lower value near the body. In the high temperature regions simple molecules such as hydrogen, oxygen, and nitrogen are not only dissociated but also are ionized. Atomic line radiation becomes significant. For energy transitions involving the outer electronic states Griem [1] has shown that atomic lines have a Lorentzian shape with the half width mainly dependent upon electron collision broadening. An investigation by Wilson and Hoshizaki[2] revealed that about 50 per cent of the radiative

transport within shock layers during re-entry comes from the atomic lines.

Reabsorption and overlapping of line wings become important as the lines become optically thick. The radiative heat transfer is significantly reduced by the effects of radiative cooling and nongray self-absorption.[3] Since nongray self-absorption is important, it is necessary to make detailed quantum mechanical calculations for the spectral absorption coefficient.

In the lower temperature regions molecular hydrogen, oxygen, etc. exist, and molecular band radiation is important. The low temperature regions occur near the boundary layer.

The continuum absorption coefficient is well defined for atomic gases. It results from bound-free and free-free transitions. The contribution resulting from bound-bound transitions requires a knowledge of the total line strength and the shape of the spectral absorption coefficient for each line; the former is well known for simple gases, but the latter is not.

II. REVIEW OF LITERATURE

Several approximate methods have been developed in radiative transfer theory. The classical approximations are the Planck and Rosseland means.[4] The Planck mean requires the radiating plasma to be optically thin, while the Rosseland mean requires the plasma to be optically thick. These restrictions limit their application to general radiation calculations.

Radiative intensity from isothermal hydrogen plasmas has been studied by Aroeste and Benton;[5] however their investigation did not include the contribution from the higher electronic transitions. They determined contributions to the intensity due to discrete transitions using approximate expressions for the absorption coefficient. They assumed the partition function to be equal to the contribution from the ground state.

Olfe[6] approximated the radiation from hydrogen plasmas at temperatures from 300 to 10,000°K. He considered contributions from the continuum, atomic lines, and molecular bands. At higher temperatures the molecular band radiation was found to be of secondary importance, since hydrogen molecules dissociate into atomic hydrogen under these conditions. He calculated the spectral absorption coefficient for the pressure-induced rotation spectrum. For a rotational line, the absorption coefficient was represented by a dispersion contour modified on the low frequency side by a Boltzman factor and with a half width proportional to the square root of the temperature.

Nelson and Goulard[7] considered line and continuum radiation from isothermal hydrogen shock layers at temperatures from 15,000 to 33,000°K. They used a trapezoidal numerical integration with variable step size to calculate the radiative intensity. The step size was adjusted by allowing the absorption coefficient to vary by no more than 50% of its previous value throughout the interval. They showed that line radiation is more important than continuum radiation at low ambient densities; however, as the ambient density increased, continuum radiation becomes more significant than line radiation. Nelson and Goulard[7] also showed that the shock layer is optically thin at low ambient densities, and it becomes optically thick as the ambient density increases.

Nelson and Crosbie[8] calculated the continuum radiative flux from nonisothermal, nongray atomic gases. They assumed linear temperature profiles in the shock layer in order to uncouple the radiative transfer from the fluid mechanics. They showed the importance of the ionization edge location and the spectral shape of the absorption coefficient. The method of superposition was used to extend the results to atomic gases with multiple electronic levels. However, they did not consider the contribution from the atomic lines. This made the integration of the spectral absorption coefficient much easier since the continuum is a relatively smooth function. They used Simpson's rule for the spectral integration.

Lasher et al.[9] calculated the radiation from hydrogen plasmas using the equivalent line width approximation for most of the atomic lines. Detailed line profiles were used for the transitions between the low electronic states, while a dispersion profile was assumed for the line shape of the transitions involving the high electronic states. The equivalent line width approximation restricts the results in that it does not take into account the effect of line overlap. Therefore, the method becomes questionable when the pressures and densities of the plasma are large.

Equivalent line grouping has also been used to facilitate the calculation of line radiation in radiative flux calculations.[10] Its unique feature is the replacement of several lines in a narrow frequency interval by a single line, thus reducing the number of necessary calculations. However, this approximation assumes that each line within the frequency interval is either optically thin or optically thick.

Nicolet[11] discusses the molecular band model as used in calculating the radiative flux. In the molecular band model the molecular spectrum is converted into an equivalent continuum, omitting the fine details of the inner band system. This method yields the correct fluxes when the layer is optically thin, optically thick, or when strong overlapping of lines occurs. For most cases within the molecular spectra, the approximation is very good.

The approximate methods discussed above for calculating the radiation from a plasma have several trade-offs. These must

be evaluated in order to determine an appropriate method for calculating the radiation emitted by a plasma. The step-wise gray approximation developed in this research evolves from these previous models. In addition to considering the radiating species of the previous models, the current model considers the effects of molecular bands. The previous work of Nelson and Goulard[7] and Lasher et al.[9] neglected molecular hydrogen and hence, did not consider molecular band radiation.

III. DEVELOPMENT OF STEP-WISE GRAY APPROXIMATION

A. Governing Equations

The equation of radiant transfer for an absorbing-emitting medium is a continuity equation for the number of photons propagating within the solid angle $d\Omega$ and within the frequency interval ν to $\nu + d\nu$. The conservation of radiant energy is given by

$$\frac{d I_\nu}{d S} = \kappa_\nu B_\nu (T) - \kappa_\nu I_\nu (S) \tag{2}$$

where I_ν is the radiant intensity, S is the direction of propagation, κ_ν is the absorption coefficient, and $B_\nu (T)$ is the Planck function. The geometry of the shock layer configuration is shown in Fig. 1, where $x = S \cos \theta$ and $\cos \theta = \mu$. Assuming local theromodynamic equilibrium exists, the Planck function is given by

$$B_\nu = \frac{2h\nu^3}{c^2} \frac{1}{\exp(h\nu / kT) - 1} \tag{3}$$

The radiative transport equation can be integrated over a path length L, assuming zero intensity at the orgin and an isothermal plasma, to give

$$I_\nu (L, \mu) = B_\nu (T) \left[1 - \exp \left(- \frac{\kappa_\nu L}{\mu} \right) \right]$$

The total intensity is obtained by integrating over the entire

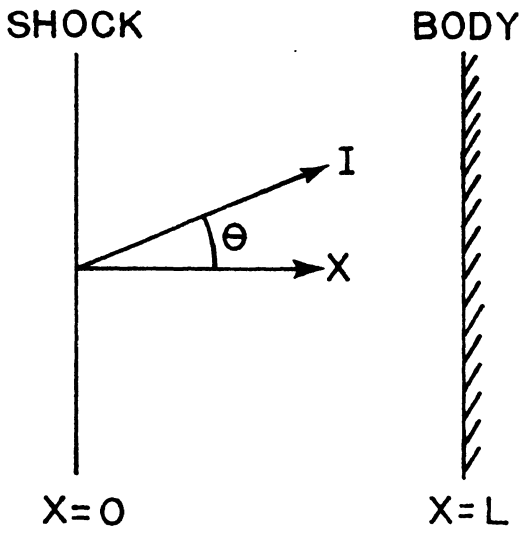

Fig. 1 Geometry of shock layer

spectrum

$$I\ (L,\mu\ ) = \int_0^\infty B_\nu\ (T)\ [\ 1 - \exp\ (-\ \frac{\kappa_\nu\ L}{\mu})]\ d\nu \qquad (5)$$

Radiative flux is found by integrating the total intensity over the solid angle, where E_3 is the exponential integral

$$F\ (L) = 2\ \pi \int_0^\infty B_\nu\ (T)[\ \tfrac{1}{2} - E_3\ (\kappa_\nu\ L)]\ d\nu \qquad (6)$$

When the plasma is optically thin, $\kappa_\nu\ L \rightarrow\ 0$ and the flux is

$$F(L) = \pi \int_0^\infty B_\nu\ (T)\ [\kappa_\nu\ L]\ d\nu \qquad (7)$$

When the plasma is optically thick, $\kappa_\nu\ L \rightarrow \infty$ and it radiates as a blackbody,

$$F(L) = \pi \int_0^\infty B_\nu\ (T)\ d\nu \qquad (8)$$

Equations (5) and (6) are well known expressions for intensity and flux. The main difficulty in their evaluation arises because the absorption coefficient varies by several orders of magnitude over the atomic lines.

B. Molecular Bands

The absorption coefficient depends on frequency, temperature, and density. When the temperature is low, molecular hydrogen becomes important in certain spectral regions. The data for the Lyman, Werner, and Photoionization molecular bands was taken from curves for absorption cross-sections of those bands,[12] see Figs. 2, 3, and 4. The curves represent averages over

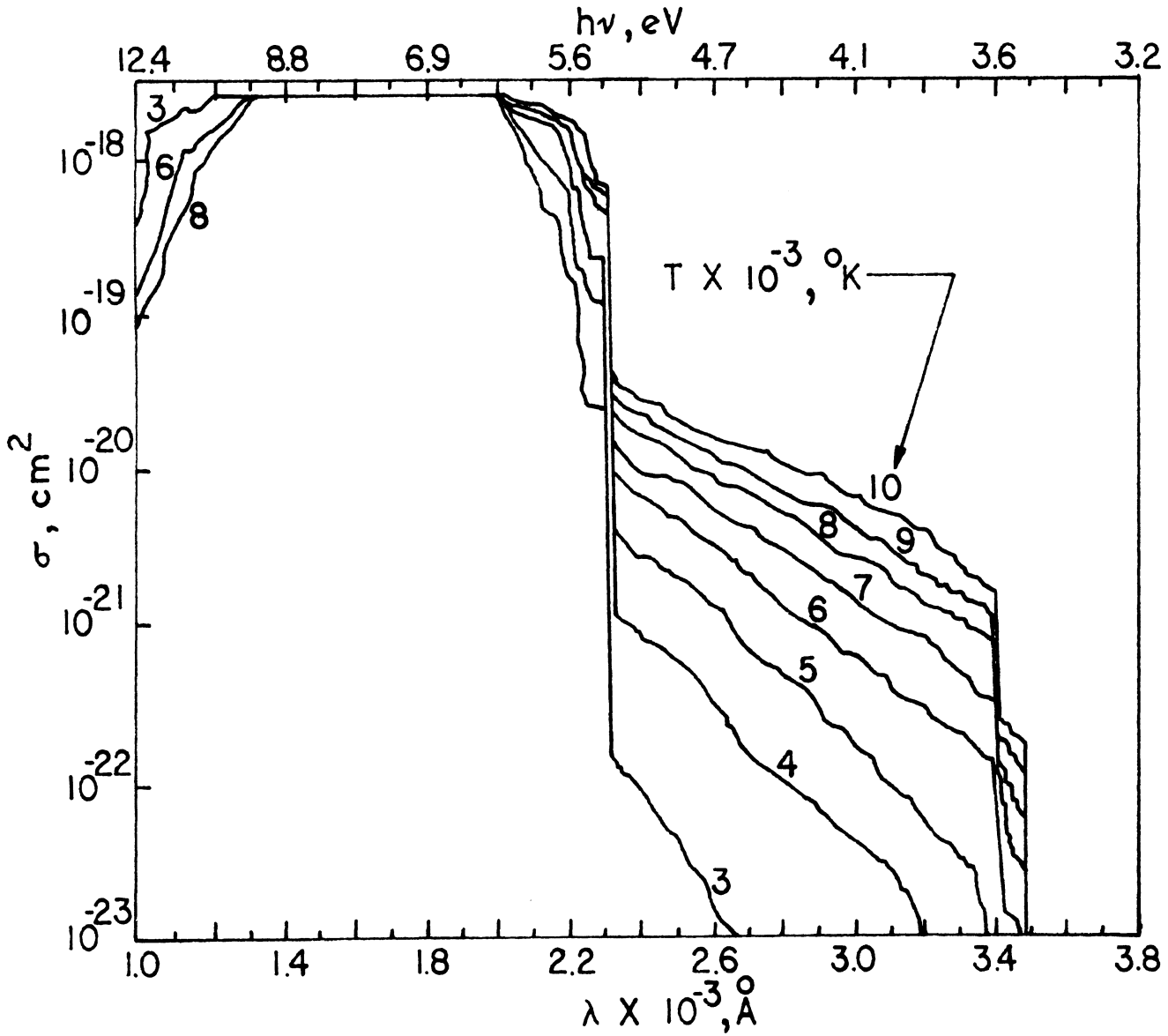

Fig. 2 H_2 Lyman band

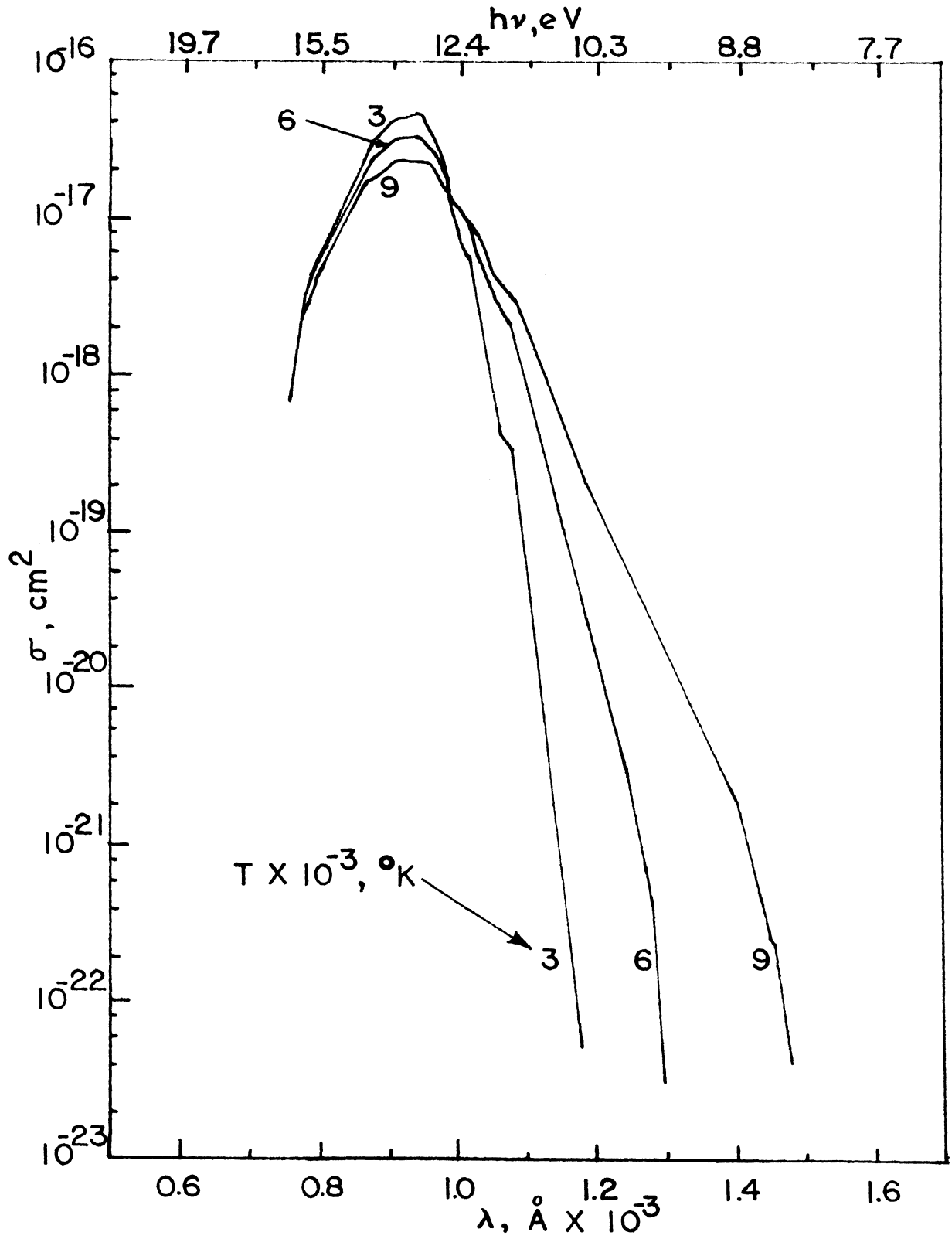

Fig. 3 H_2 Werner band

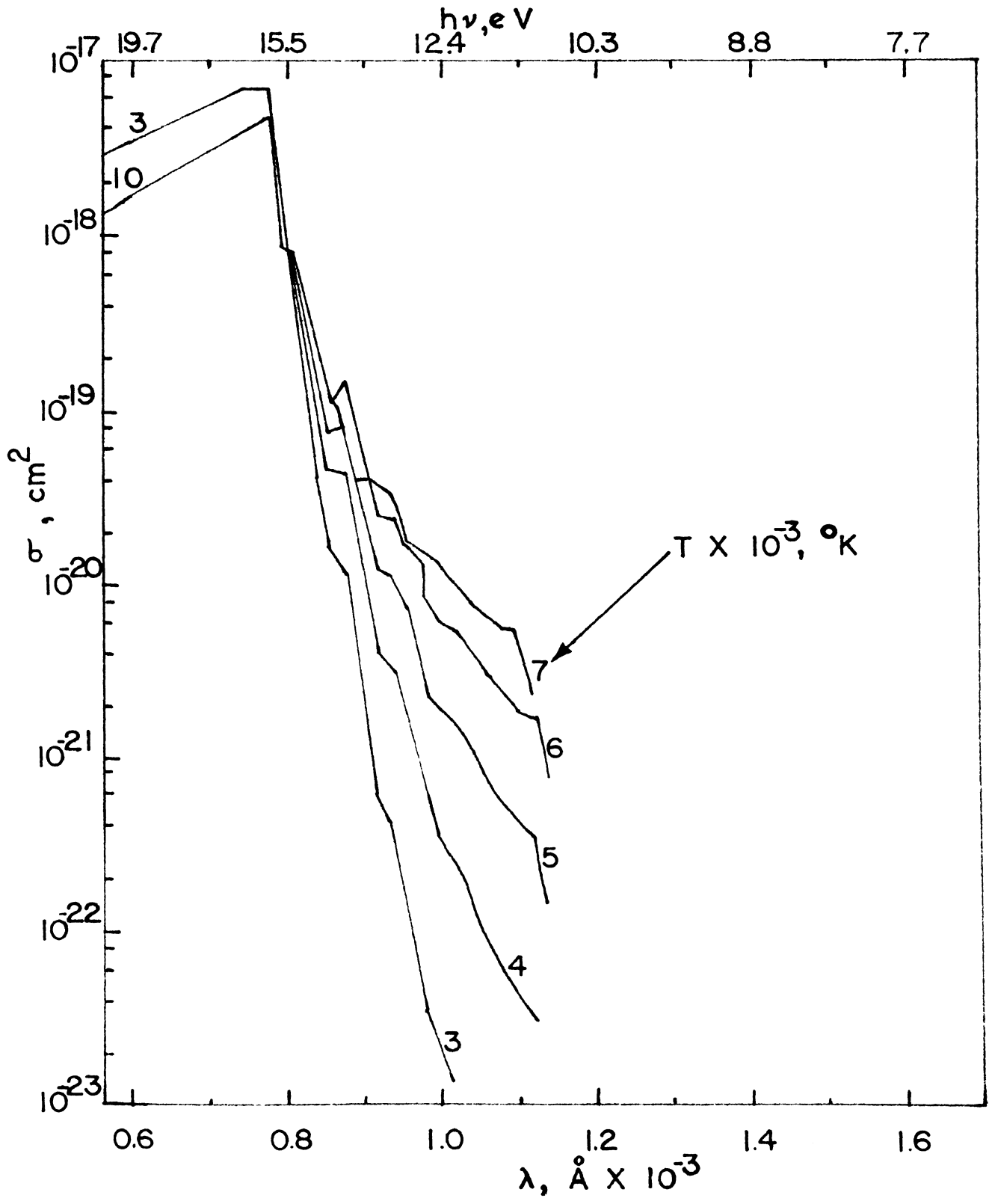

Fig. 4 H_2 Photoionization band

the vibration-rotation lines. As the temperature increases and the molecules dissociate, the effect of molecular hydrogen becomes negligible. Atomic hydrogen is the primary source of emission. When extremely high temperatures are reached, the hydrogen atoms become ionized, and free-free radiation between protons and electrons is the primary source of emission. The temperature and density of the plasma control the population of molecular, atomic, and ionized hydrogen.

C. Step-Wise Gray Approximation

In order to develop the step-wise gray approximation, the spectral frequency range is divided into several intervals of varying width $\Delta\nu$. They are large (about one eV) when only continuum radiation is present; however, $\Delta\nu$ must be very small when line centers are located in the interval. A quadratic fit is used in the numerical process of approximating the continuum absorption coefficient when a line center is not in the frequency interval. If a line center is in the interval, a simple averaging process is used to determine the average continuum absorption coefficient. A Lorentz line shape is assumed in order to calculate the bound-bound absorption coefficient of lines with centers in the spectral interval. The continuum contains the line wings of lines with centers outside the spectral interval of interest, as well as free-free and bound-free radiation.

The model developed in this research averages the absorption coefficient in each frequency interval. An average absorption coefficient is calculated for each line with its

line center located in the spectral interval. The individual line contribution is then summed to determine the total bound-bound absorption coefficient for the interval. This value is added to the average continuum absorption coefficient in the interval to obtain the total average absorption coefficient.

The continuum absorption coefficient is calculated in two ways, depending on whether or not a line is encountered within the frequency interval. If a line center is not contained in the frequency interval, a quadratic fit is used in the approximation of the continuum absorption coefficient. The line wings are considered as being part of the continuum. Three points are chosen, point one at the beginning, point two at the middle, and point three at the end of the frequency interval. The exact values for the total absorption coefficients at the three points are taken from a program developed by Nelson and Goulard.[7] The average absorption coefficient becomes

$$\bar{\kappa}_c = \frac{\kappa_{\nu_1} + 4\,\kappa_{\nu_2} + \kappa_{\nu_3}}{6} \tag{9}$$

where κ_{ν_1}, κ_{ν_2}, and κ_{ν_3} are the absorption coefficients at the three points. This yields the average continuum absorption coefficient for the spectral interval. It is especially useful when line wings are present.

When a line center is in the frequency interval, the continuum absorption coefficient is assumed to vary linearly in the frequency interval ν_1 to ν_3. The average absorption

coefficient becomes

$$\bar{\kappa}_c = \frac{\kappa_{\nu_1} + \kappa_{\nu_3}}{2} \tag{10}$$

The average bound-bound absorption coefficient is found by averaging the atomic line absorption coefficients over the spectral interval, assuming a Lorentz line shape.

$$\bar{\kappa}_l = \frac{h}{\nu_3 - \nu_1} \int_{\nu_1}^{\nu_3} \frac{S_i^* \gamma_i}{\pi [(\nu - \nu_{o_i})^2 + \gamma_i^2]} d\nu \tag{11}$$

If a line center is not in the spectral interval, the average line absorption coefficient is zero. After performing the integration, the bound-bound absorption coefficient is

$$\bar{\kappa}_l = \frac{h}{(\nu_3 - \nu_1)\pi} \sum_{i=1}^{n} S_i^* \left[\tan^{-1}\left|\frac{\nu_3 - \nu_{o_i}}{\gamma_i}\right| + \tan^{-1}\left|\frac{\nu_1 - \nu_{o_i}}{\gamma_i}\right|\right] \tag{12}$$

Here κ_l has been summed over all the lines with centers in the frequency interval $\nu_3 - \nu_1$. Equation (11) does not contain the stimulated emission factor $(1-\exp(-h\nu/kT))$; however, the continuum contribution in the spectral interval contains the stimulated emission factor.

The average total absorption coefficient in the frequency interval is found by adding the average continuum and average line absorption coefficients together

$$\bar{\kappa} = \bar{\kappa}_c + \bar{\kappa}_l \tag{13}$$

Using this, the average total intensity is found by summing the spectral intensity over each frequency interval,

$$I(L,\mu) = \sum_i B_\nu(T)\left[1-\exp\left(\frac{-\kappa_i L}{\mu}\right)\right]\Delta\nu_i \qquad (14)$$

The average total flux is calculated in a similar manner,

$$F(L) = \sum_i 2\pi B_\nu(T)\left[\tfrac{1}{2} - E_3(\kappa_i L)\right]\Delta\nu_i \qquad (15)$$

Now the step model is complete and the radiative intensity and flux can be calculated. Figure (5) shows graphically the step-wise gray absorption coefficient as a function of frequency. Each frequency interval has an average absorption coefficient of its own, which when placed along side that of the other frequency intervals depicts a graph similar to the exact graph of absorption coefficient versus frequency. The only difference is that there are "steps" in each interval rather than a continuous curve.

Once the total average absorption coefficient is obtained, it is used in the radiative intensity and flux calculations. The average intensity and flux are calculated for each interval $\Delta\nu$; these are summed for all the intervals to determine the intensity and flux for a particular temperature, density, and shock layer thickness.

D. Accuracy of Approximation

In this study various numbers of steps were tried with varying accuracy. In general, increasing the number of steps increased the accuracy. For the data presented 135 steps were taken in a spectral

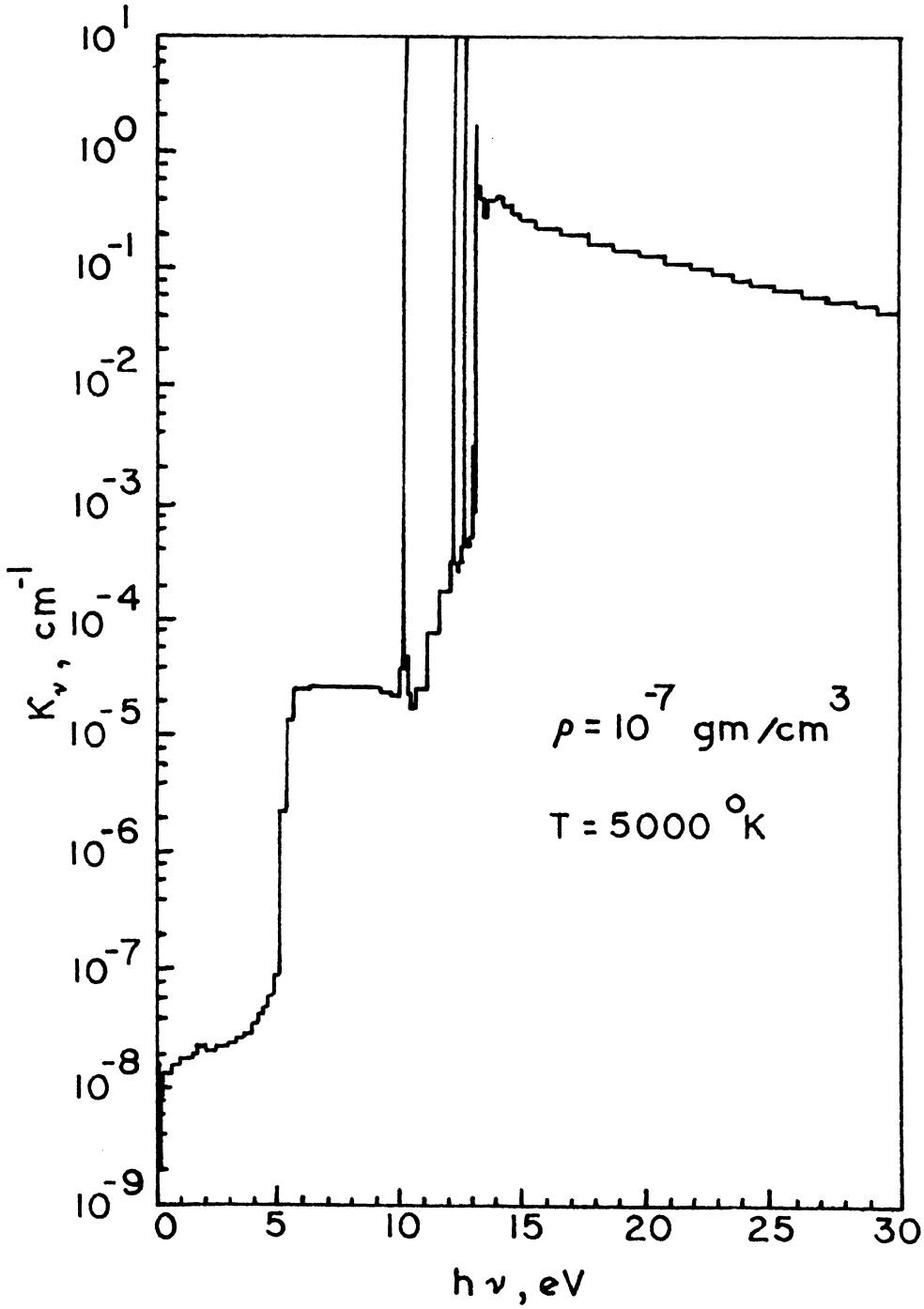

Fig. 5 Physical model

interval from zero to fifty electron volts. Where only continuum radiation is significant, the step sizes were quite large (as much as one eV). However, when atomic lines occur within a frequency interval, step sizes were as small as 0.0001eV.

The position of the steps was determined through a trial and error procedure until an accurate approximation was obtained. This was done by investigating the contribution to the total flux of the i^{th} interval (ΔF_i). ΔF_i was limited by

$$\Delta F_i < \frac{1}{10} \sum_{j-1}^{i-1} \Delta F_j . \qquad (16)$$

If this criteria was not satisfied, the i^{th} interval was decreased. The spectral position of each step is shown in Table I.

The accuracy of the step-wise gray approximation is shown in Table II. Plasma conditions of interest are for temperatures of 20,000°K and 40,000°K at densities of 3.1415×10^{-8} gm/cm^3 and 1.55×10^{-6} gm/cm^3 respectively. When the frequency spectrum is divided into a small number of intervals, the accuracy is poor compared to when it is divided into many intervals of varying length $\Delta\nu$. The per cent deviation from exact results obtained using the numerical program developed by Nelson and Goulard [7] is shown in Table II. At 20,000°K Nelson and Goulard obtained for the flux 2.96×10^9 ergs/sec-cm^2 and for the intensity 5.80×10^8 ergs/sec-cm^2-sr. At 40,000°K they obtained for the flux 3.06×10^{12} ergs/sec-cm^2 and for the intensity 5.39×10^{11} ergs/sec-cm^2-sr.

The 20,000°K case is less accurate than the 40,000°K case.

TABLE I

LISTING OF FREQUENCY INTERVALS (ev)

50.0000	16.0000	12.1500	10.2040	10.1960	4.2500
46.0000	15.0000	12.1000	10.2020	10.1950	4.0000
44.0000	14.5000	12.0950	10.2010	10.1940	3.7500
42.0000	14.0000	12.0900	10.2000	10.1920	3.5000
40.0000	13.8500	12.0880	10.1995	10.1900	3.2500
38.0000	13.7500	12.0865	10.1990	10.1850	3.0000
36.0000	13.6000	12.0860	10.1988	10.1800	2.8500
34.0000	13.5000	12.0850	10.1986	10.1700	2.7000
32.0000	13.3500	12.0830	10.1985	10.1000	2.5000
30.0000	13.2000	12.0800	10.1984	10.0000	2.0000
29.0000	13.1000	12.0600	10.1982	9.5000	1.8000
28.0000	13.0500	12.0400	10.1981	9.0000	1.5000
27.0000	13.0200	12.0000	10.1980	8.5000	1.2000
26.0000	13.0000	11.5000	10.1979	8.0000	1.0000
25.0000	12.9600	11.0000	10.1978	7.5000	0.5000
24.0000	12.9200	10.7500	10.1977	7.0000	0.2000
23.0000	12.9000	10.5000	10.1976	6.5000	0.1000
22.0000	12.8000	10.3000	10.1975	6.0000	0.0500
21.0000	12.7750	10.2600	10.1973	5.5000	0.0200
20.0000	12.7500	10.2300	10.1972	5.2500	0.0100
19.0000	12.7250	10.2150	10.1970	5.0000	
18.0000	12.6000	10.2080	10.1968	4.7500	
17.0000	12.3500	10.2060	10.1965	4.5000	

TABLE II

Accuracy of Intensity Calculations at

$20{,}000^{\circ}K$ and $40{,}000^{\circ}K$

(Plasma thickness = 1.0 cm)

NUMBER OF INTERVALS	TIME (SEC.)	T = 20,000°K INTENSITY (ERGS/ SEC-CM^2-SR)	ERROR (%)	T = 40,000°K INTENSITY (ERGS/ SEC-CM^2-SR)	ERROR (%)
25	18	1.59×10^{11}	27,400	1.14×10^{12}	111
50	21	6.66×10^{9}	1,050	3.99×10^{11}	26
70	25	3.22×10^{9}	472	1.35×10^{12}	150
80	26	9.44×10^{8}	63	6.02×10^{11}	11.5
100	29	4.56×10^{9}	690	2.97×10^{11}	45
120	33	6.74×10^{8}	16.2	5.80×10^{11}	7.4
135	35	6.58×10^{8}	13.4	5.74×10^{11}	6.5

At 20,000°K there is a significant amount of atomic hydrogen present in the shock layer. Hence, this makes it possible for more bound-bound energy transitions to occur which give rise to atomic lines. The lines are difficult to integrate over accurately. The frequency interval in which a line center occurs must be divided into many small intervals to accurately approximate the atomic line absorption coefficient.

At 40,000°K the plasma is nearly fully ionized with only electrons and protons present. Therefore, only a few lines exist. The radiation is mostly due to the continuum at 40,000°K, which is easily approximated.

The location of the beginning and end (cuts) of each spectral interval has a large effect on the accuracy. For instance, when 100 cuts are used, the accuracy is less than for 80 cuts. This is because of the spacing of the cuts. The cuts are located in a manner that does not yield a true average of the absorption coefficient; instead, a much higher absorption coefficient than the one which actually existed is predicted by the model.

The flux and intensity are found to have about the same per centage error. Therefore, only the intensity results are shown in Table II.

The time required to make the intensity and flux calculations increased as the number of steps increased. Required computer time versus the number of intervals is shown in Table II.

IV. RESULTS

An IBM System/360, model 50 computer was used for the numerical calculations in this study. Approximately 35 seconds of computer time was required to model the absorption coefficient and calculate the flux and intensity for ten shock layer thicknesses at one temperature and density. The shock layer was assumed to be isothermal. The flux and intensity numerical results are presented in tabular form in Appendix B, while the results are presented in graphical form in the discussion that follows. The numerical computer program that was used for the calculations is listed in Appendix C.

A. Absorption Coefficient

The absorption coefficient (cm^{-1}) as a function of frequency (eV) is shown in Figs. 6 through 9. κ_ν is plotted in Figs. 6 through 8 for temperatures of 10,000°K and 40,000°K at constant density. Fig. 6 is for a density of 10^{-5} gm/cm^3, Fig. 7 for a density of 10^{-6} gm/cm^3, and Fig. 8 for a density of 10^{-7} gm/cm^3. Fig. 9 gives the absorption coefficient for a density of 10^{-5} gm/cm^3 at a temperature of 5000°K.

The photoionization edges occur at approximately 13.6eV (Lyman series), 3.4eV (Balmer series), 1.5eV (Paschen series), and 0.85eV (Brackett series). The Lyman edge is clearly visible in the figures; however, the other edges are hidden by the contribution from the molecular band and free-free radiation.

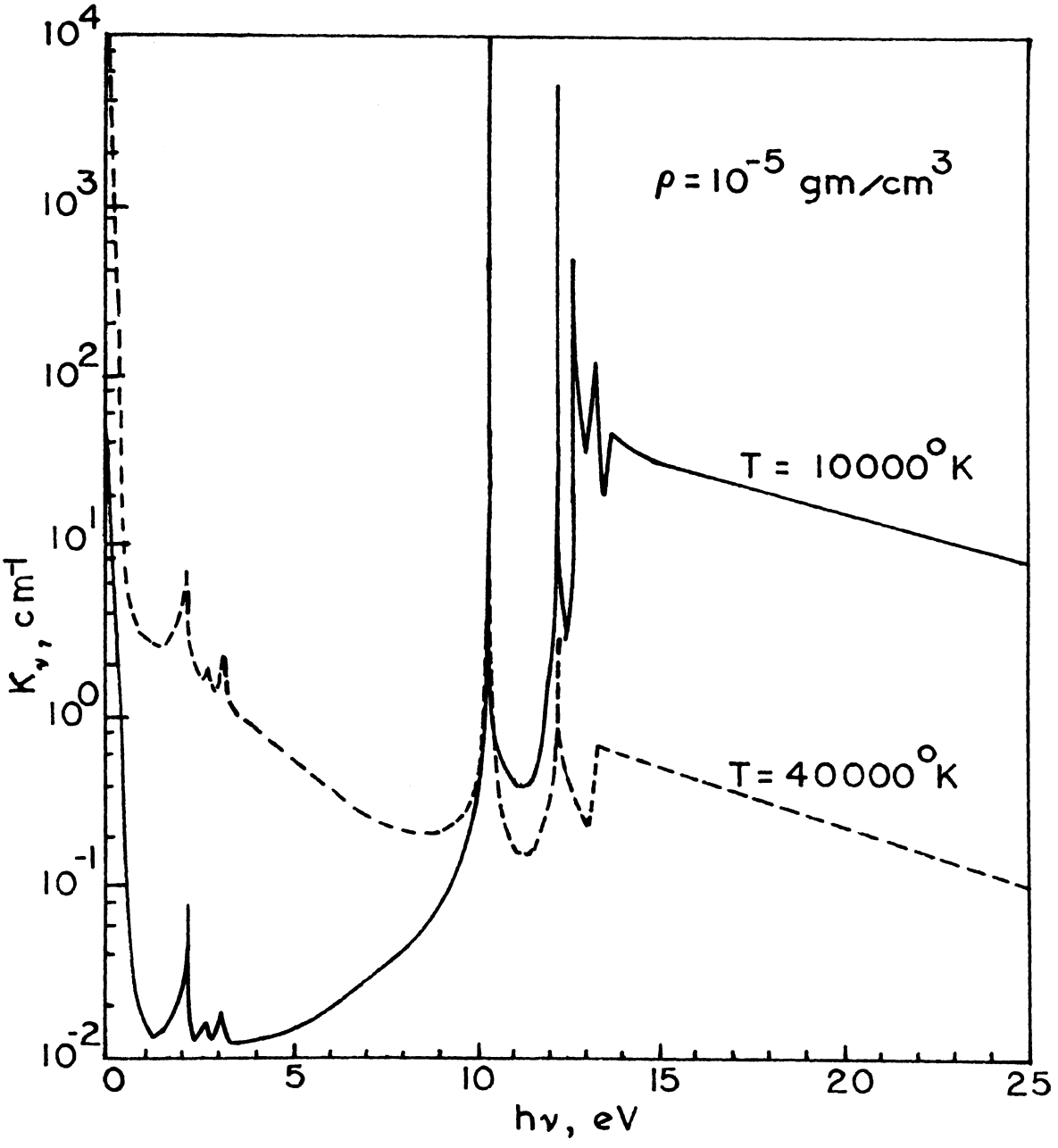

Fig. 6 Spectral absorption coefficient for $\rho = 10^{-5}$

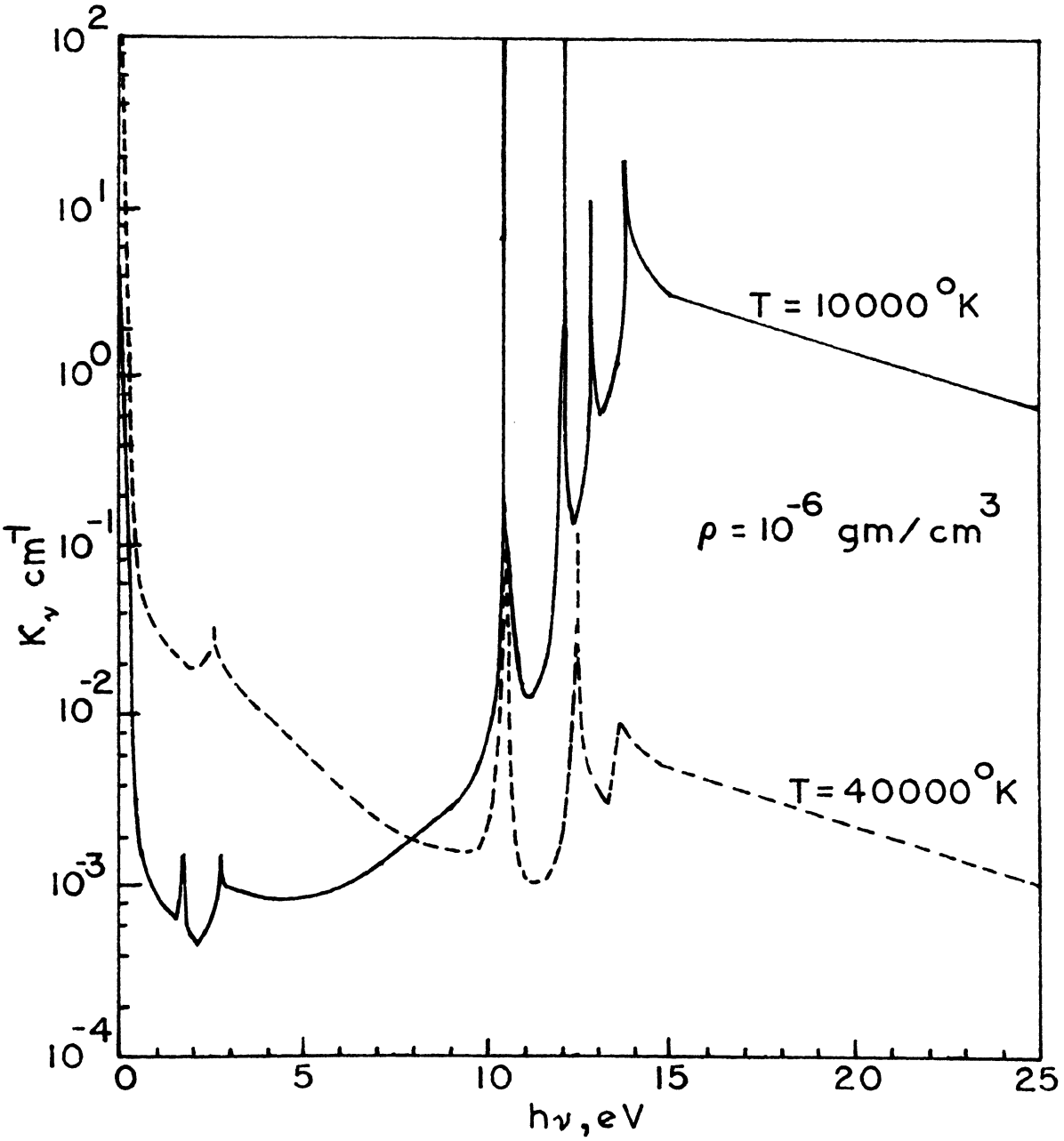

Fig. 7 Spectral absorption coefficient for $\rho = 10^{-6}$

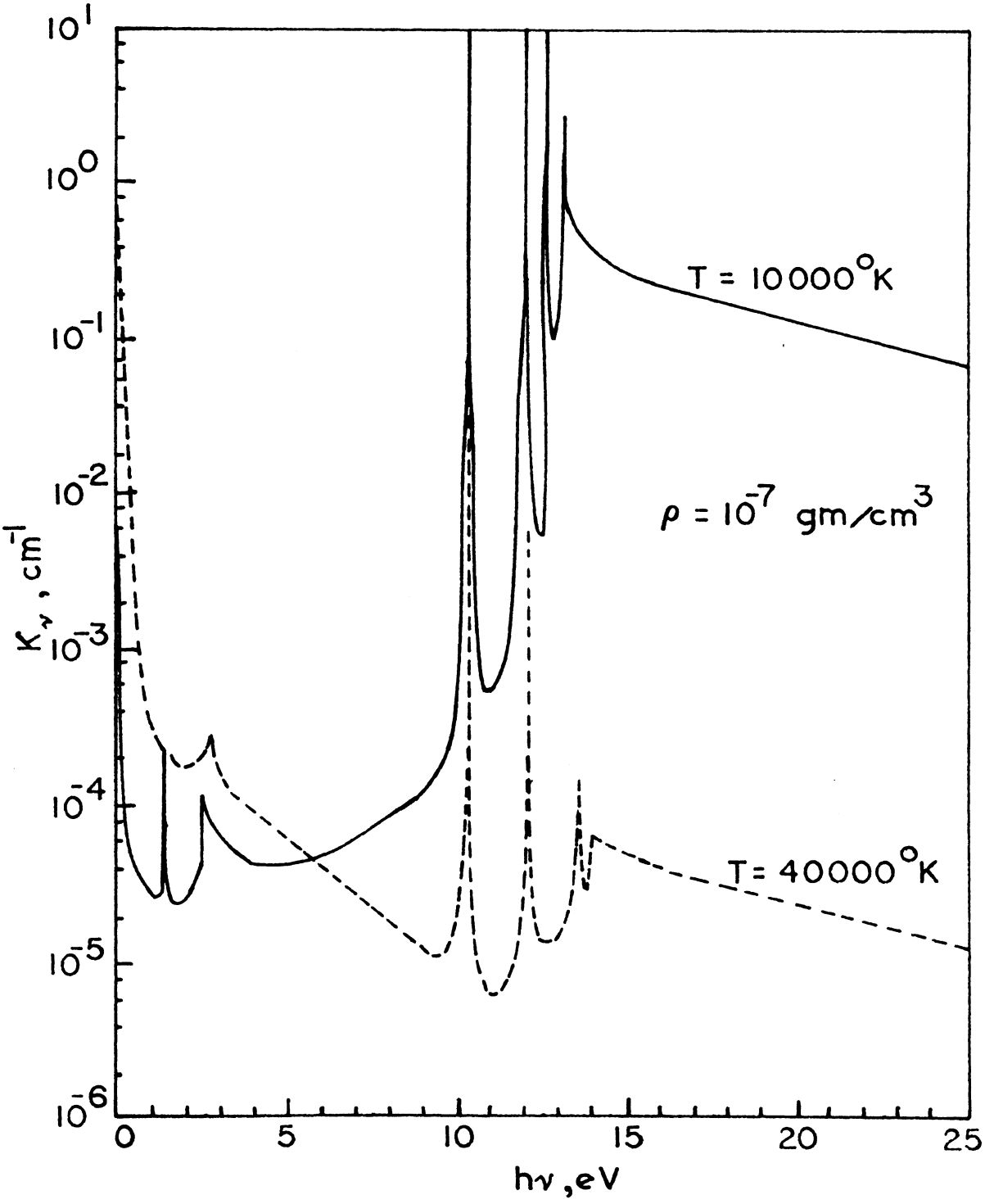

Fig. 8 Spectral absorption coefficient for $\rho = 10^{-7}$

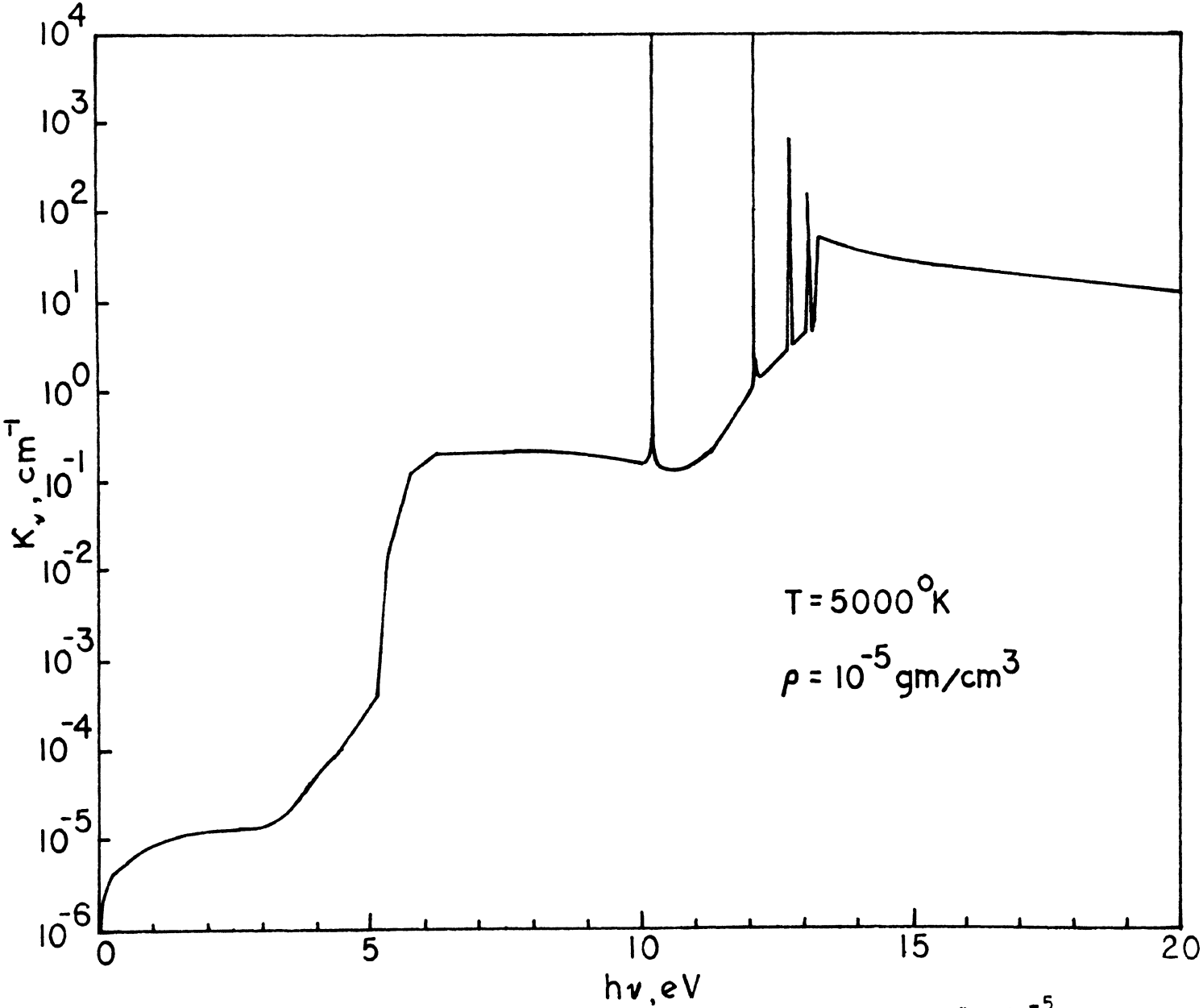

Fig. 9 Spectral absorption coefficient for T = 5000 and $\rho = 10^{-5}$

The Lyman lines are also visible in Figs. 6 through 9. The Ly_α is seen at 10.2eV, Ly_β at 12.1eV, and Ly_γ at 12.5eV. The other Lyman lines are also present; however, they are so close together that they appear as continuum on the graphs. In Figs. 7, 8, and 9 the H_α and H_β lines are visible at 1.8eV and 2.5eV. The Paschen and Brackett lines are masked by the free-free radiation process.

1. Effect of temperature at constant density

The effect of temperature at constant density on the radiation absorption coefficient is seen in Figs. 6 through 8. At $10{,}000^\circ K$ and 10^{-5} gm/cm^3, κ_ν first decreases as $h\nu$ increases because the free-free absorption cross section decreases as $1/\nu^3$ and also because the excited atomic hydrogen states are not populated sufficiently to contribute to the absorption coefficient. As $h\nu$ increases beyond 2.5eV, the absorption coefficient begins to increase first due to the Balmer lines and continuum and then due to the Ly_α line wing. The H_2 Lyman molecular band does not significantly influence κ_ν because the H_2 population is so small.

The absorption coefficient continues its general increase between 10 and 13.9eV due to the Lyman lines. After passing the Lyman ionization edge, the ground state continuum process is responsible for the absorption coefficient. At $10{,}000^\circ K$ the ground state is highly populated; hence, the absorption coefficient in this range is large.

At $40{,}000^\circ K$ and 10^{-5} gm/cm^3, κ_ν continually decreases as $h\nu$

increases from zero to about 10eV. It first decreases because of the free-free radiation process. It continues to decrease as $h\nu$ increases from 2eV because the higher excited states of hydrogen are more highly populated than the lower excited states, and the bound-free continuum process drops off as $1/\nu^3$. Also, the Ly_α line is not as strong as it was at 10,000°K because the ground state population has decreased. Hence, the Ly_α line wing does not increase κ_ν from 5 to 10eV as it did at 10,000°K. Between 10 and 13.9eV the Lyman lines appear, while beyond 13.9eV the ground state continuum is responsible for the absorption coefficient.

At densities of 10^{-6} and 10^{-7} gm/cm^3, trends similar to those discussed above are observed. However, as density decreases the Balmer lines increase in importance.

As the temperature increases from 10,000°K to 40,000°K, the absorption coefficient increases in the frequency interval from zero to approximately 10eV and decreases in the frequency interval from 10eV to infinity. This can be attributed entirely to the population of the hydrogen electronic states.

At low temperatures only the ground state of atomic hydrogen is significantly populated, and the electron number density is low. This causes the ground state continuum process and the Lyman series bound-bound processes to be the major contributors to the radiative absorption coefficient.

At high temperatures the electron number density is high, and the ground state population is small. This causes the free-free process and the excited state bound-free processes to be the

major contributors to the radiative absorption coefficient.

2. Effect of density at constant temperature

The effect of density at constant temperature can be considered by investigating Figs. 6 through 8. First, a temperature of 10,000°K will be considered.

The free-free absorption coefficient varies directly with density as density changes from 10^{-5} to 10^{-7} gm/cm^3. It is related to the population of the electrons[10] which changes directly with the density.

In the frequency region from 2.5 to 10eV, the absorption coefficient is influenced by the Balmer lines and continuum as well as the Ly_α line wing. The absorption coefficient in the Ly_α line wing increases as density increases at 10,000°K. This is because the number density of the electrons increases (see Figs. A-1, A-2, and A-3), thus, broadening the Ly_α line wing. The continuum absorption coefficient increases directly with density. Hence, the absorption coefficient in the interval from 5 to 10eV increases slightly faster than the density for density changes at 10,000°K.

The Balmer lines influence the rate of change of κ_ν with frequency near 2.5eV. As the density increases, the Balmer lines become less important in defining the absorption coefficient.

The population of the ground state and the excited states of the hydrogen atom vary directly with the density. At a given frequency, the ratio of the continuum absorption coefficient at two different densities is proportional to the ratio of the

populations at the two densities.

In the frequency region beyond 13.9eV, the absorption coefficient varies directly with the ground state population at 10,000°K. The ground state populations are given in Table III. They vary directly with density for a temperature of 10,000°K, thus accounting for the factor of 10 change in the absorption coefficient for a factor of 10 change in density.

TABLE III

Populations of the Hydrogen Ground State and the First Excited State

DENSITY	T = 10,000°K		T = 40,000°K	
	N_0 (cm^{-3})	N_1 (cm^{-3})	N_0 (cm^{-3})	N_1 (cm^{-3})
10^{-5} gm/cm^3	5.9×10^{18}	1.7×10^{14}	7.9×10^{16}	1.6×10^{16}
10^{-6}	5.8×10^{17}	1.7×10^{13}	9.0×10^{14}	1.8×10^{14}
10^{-7}	5.5×10^{16}	1.6×10^{12}	9.3×10^{12}	1.9×10^{12}

Now, the effect of density at 40,000°K will be considered. Between zero and 2.0eV the free-free radiation is much stronger than the molecular band radiation and the high excited state bound-free radiation. The free-free absorption coefficient varies directly with the square of the electron number density.[13] The electron number density changes directly as the density of the plasma changes; therefore, at 40,000°K the free-free absorption coefficient changes as the square of the density.

For $h\nu$ between 2.0 and 5.0eV, the bound-free absorption

coefficient varies as the population of the first excited state. The populations of the first excited state are given in Table III. They change by a factor of 100 for density changes of a factor of 10. This is because the partition function at 40,000°K varies directly with density. When the density decreases, the reduction of the ionization potential also decreases. This causes the electronic partition function to increase, which in turn causes the hydrogen population to decrease by a factor of 100 when density decreases by a factor of 10. At 10,000°K the higher terms in the partition function are negligible and the partition function is relatively constant with density.[14] The factor of 100 is coincidental to 40,000°K; at 30,000°K it would be smaller; and at 50,000°K it would be somewhat larger.

The absorption coefficient decreases in the entire spectral region from zero to 10eV at 40,000°K. As the density increases, the Ly_α line undergoes greater broadening, which increases the absorption coefficient in the line wing. Thus, as density increases, κ_ν decreases less rapidly in the frequency interval 5 to 10eV.

The Lyman lines occur in the spectral interval between 10 and 13.9eV. Above 13.9eV the ground state continuum determines the magnitude of the absorption coefficient. The populations of the ground state differ by about 100, as explained above, causing the absorption coefficient to vary as the square of the density.

3. Effect of molecular band

Fig. 9 shows the absorption coefficient at a temperature of 5000°K and a density of 10^{-5} gm/cm^3. At 5000°K there is very little effect from the free-free process due to the low degree of ionization. Also, the excited states of atomic hydrogen are essentially unpopulated. Therefore, the atomic hydrogen absorption coefficient is quite low in the zero to 5eV frequency range.

At approximately 5.5eV, κ_ν increases very rapidly due to the H_2 Lyman molecular band. The absorption coefficient for the H_2 Lyman band, which is shown in Fig. 2, remains strong up to about 12eV. Over this range of $h\nu$ (5.5 to 12eV), the H_2 Photoionization band is still relatively weak (see Fig. 4). However, the H_2 Werner band becomes strong at approximately 10eV (see Fig. 3). Thus, in Fig. 9 the effect of the H_2 Lyman band appears from 5.5 to 10eV; however, the Lyman lines are strong enough to mask the Werner molecular band above 10eV.

At 5000°K the ground state is highly populated. This causes the ground state continuum process to be large for $h\nu$ greater than 13.9eV. Above this frequency, as frequency increases the ground state continuum decreases as $1/\nu^3$.

B. Total Intensity

The integral of intensity (ergs/cm^2-sr) from infinity to $h\nu$ as a function of frequency is shown in Figs. 10 through 12. The integral of intensity is the normal intensity to the body ($\mu = 1$)

$$I_{\infty,\nu} = -\int_{h\nu}^{\infty} B_\nu(T)[\ 1-\exp(-\kappa_\nu L)\ ]d\nu \qquad (17)$$

The graphs are plotted for temperatures of 10,000, 20,000, 30,000, and 40,000°K at densities of 10^{-5} gm/cm^3 (Fig. 10), 10^{-6} gm/cm^3 (Fig. 11), and 10^{-7} gm/cm^3 (Fig. 12). All of the figures are for a plasma thickness of 1.0 cm.

Figs. 10 through 12 allow the following conclusions to be made. When the integral of intensity curves are flat over a spectral region, there is no major contribution to intensity from either the lines or the continuum. When the integral of intensity curves have a steep increase over a spectral region, it indicates that a strong atomic line exists. This is especially noticeable in Figs. 11 and 12 at approximately 10 and 12eV at the locations of the Ly_α and Ly_β lines. The sharp increase indicates that these lines make very important contributions to the total intensity. For instance, in Fig. 12 at a temperature of 40,000°K and between a frequency of about 10.2 and 10eV, the intensity doubles because of the contribution due to the Ly_α line.

Note that in Fig. 11 the T=40,000°K and T=30,000°K curves cross at approximately 14eV, and in Fig. 12 the T=20,000°K, T=30,000°K, and T=40,000°K curves cross at about 14.5eV. This is caused by the shift in the maximum of the Planck function to higher frequencies as the temperature increases. For instance, at 10,000°K

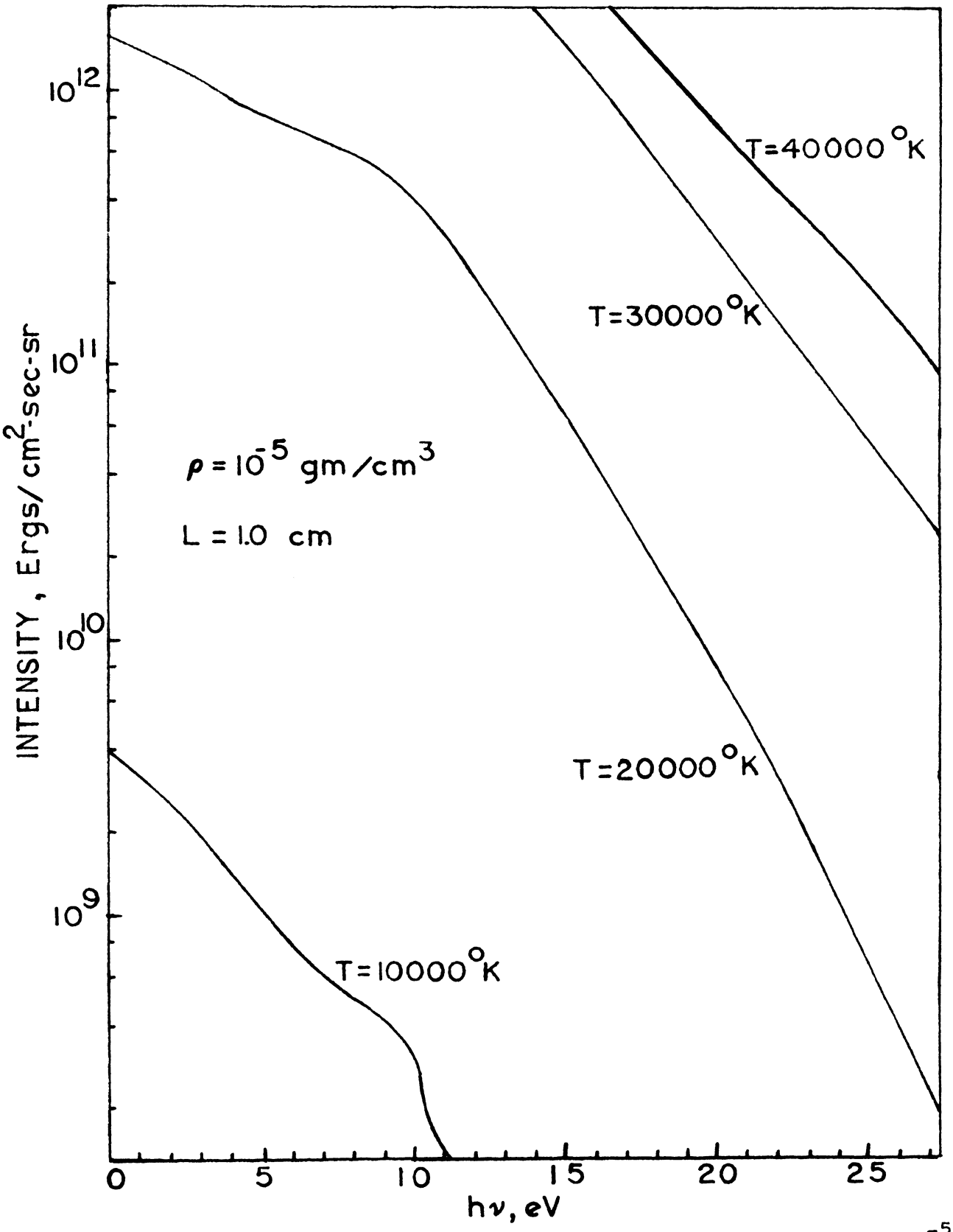

Fig. 10 Integral of intensity over the frequency spectrum for $\rho = 10^{-5}$

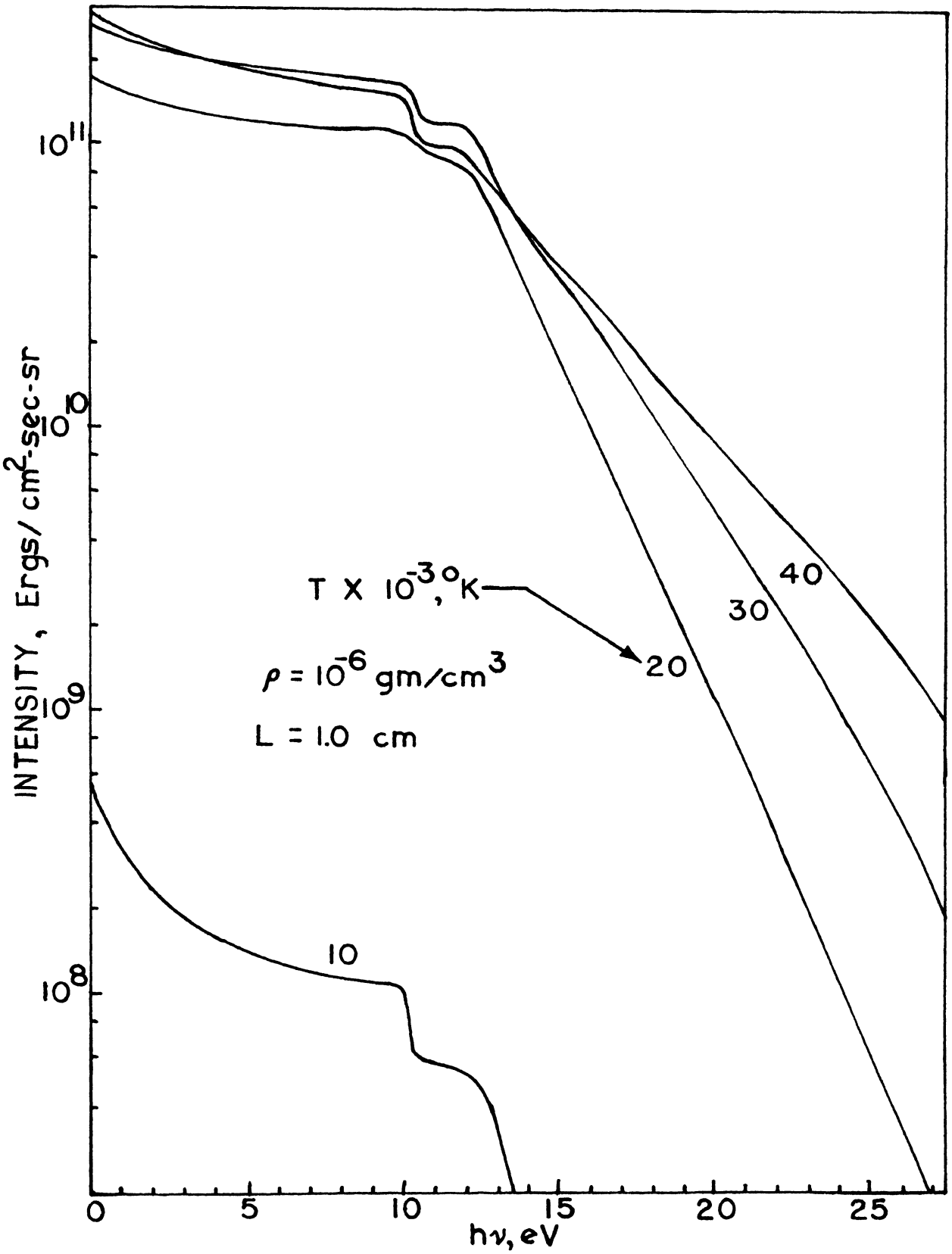

Fig. 11 Integral of intensity over the frequency spectrum for $\rho = 10^{-6}$

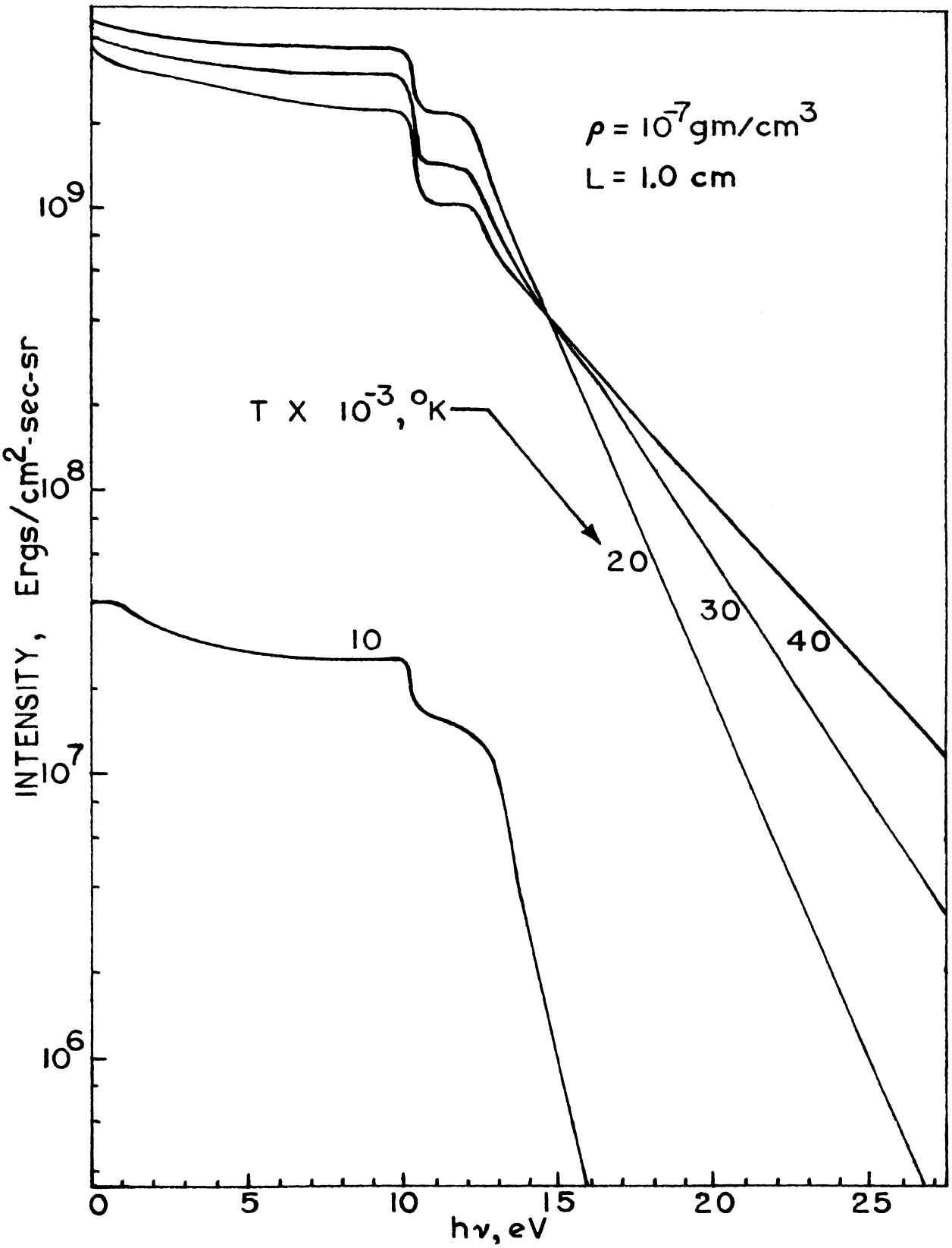

Fig. 12 Integral of intensity over the frequency spectrum for $\rho = 10^{-7}$

the maximum of the Planck function is at 3.9eV, while at 40,000°K the maximum of the Planck function is at 9.5eV. Therefore, for a density of 10^{-7} gm/cm^3, the source function for ground state continuum radiation in the spectral interval from infinity to $h\nu$ is greater at 40,000°K than at 30,000°K. Although the ground state population is less at 40,000°K than it is at 30,000°K, the increase in the source function is strong enough to increase the intensity in the spectral region from infinity to about 15eV. At higher densities the population of the electronic states at 40,000°K is great enough to increase $I_{\infty,\nu}$ above that for T=30,000°K throughout the frequency spectrum.

In the spectral range below 15eV, lower temperature plasmas radiate more strongly than the high temperature ones. At 40,000°K the excited states and free states are highly populated. But since the maximum of the Planck function is shifted to 9.5eV, the source function is not strong enough for the radiation from the highly populated excited states to have a great effect in the zero to five eV range.

C. Spectral Distribution of Intensity

Figs. 13 and 14 show the spectral distribution of intensity at densities of 10^{-5} and 10^{-6} gm/cm^3 and a plasma thickness of 1.0 cm. These graphs are for temperatures of 10,000 and 40,000°K. The area under the curves is equal to the total intensity emitted by the plasma at those specific theromodynamic conditions.

1. Effect of temperature at constant density

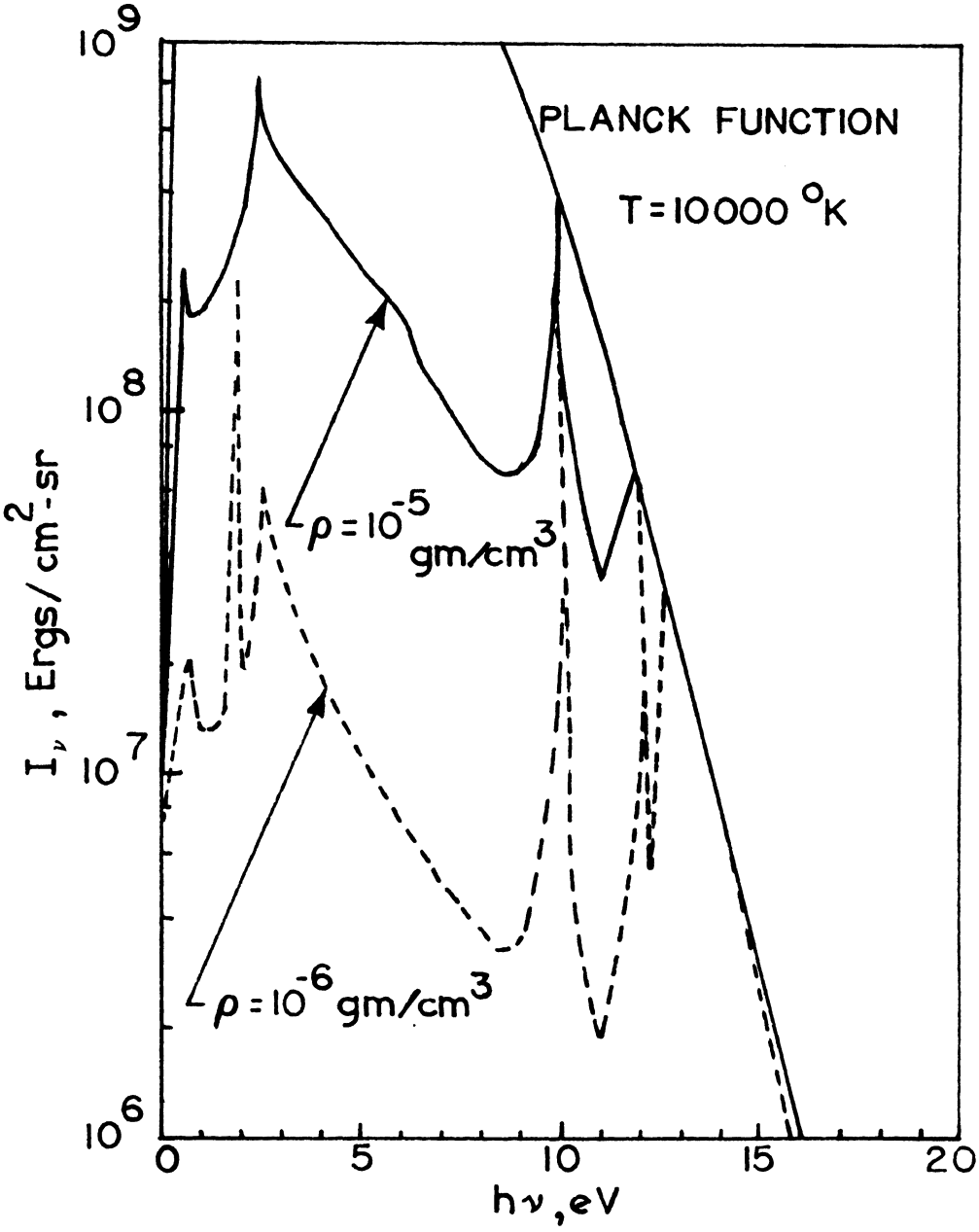

Fig. 13 Spectral distribution of intensity for T = 10,000

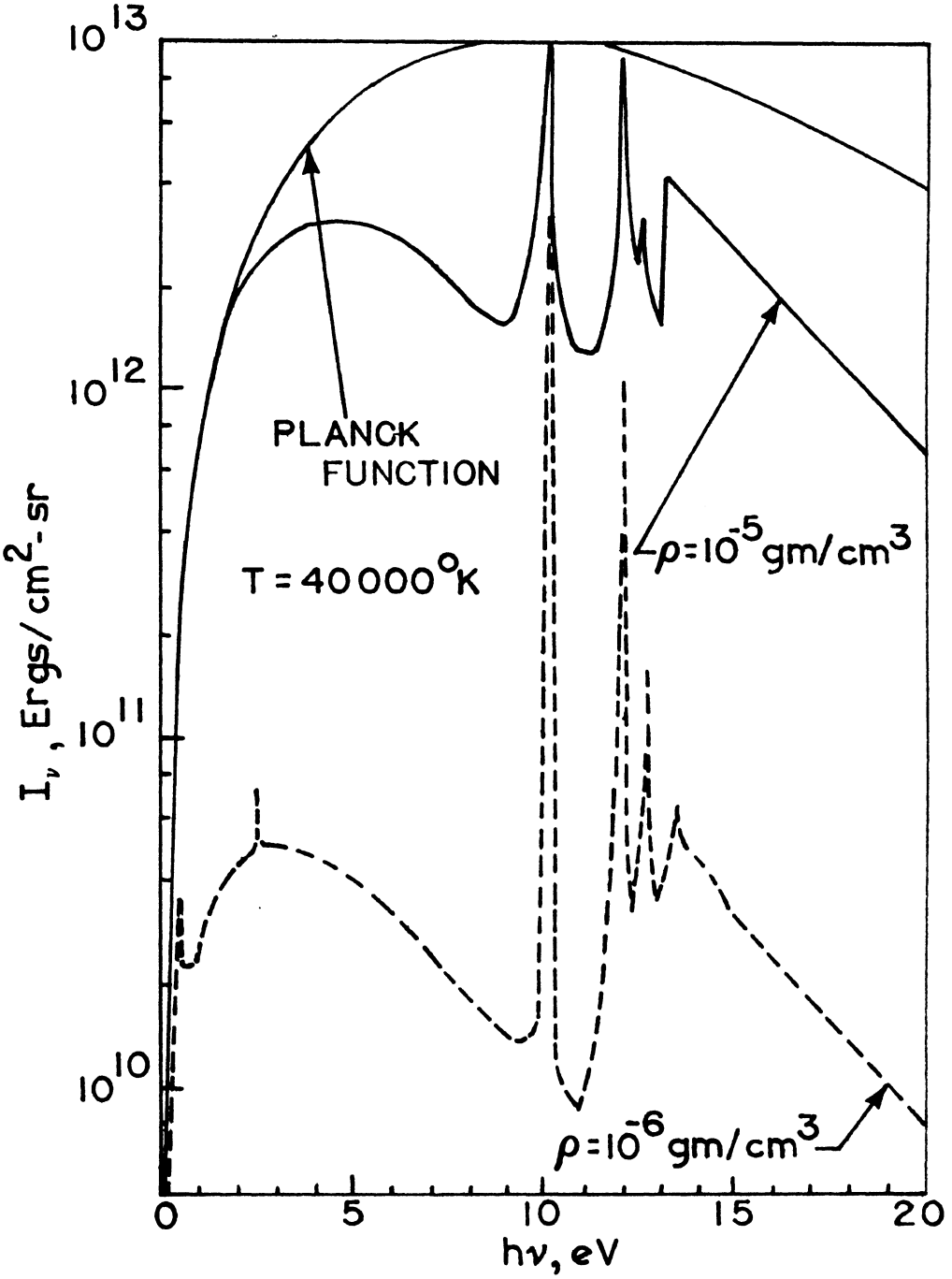

Fig. 14 Spectral distribution of intensity for T = 40,000

In Figs. 13 and 14 at a density of 10^{-5} gm/cm^3, the effect of temperature on the spectral intensity is seen. First, the 10,000°K case will be considered.

In the zero to 0.5eV range, the plasma radiates as approximately a blackbody. The radiation is optically thick in this frequency range.

The radiative contribution from the Balmer and Paschen lines is seen from 0.5 to 3.5eV. They are optically thin at this temperature and, therefore, contribute only a small amount to the spectral intensity. The effect of the H_α and the H_β lines is seen at 1.8 and 2.5eV in Fig. 13.

As the frequency increases above 3.9eV, the spectral intensity drops off rapidly because the Planck function is decreasing and the plasma is optically thin.

Effects from the Ly_α line wing on the spectral intensity begin to appear at about 9.0eV. The Ly_α emission near the line center is strongly reabsorbed and radiates like a blackbody. Other Lyman line effects are seen between 10 and 13.9eV. The Ly_β line is also thick and radiates like a blackbody.

Above 13.9eV the plasma is optically thick and radiates like a blackbody. However, since the source function is so small above 13.9eV, the total effect of the ground state continuum radiation is also small even though the ground state is highly populated.

Now a temperature of 40,000°K will be considered at a density of 10^{-5} gm/cm^3. At this temperature the maximum of the

Planck function has been shifted to 9.5eV. The plasma radiates as a blackbody from zero to 2.0eV since the absorption coefficient is large due to the highly populated excited and free states.

The Balmer lines are optically thick at 40,000°K; however, their effect on the total intensity is small because the source function is about a factor of five less than its maximum in the frequency range where the Balmer lines occur.

Above the Balmer ionization edge (3.5eV), the continuum drops off less steeply for 40,000°K than 10,000°K due not only to the increase in the population of the excited states, but also because the source function is still increasing at 40,000°K.

The Ly_α and Ly_β lines are optically thick near their line centers and are strongly reabsorbed. Other Lyman lines are optically thin and have no significant contribution to the spectral intensity.

Above the Lyman ionization edge the continuum is optically thin and it radiates like κ_ν times the Planck function; whereas, the ground state continuum was optically thick and radiated like the Planck function.

For a density of 10^{-6} gm/cm^3, similar trends occur to those observed for the case discussed above. However, since the plasma is less dense, and therefore, more optically thin, the spectral intensity is less.

2. Effect of density at constant temperature

The effect of density at a temperature of 10,000°K is shown in Fig. 13. At a density of 10^{-5} gm/cm^3 the continuum

is the most significant radiation process. At this temperature and density the plasma is highly populated with neutral atoms in which bound-free transitions can occur. Thus, the bound-free contribution is large in comparison with the atomic line contribution.

The Balmer lines are optically thin, hence , they contribute little to the total intensity. The Lyman lines are optically thick and are reabsorbed, but they also have only a small effect since the source function is small where they occur.

At a density of 10^{-6} gm/cm^3, the population of the plasma is decreased by approximately a factor of 10 from the previous case; hence, the spectral absorption coefficient has decreased which causes the spectral intensity to decrease. Line radiation increases in importance as density decreases because the continuum becomes optically thin faster than the lines.

Now, the effects of density at 40,000°K will be considered. For a density of 10^{-5} gm/cm^3, the plasma radiates as a blackbody from zero to 2.0eV because the higher electronic states and free states are significantly populated.

At 40,000°K there are relatively few neutral atoms in which a bound-bound transition can occur. Thus, the continuum bound-free transitions completely mask the Balmer lines at this density. The Ly_α line occurs near the maximum of the source function and radiates like a blackbody near its center. Thus, the Lyman line contribution to the spectral intensity increases.

At a plasma density of 10^{-6} gm/cm^3 and temperature of 40,000°K, the plasma radiates as a blackbody from zero to 0.5eV. Blackbody

radiation is not found from 0.5 to 2.0eV (as was the case for $\rho = 10^{-5}$ gm/cm^3) because the plasma is less dense which causes the population of the higher electronic states to decrease relative to the previous case of $\rho = 10^{-5}$ gm/cm^3. This, in turn, causes the plasma to become more optically thin.

The Balmer lines increase in importance since the bound-free continuum radiation has been reduced; however, their effect on the total intensity is relatively small. The continuum radiation decreases with frequency between 3.5 and 9.5eV. The Planck function is still increasing in this frequency range, so the decrease in continuum intensity is gradual compared to the 10,000°K case.

The Ly_α and Ly_β lines are optically thick for these plasma conditions, causing the spectral intensity to increase significantly. The Ly_α radiates as a blackbody, and the Ly_β approaches blackbody radiation.

The ground state continuum process decreases with frequency but the contribution is much less at a density of 10^{-6} gm/cm^3 than at 10^{-5} gm/cm^3 because it is more optically thin due to the decrease in the number of particles.

D. Intensity as a Function of Thickness

Figs. 15 through 17 show the total intensity (ergs/sec-cm^2-sr) as a function of shock layer thickness (cm) at constant density and temperatures of 20,000, 30,000, 40,000, and 60,000°K. All the results are for $\mu = 1$. Fig. 15 is for a density of 10^{-5} gm/cm^3, Fig. 16 for a density of 10^{-6} gm/cm^3, and Fig. 17 for a

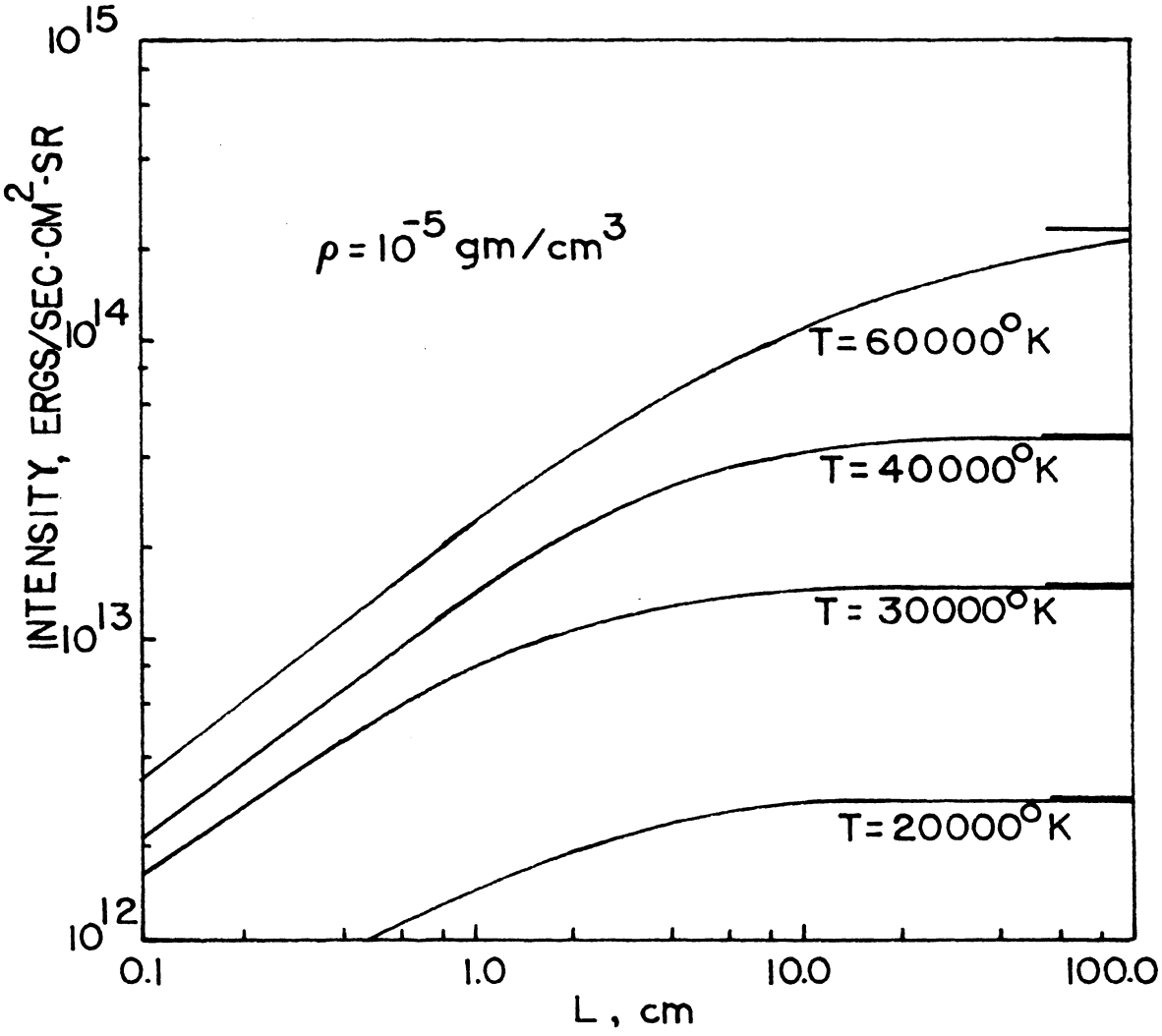

Fig. 15 Intensity variation with shock layer thickness for $\rho = 10^{-5}$

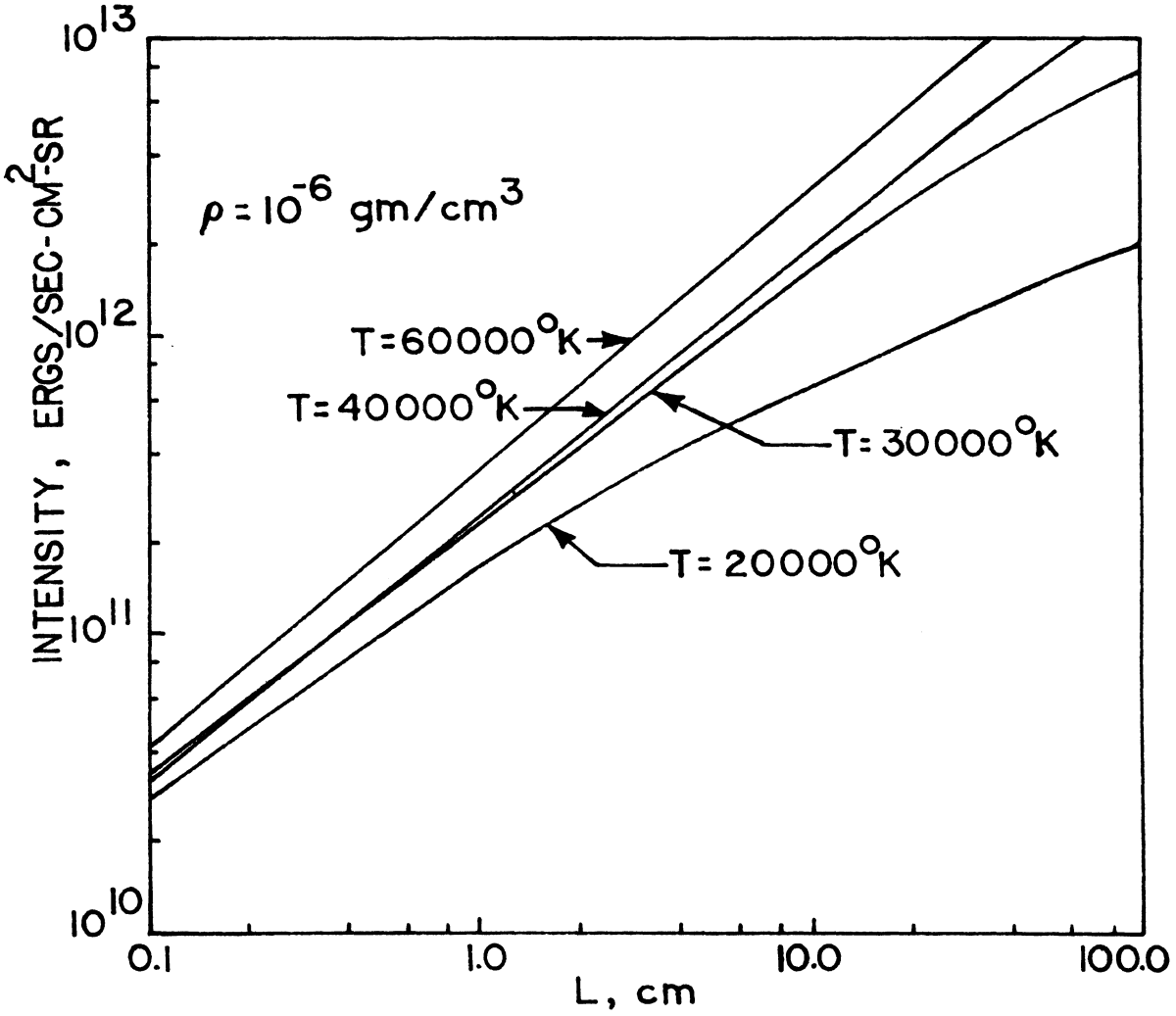

Fig. 16 Intensity variation with shock layer thickness for $\rho = 10^{-6}$

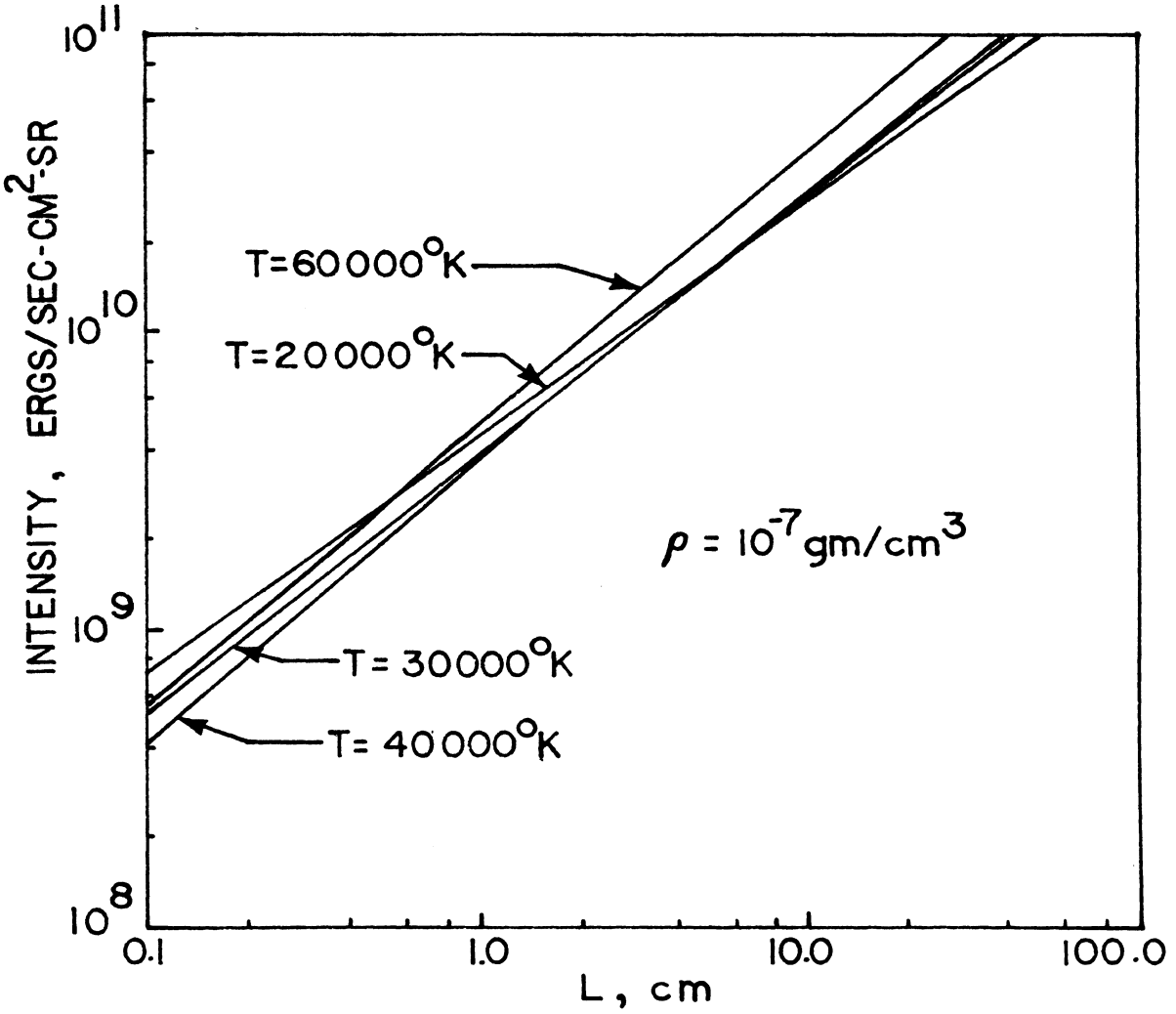

Fig. 17 Intensity variation with shock layer thickness for $\rho = 10^{-7}$

density of 10^{-7} gm/cm^3.

First, a density of 10^{-5} gm/cm^3 will be considered. From Fig. 15 several conclusions can be drawn. When the plasma is optically thin, the intensity increases linearly with thickness. At higher temperatures the plasma remains optically thin for larger path lengths than at lower temperatures. As the temperature increases and the maximum of the Planck function moves to higher frequencies, the population moves to the excited states. Thus, the ground state is relatively unpopulated which causes the plasma to remain optically thin over a larger path length at higher temperatures (see Fig. 14).

As the shock layer thickness increases, the intensity increases less rapidly until finally it attains that of a blackbody, which is shown as a straight line extending from the right side of the graph. Once the intensity has attained that of a blackbody, an increase in shock layer thickness yields no further increase in the total intensity.

In Fig. 16 at a density of 10^{-6} gm/cm^3, similar trends to those in Fig. 15 are observed. The main difference between the two densities is that the plasma remains optically thin for greater thicknesses because of the decrease in the total number of species with a decrease in density. The intensity, therefore, varies linearly with thickness over a greater range of plasma thicknesses.

Also, the magnitude of the intensity decreases as density decreases. The intensity is less at a lower density because the

absorption coefficient, which varies directly with density, is smaller as was discussed previously. In other words, the optical thickness of a plasma of given thickness L decreases with density.

The curves in Fig. 16 at temperatures of 30,000°K and 40,000°K intersect at L = 0.3 cm. Here, the emitted intensity for the two temperatures is equal. At a thickness of 0.1 cm, a plasma at 40,000°K emitts less energy than a plasma at 30,000°K. This can be explained by considering the shift in the maximum of Planck function to higher frequencies as the temperature increases, while the population of the hydrogen levels moves more away from the ground state and towards the excited states. As the temperature increases, the population forces the plasma to radiate at lower frequency; however, the maximum of the source function moves to larger frequencies. Thus, the curves for temperatures of 30,000°K and 40,000°K in Fig. 16 intersect due to the trade-off between the shift in the maximum of the Planck function and the population of the excited electronic states.

Curves for a density of 10^{-7} gm/cm^3 are shown in Fig. 17. Trends are similar to those discussed above. However, at a density this low, the plasma is essentially optically thin for all of the temperatures and thicknesses shown because there are relatively few species present. As the density decreases, the trade-off between the maximum of the source function and the excited state population has a more pronounced effect, causing several of the curves to intersect.

E. Intensity as a Function of Temperature

The total normal intensity ($\mu = 1$) as a function of temperature is shown in Figs. 18 through 20 at densities of 10^{-5}, 10^{-6}, and 10^{-7} gm/cm^3. Intensity curves are shown for shock layer thicknesses of 0.1, 1.0, 10, and 100 cm. The reference blackbody intensity is also shown. The pressure is plotted with its ordinate at the right hand side of the graph. Individual data points on the graphs are from Lasher, Wilson, and Grief[9] and Nelson[15]. A comparison with these results will be made later.

1. Effect of temperature and density

At a density of 10^{-5} gm/cm^3 in Fig. 18, the emitted intensity at low temperatures is much less than at high temperatures because the Planck function varies directly with T^4. From temperatures of 5000°K to 20,000°K, the plasma radiation increases faster than the Planck function because the electronic levels are all becoming populated, allowing the plasma to radiate throughout the entire frequency spectrum.

For a density of 10^{-5} gm/cm^3, the plasma radiates as a blackbody between temperatures of 20,000 to 35,000°K when the thickness is greater than 10 cm. This effect was also visible in Fig. 15 where the intensity curves became flat for thicknesses greater than 10 cm in the temperature range mentioned.

As the temperature increases further, the plasma becomes fully ionized and only the free-free continuum and high excited state radiation processes are important. The spectral interval available to the plasma for radiation becomes smaller, and the

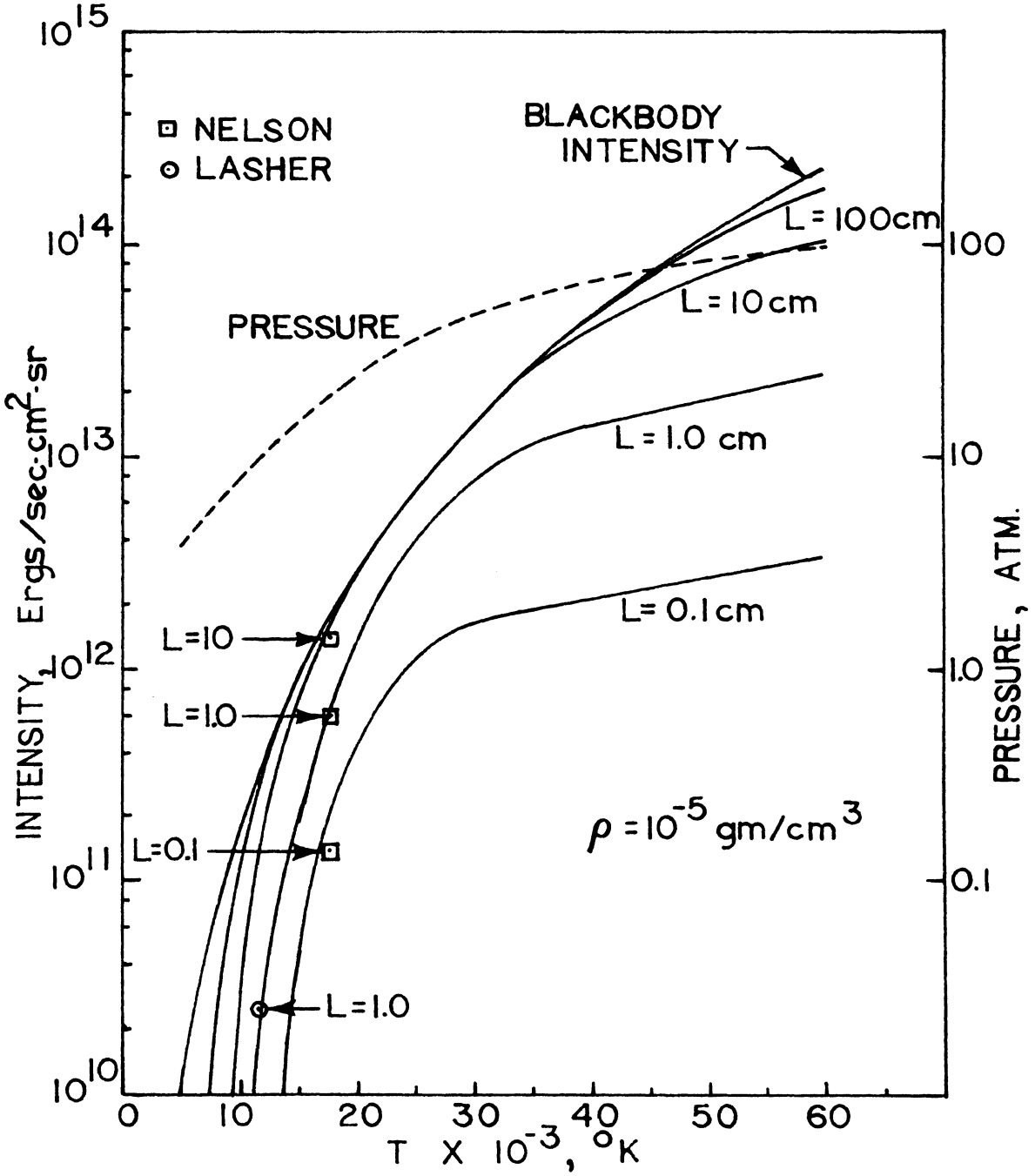

Fig. 18 Temperature distribution of intensity for $\rho = 10^{-5}$

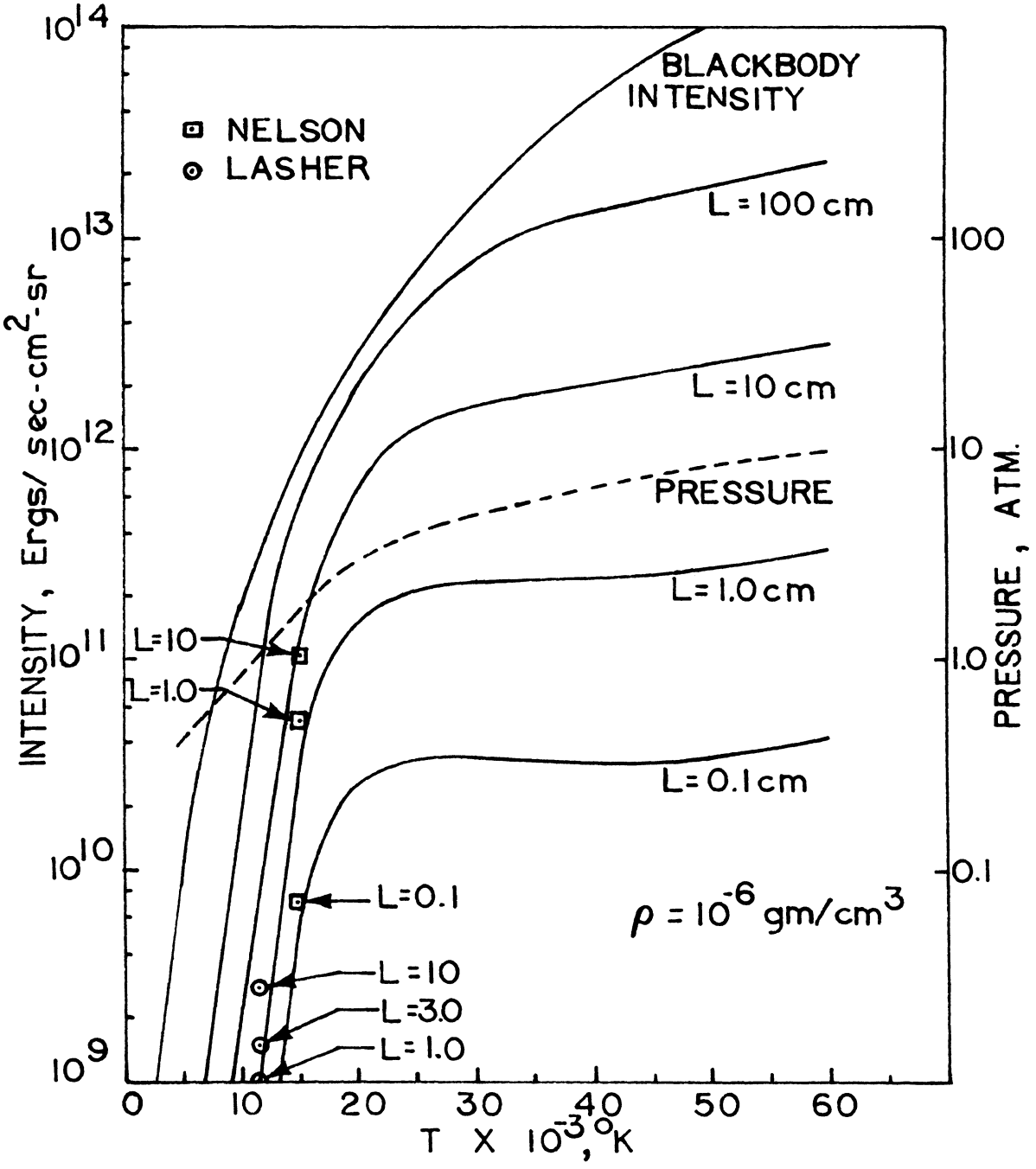

Fig. 19 Temperature distribution of intensity for $\rho = 10^{-6}$

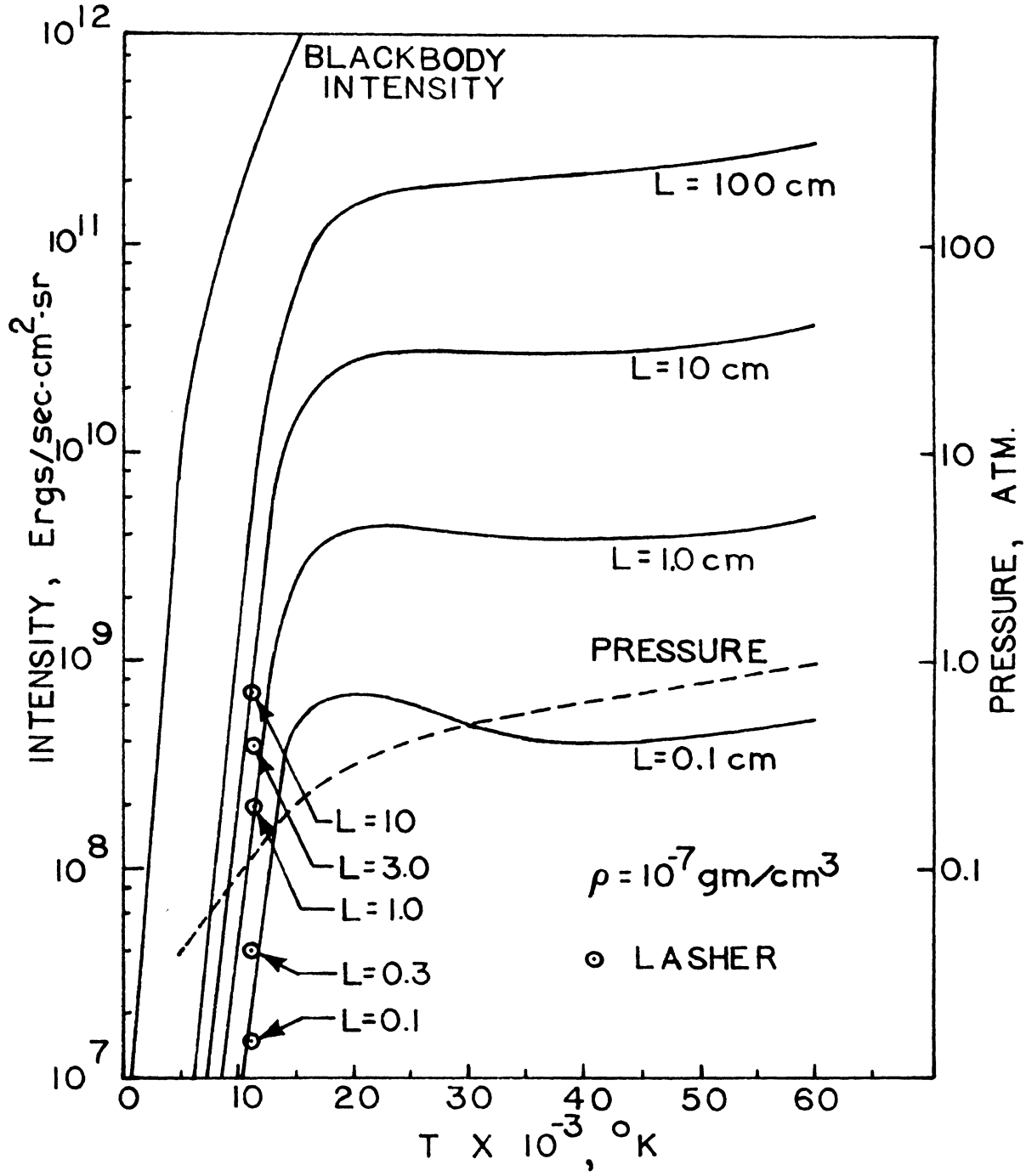

Fig. 20 Temperature distribution of intensity for $\rho = 10^{-7}$

total intensity decreases relative to the Planck function.

For lower densities of 10^{-6} and 10^{-7} gm/cm^3 (Fig. 19 and 20), the intensity varies in a similar manner to that discussed above. However, as the density decreases, the emitted intensity decreases relative to that of a blackbody because of the decrease in hydrogen population.

In Figs. 19 and 20 a deflection point appears in some of the curves. This occurs for a thickness of 0.1 cm in Fig. 19 and for thicknesses of 0.1, 1.0, and 10 cm in Fig. 20. There is less intensity emitted at 40,000°K for these cases than for 20,000°K or 60,000°K. This fact was also seen in Figs. 16 and 17, which caused the curves to intersect. It is due to the trade-off between the shift of population to free and high electronic states and the shift of the maximum of the Planck function to larger frequencies.

2. Comparison with previous results

The radiation from hydrogen plasmas was claculated by Lasher, Wilson, and Grief[9] up to 40,000°K and by Nelson[15] between temperatures of 15,000°K and 33,000°K. The data they obtained is shown on Figs. 18, 19, and 20 by the square (Nelson) and the circular (Lasher et al.) data points.

Results from the Lasher et al. study were obtained at constant pressure. Pressure is shown on the figures for reference to the work of Lasher et al. Their results were for pressures of 0.1, 1.0, and 10.0 atmospheres, and they agree

closely with those of this study except at a density of 10^{-6} gm/cm^3, where they differ by about a factor of two at a plasma thickness of 10.0 cm.

Nelson[15] made his calculations at constant density as was done in the present study. He considered plasma densities of 10^{-4}, 10^{-5}, and 10^{-6} gm/cm^3. Therefore, comparison with his results is limited to Figs. 18 and 19.

The results of this study agree with the previous results of Nelson within about 15% at the points compared. The present study seems to give intensities that are generally slightly higher than those obtained previously by Lasher et al. as well as those of Nelson. This is because the present study predicts an absorption coefficient in the line wing regions to be slightly higher than that predicted by Nelson[15] and Lasher et al.[9]

F. Total Flux

The total radiative flux (ergs/sec-cm^2) is shown as a function of temperature in Fig. 21 at various thicknesses and a density of 10^{-5} gm/cm^3. The Planck function is shown for reference.

The radiative flux is calculated in this study because in the previous work of Lasher et al.[9] and Nelson[15] it was not determined.

The trends are exactly the same for the flux as they were for the intensity at this density. The flux is greater than the intensity by approximately a factor of π. The flux at other densities is also a factor of π times the intensity. When the plasma is optically thick, the flux is exactly π times the

intensity. As the plasma becomes optically thin, the flux deviates slightly from π times the intensity. (See equations 6,7, and 8.)

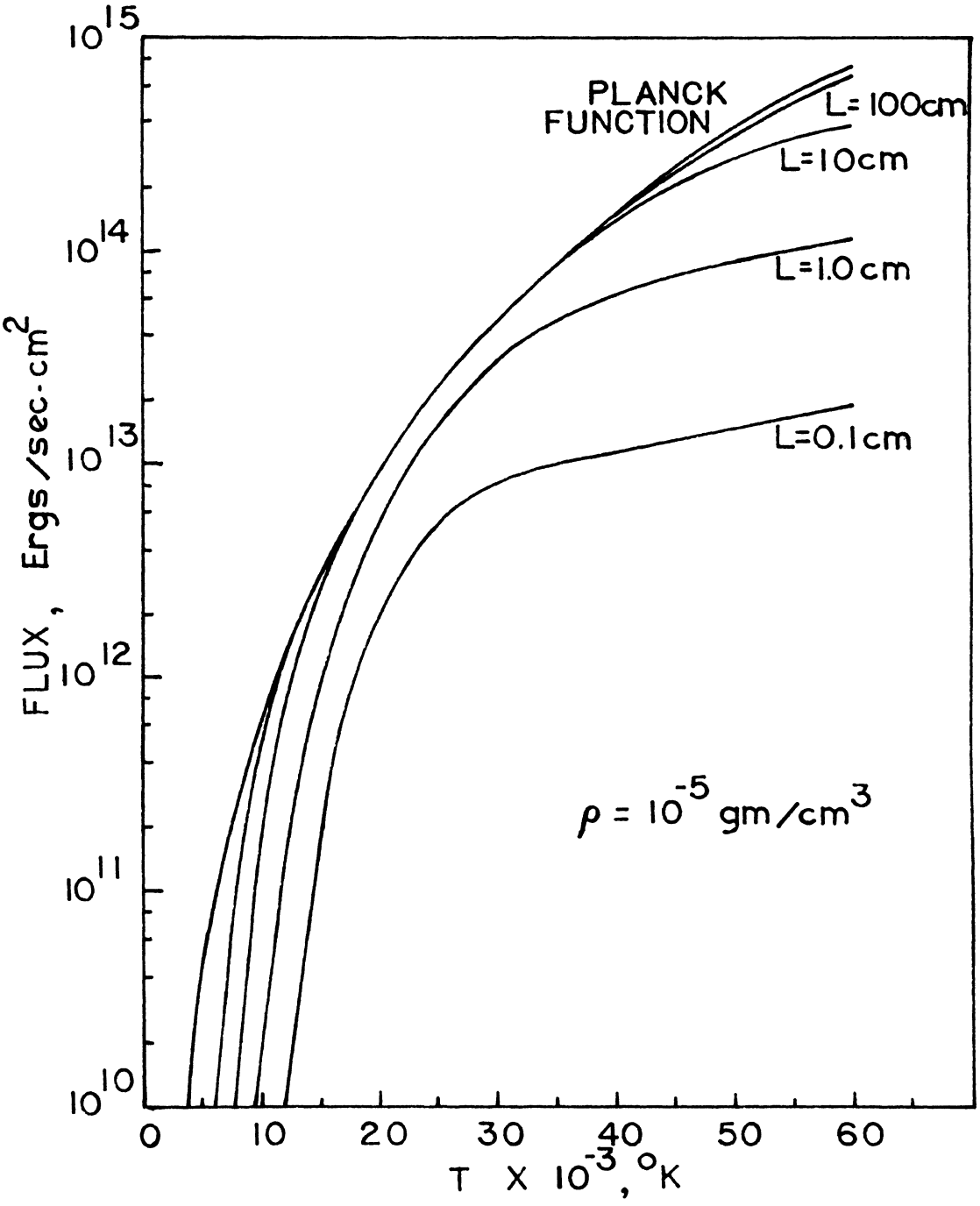

Fig. 21 Temperature distribution of flux

V. SUMMARY AND CONCLUSIONS

The goal of this study was to accurately approximate the radiative absorption coefficient of an isothermal hydrogen plasma while reducing the numerical computer time involved. In this study a step-wise gray approximation was used to approximate the radiative absorption coefficient, with 135 steps being taken in the entire frequency spectrum. The data was presented in graphical and tabular form for various plasma conditions. The plasma was between temperatures of 5000 and 60,000^{o}K, between densities of 10^{-5} and 10^{-7} gm/cm^{3}, and between thicknesses of 0.1 and 100 cm.

Using the step-wise gray absorption coefficient, the radiative flux and intensity were calculated and several trends were noticed. Various numbers of steps were tried with the general trend being more steps increasing the accuracy but at the same time requiring more computer time. Using 135 steps, the numerical computer time required to approximate the absorption coefficient and calculate the intensity and flux was reduced by about a factor of 10 from previous calculations.[15]

The results bring out the importance of the trade-off between the shift of the maximum of the Planck function and the population of the higher electronic states. They show that even though the plasma may radiate as a blackbody in a certain frequency interval, the emitted radiation may be small because the excited states are relatively unpopulated.

At a low density (10^{-7} gm/cm^3), the plasma was seen to be essentially thin because relative few species were present. At a density of 10^{-7} gm/cm^3, it was observed that the intensity remained relatively constant in the temperature range from 20,000°K to 40,000°K.

The results can be extended to include plasmas made up of several species as well as non-isothermal plasmas. When a plasma has several species present, the spectrum is divided into several frequency intervals for each specie and then summed with that of the other species present. By making the frequency intervals very small and letting each be at a slightly different temperature, an arbitrary temperature profile can be approximated to give non-isothermal results.

BIBLIOGRAPHY

1. Griem, H.R. "Stark Broadening of Higher Hydrogen and Hydrogenlike Lines by Electrons and Ions," Astrophysical Journal, 132, 883 (1960).

2. Wilson, K.H. and Hoshizaki, H. "A Study of Superorbital Heating Problems," Vol. I, Lockheed, Preprint No. 4-17-67-11, 1968.

3. Anderson, J.D. "Nongray Radiative Transfer Effects on the Radiating Stagnation Region Shock Layer and Stagnation Point Heat Transfer," NOLTR 67-104, 1967.

4. Sparrow, E.M. and Cess, R.D., Radiation Heat Transfer, Wadsworth, 1970.

5. Aroeste, H. and Benton, W.C. "Emissivity of Hydrogen Atoms at High Temperatures," Journal of Applied Physics 27, 117 (1956).

6. Olfe, D.B., Journal of Quantitative Spectroscopy and Radiative Transfer, 1, 104 (1961).

7. Nelson, H.F. and Goulard, R. "Equilibrium Radiation from Isothermal Hydrogen-Helium Plasmas," Journal of Quantitative Spectroscopy and Radiative Heat Transfer, 8, 1351 (1968).

8. Nelson, H.F. and Crosbie, A.L. "Radiative Flux from Nonisothermal Nongray Atomic Gases," American Institute of Aeronautics and Astronautics, Preprint No. 70-837, 1970.

9. Lasher, L.E., Wilson, K.H., and Grief, R. "Radiation from an Isothermal Hydrogen Plasma at Temperatures up to 40,000°K," Journal of Quantitative Spectroscopy and Radiative Transfer, 7, 305 (1967).

10. Wilson, K.H. "Stagnation Point Analysis of Coupled Viscous-Radiating Flow with Massive Blowing," American Institute Of Aeronautics and Astronautics, Preprint No. 70-203, 1970.

11. Nicolet, W.E. "Advanced Methods for Calculating Radiation Transport in Ablation-Product Contaminated Boundary Layers," NASA CR-1656 (1970).

12. Soshnikov, V.N. "Absolute Intensities of Electronic Transitions in Diatomic Molecults," Soviet Physics, Uspelshi 4, 425 (1961).

13. Zel'dovich, Ya.B. and Raizer, Yu.P., Physics of Shock Waves and High Temperature Hydrogynamic Phenomena, Academic Press, 259, 1966.

14. Nelson, H.F. "Thermodynamic Properties of Hydrogen-Helium Plasmas," University of Missouri-Rolla Report, January, 1971.

15. Nelson, H.F. "Equilibrium Radiation from Isothermal Hydrogen-Helium Slabs," Purdue University Report, July, 1967.

16. Singh, B. "The Influence of a Carbon Ablation Layer on Radiation from a Hydrogen Shock Layer," Master's Thesis, University of Missouri-Rolla, 1970.

VITA

Keith Harlan Browne was born on August 20, 1948, in Springfield, Missouri to Mr. and Mrs. J. Robert Browne. In 1952 he moved to Independence, Missouri where he received his primary and secondary education. His college education was obtained at the University of Missouri-Rolla, in Rolla, Missouri. In May of 1970 he received a Bachelor of Science degree in Mechanical Engineering from the University of Missouri-Rolla.

Following his undergraduate education, he enrolled in June of 1970 in the Graduate School of the University of Missouri-Rolla. His research was supported by NASA grant NGR 26-003-055 from the period of June 1970 to January 1971 and NSF grant GK 10954 during June and July of 1971. He was a graduate assistant during the spring of 1971 in the Department of Mechanical Engineering.

Appendix A

COMPOSITION OF HYDROGEN PLASMA*

To calculate the equilibrium composition of hydrogen plasma at high temperatures, the following reactions must be considered.

$$H_2 \rightleftarrows H + H \qquad (A - 1a)$$

$$H \rightleftarrows P + e \qquad (A - 1b)$$

$$H + e \rightleftarrows H^- \qquad (A - 1c)$$

$$H_2 \rightleftarrows H_2^+ + e \qquad (A - 1d)$$

The total number of hydrogen molecules is

$$N'_{H_2} = \rho / m_{H_2} \qquad (A - 2)$$

where the gas density ρ is assumed to be known. The hydrogen layer temperature is also known from the solutions of Rankine-Hugoniot equations.

* This development closely follows that of Ref. 16.

Let Ψ be the fraction of the molecular hydrogen that has dissociated (Equation A-1a); therefore, the number density of molecular hydrogen is $(1 - \Psi)N'_{H_2}$, while $N_H = 2\Psi N'_{H_2}$, because two hydrogen atoms are formed in each dissociation process.

Let α be the fraction of N_H that exists as protons, then $N_P = 2\alpha\Psi N'_{H_2}$. For each proton that is formed an electron also becomes free; therefore, $N_e = N_P$. The number density of remaining atomic hydrogen is $N_H = 2\Psi(1 - \alpha) N'_{H_2}$.

The negative hydrogen ion is formed by the reaction given in Equation (A - 1c). Let δ be the fraction of atomic hydrogen that exists as the negative hydrogen ion, then $N_{H^-} = \delta(1-\alpha) 2\Psi N'_{H_2}$. The remaining number density of atomic hydrogen is $N_H = (1 - \delta)(1 - \alpha) 2\Psi N'_{H_2}$ and that of the electrons is $N_e = 2\Psi [\alpha - \delta(1 - \alpha)] N'_{H_2}$, because an electron is used for each H^- that is formed.

In addition the molecular ion H_2^+ is formed by the process of Equation (A-1d). Let η be the fraction of H_2 that exists as H_2^+. Then $N_{H_2^+} = \eta(1 - \Psi) N'_{H_2}$ and $N_{H_2} = (1 - \eta)(1 - \Psi) N'_{H_2}$. For each H_2^+ ion that is formed an electron becomes free; therefore, the electron number density becomes $N_e = [(\alpha - \delta)(1 - \alpha)) 2\Psi + \eta(1 - \Psi)] N'_{H_2}$.

In summary, the final number densities are related to the initial number densities as follows:

$$N_{H_2} = (1 - \eta)(1 - \Psi) N'_{H_2} \qquad (A - 3a)$$

$$N_H = 2\Psi(1 - \alpha)(1 - \delta) N'_{H_2} \qquad (A - 3b)$$

$$N_P = 2\alpha\Psi N'_{H_2} \qquad (A - 3c)$$

$$N_{H^-} = 2\Psi\ (1 - \alpha)\delta\ N'_{H_2} \qquad (A - 3d)$$

$$N_{H_2^+} = \eta\ (1 - \Psi)\ N'_{H_2} \qquad (A - 3e)$$

$$N_e = [\,2\Psi\ (\alpha - \delta\,(1 - \alpha) + \eta\,(1 - \Psi)\,]\ N'_{H_2} \qquad (A - 3f)$$

The condition of macroscopic neutrality

$$N_e + N_{H^-} = N_P + N_{H_2^+} \qquad (A - 4)$$

as well as the conservation of nuclei are satisfied identically by the relations of Equation (A - 3).

The equilibrium relationships between the atoms and ions as defined in Equation (A - 1) are given in terms of the complete partition functions as

$$kT\,\frac{N_P N_e}{N_H} = \frac{\alpha P_e}{(1 - \delta)\,(1 - \alpha)} = \frac{Z_P Z_e}{Z_H}\,kT = \beta_3, \qquad (A - 5)$$

$$kT\,\frac{N_H N_H}{N_{H_2}} = \frac{[2\Psi\,(1 - \delta)\,(1 - \alpha)]^2}{(1 - \eta)\,(1 - \Psi)} = \frac{Z_H Z_H}{Z_{H_2} N'_{H_2}} = \beta_4, \qquad (a - 6)$$

$$kT\,\frac{N_H N_e}{N_{H^-}} = \frac{(1 - \delta)P_e}{\delta} = \frac{Z_H Z_e}{Z_{H^-}}\,kT = \beta_5, \qquad (A - 7)$$

and

$$kT\,\frac{N_{H_2^+} N_e}{N_{H_2}} = \frac{\eta\,P_e}{1 - \eta} = \frac{Z_{H_2^+} Z_e}{Z_{H_2}}\,kT = \beta_6, \qquad (A - 8)$$

where the electron pressure P_e is defined as

$$P_e = [\,2\Psi\ (\alpha - \delta(1 - \alpha)) + \eta(1 - \Psi\ )\,]\ N'_{H_2}\ kT. \qquad (A - 9)$$

The set of Equations (A-5) through (A-9) represents five unknowns; α, Ψ, δ, η and P_e, which can be found as functions of temperature and density.

An iterative method is used to solve the set of Equations (A-5) through (A-8). The solution begins by assuming $\delta = \eta = 0$. Thus, Equations (A-5) through (A-9) become

$$\alpha P_e = \beta_3 \quad (1 - \alpha) \qquad (A - 10)$$

$$4\Psi^2 (1 - \alpha)^2 = \beta_4 \quad (1 - \Psi) \qquad (A - 11)$$

$$P_e = 2\Psi \alpha N'_{H_2} kT \qquad (A - 12)$$

Eliminating P_e and Ψ one arrives at an equation in terms of α

$$(1 - \alpha)^4 \left[\frac{\beta_3}{kT\ N'_{H_2}} \right]^2 + \frac{(1 - \alpha)\alpha^2}{2N'_{H_2}} \frac{\beta_3\beta_4}{kT} - \alpha^4\beta_4 = 0 \qquad (A - 13)$$

which can be solved to give the initial value of α, $(\alpha^{(0)})$. Combining Equations (A-10) and (A-12) and using $\alpha^{(0)}$, the initial value of Ψ becomes

$$\Psi^{(0)} = \frac{1 - \alpha^{(0)}}{2(\alpha^{(0)})^2} \quad \frac{\beta_3}{kTN'_{H_2}} \qquad (A - 14)$$

and the other initial values become

$$P_e^{(0)} = 2\Psi^{(0)}\ \alpha^{(0)}\ N'_{H_2}\ kT \qquad (A - 15)$$

$$\delta^{(0)} = \frac{P_e^{(0)}}{P_e^{(0)} + \beta_5} \qquad (A - 16)$$

$$\eta^{(0)} = \frac{\beta_6}{\beta_6 + P_e^{(0)}} \qquad (A - 17)$$

Once the initial values are known the ith value of the variable is arrived at in the following manner.

$$P_e^{(i)} = \left[2\Psi^{(J)} \left[\alpha^{(J)}(1 + \delta^{(J)}) - \delta^{(J)}\right] + \eta^{(J)}(1 - \Psi^{(J)})\right] N_{H_2}' kT \qquad (A - 18)$$

$$\eta^{(i)} = \frac{\beta_6}{\beta_6 + P_e^{(i)}} \qquad (A - 19)$$

$$\delta^{(i)} = \frac{P_e^{(i)}}{P_e^{(i)} + \beta_5} \qquad (A - 20)$$

$$\alpha^{(i)} = \frac{\beta_3(1 - \delta^{(i)})}{P_e^{(i)} + \beta_3(1 - \delta^{(i)})} \qquad (A - 21)$$

$$\Psi^{(i)} = \frac{X^{(i)}}{2} \left[1 + \frac{4}{X^{(i)}}\right]^{1/2} - 1 \qquad (A - 22)$$

where

$$X^{(i)} = \frac{\beta_4(1 - \eta^{(i)})}{4(1 - \delta^{(i)})(1 - \alpha^{(i)})^2} \qquad (A - 23)$$

and

$$J = i - 1$$

The iteration is continued until successive values of P_e are the same to a specified number of places.

Figures A-1, A-2, and A-3 show the equilibrium composition of hydrogen plasmas as a function of temperature for $\rho = 10^{-5}$, $\rho = 10^{-6}$, and $\rho = 10^{-7}$ grams/cm^3. At a given density as temperature increases, the number density of atomic hydrogen rapidly decreases initially and then becomes almost constant at higher temperatures. The number density of electrons and protons initially increases and then becomes almost constant at higher temperatures when the plasma is fully ionized. Note that molecular hydrogen is unimportant at temperatures above 10,000°K.

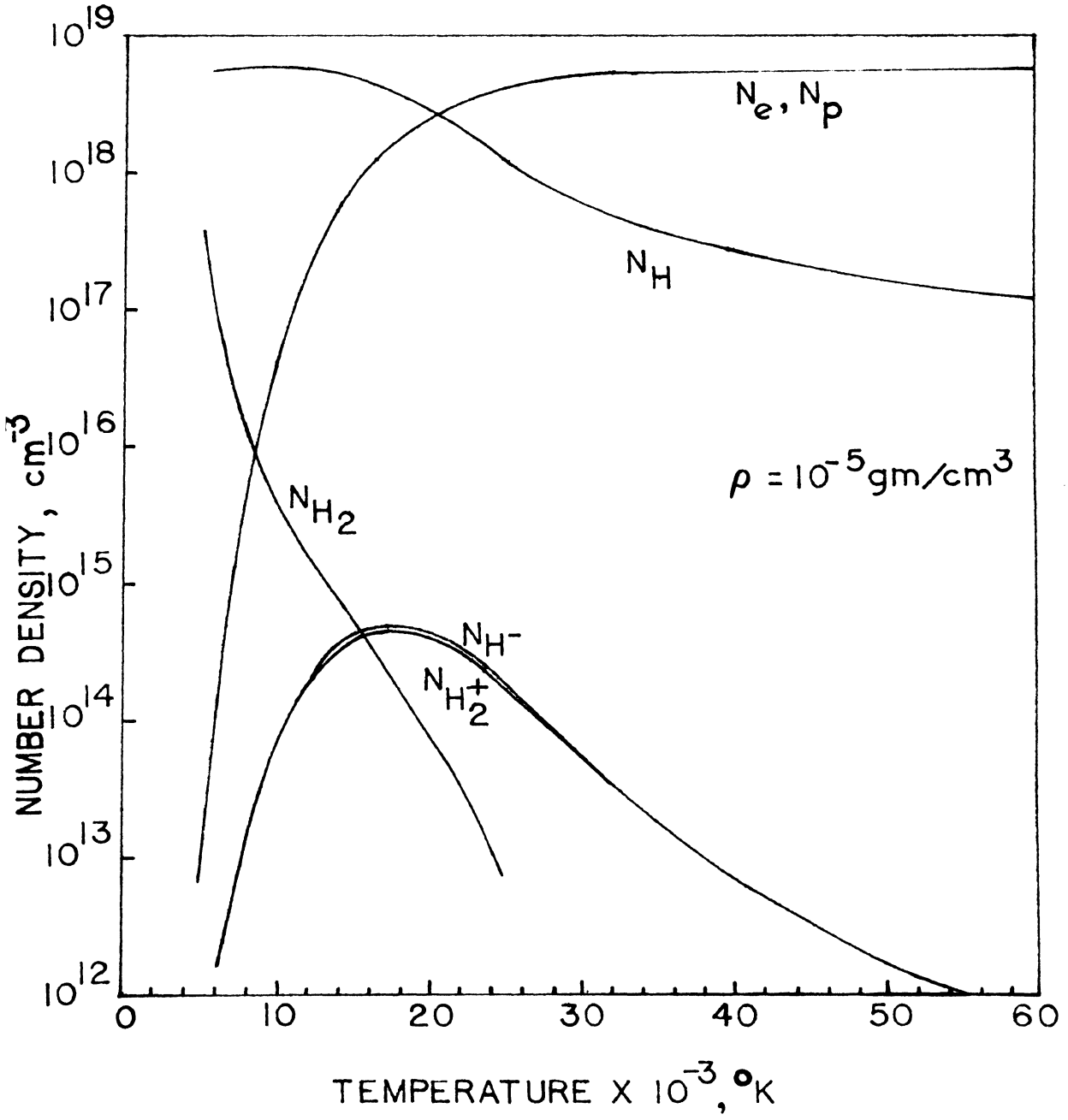

Fig. A-1. Equilibrium composition of Hydrogen for $\rho = 10^{-5}$

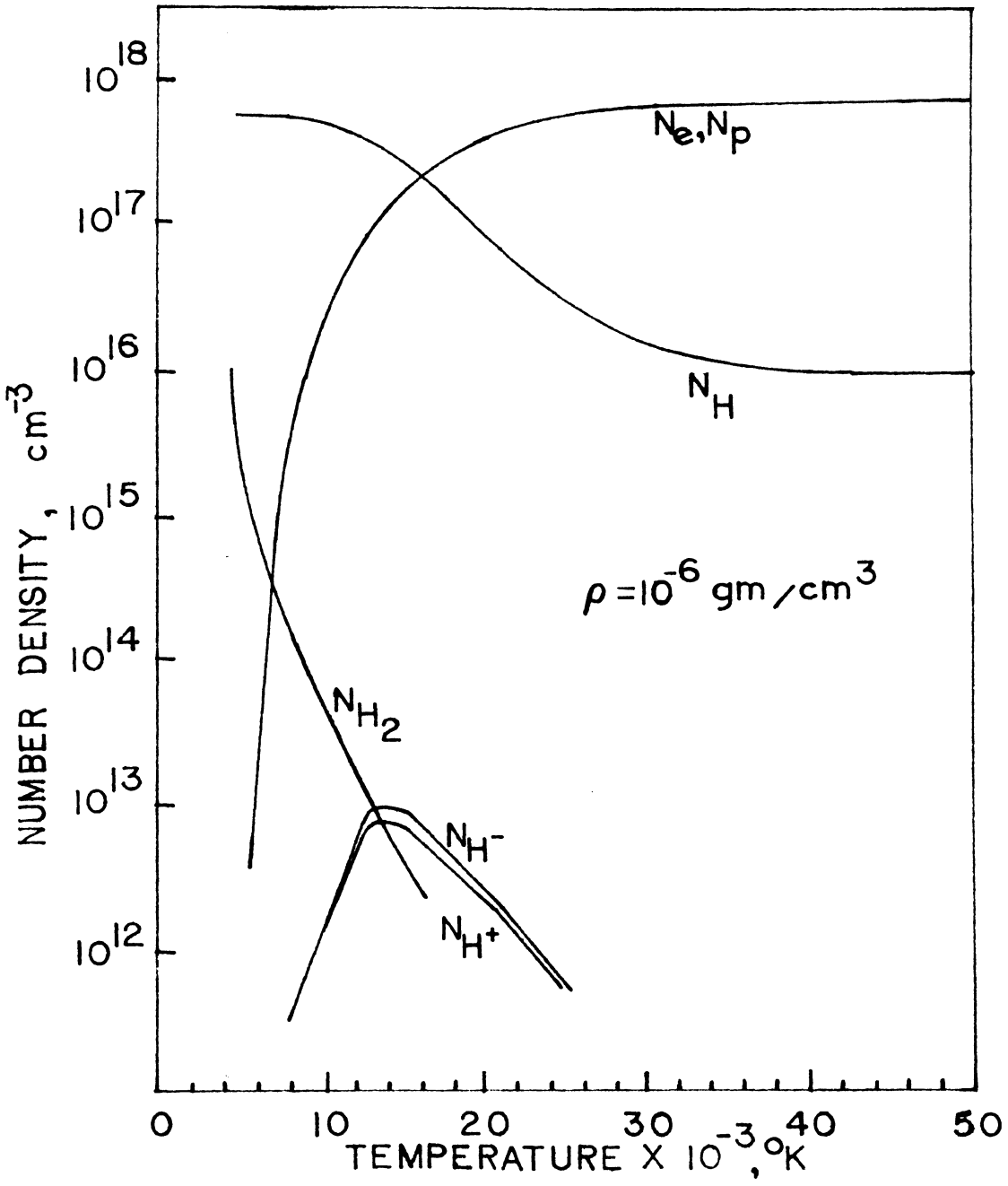

Fig. A-2. Equilibrium composition of Hydrogen for $\rho = 10^{-6}$

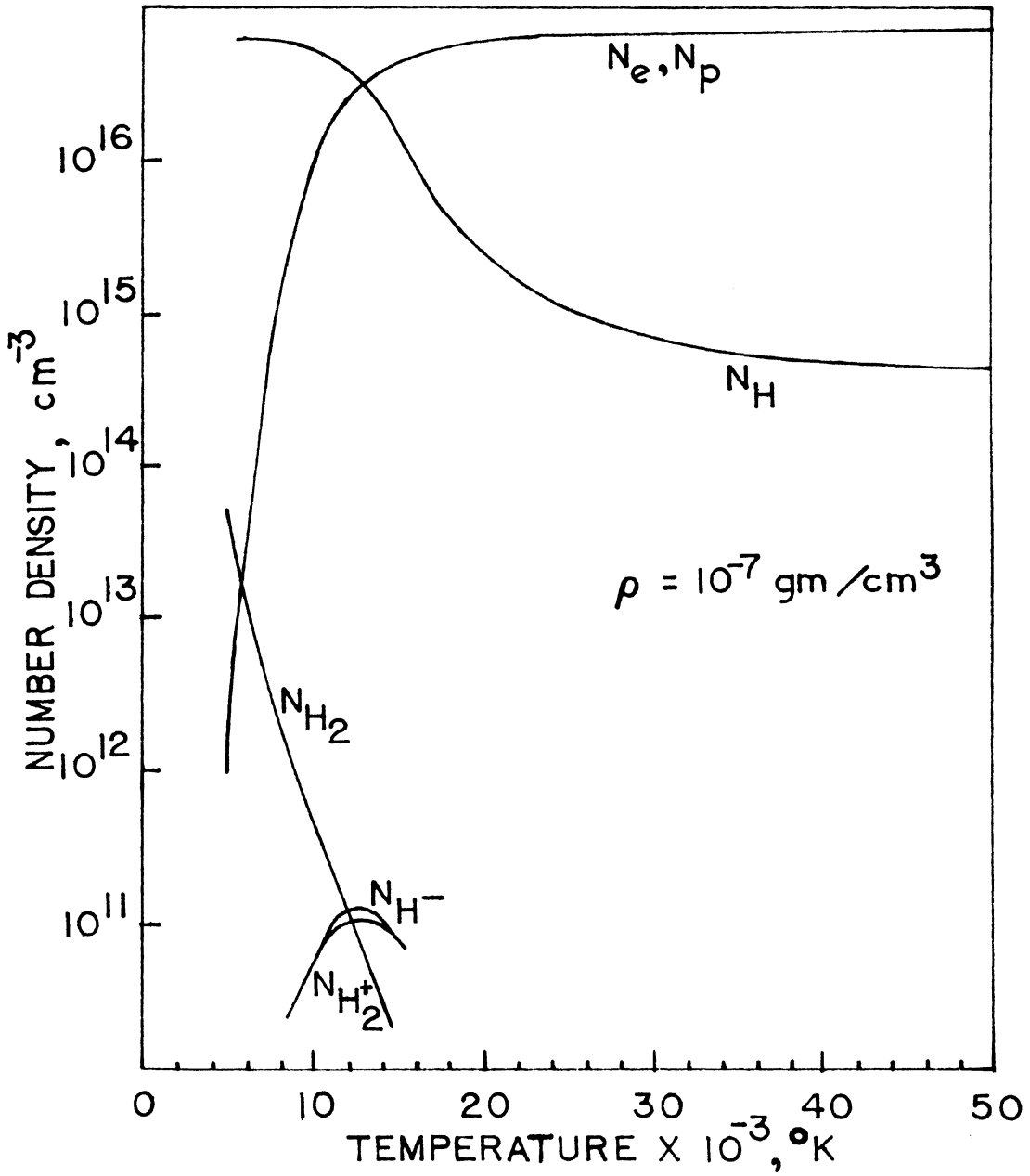

Fig. A-3. Equilibrium composition of Hydrogen for $\rho = 10^{-7}$

APPENDIX B

TABLES OF INTENSITY AND FLUX

TABLE B-I

RADIATIVE FLUX AT $\rho = 10^{-5}$ gm/cm^3

FLUX (ERGS/SEC-CM^2)

THICKNESS (cm)	0.1	1.0	10.0	100.0
TEMPERATURE (°K)				
5000	1.29×10^{6}	1.07×10^{7}	4.89×10^{7}	1.44×10^{8}
10000	2.53×10^{9}	1.99×10^{10}	1.41×10^{11}	4.81×10^{11}
15000	2.21×10^{11}	9.17×10^{11}	2.53×10^{12}	2.87×10^{12}
20000	1.88×10^{12}	5.51×10^{12}	8.95×10^{12}	9.07×10^{12}
25000	5.23×10^{12}	1.50×10^{13}	2.19×10^{13}	2.21×10^{13}
30000	8.15×10^{12}	3.00×10^{13}	4.54×10^{13}	4.59×10^{13}
35000	1.00×10^{13}	4.70×10^{13}	8.33×10^{13}	8.50×10^{13}
40000	1.15×10^{13}	6.23×10^{13}	1.36×10^{14}	1.45×10^{14}
50000	1.47×10^{13}	8.94×10^{13}	2.70×10^{14}	3.49×10^{14}
60000	1.89×10^{13}	1.17×10^{14}	4.08×10^{14}	6.80×10^{14}

TABLE B-II

RADIATIVE INTENSITY AT $\rho = 10^{-5}$ gm/cm^3

	INTENSITY (ERGS/SEC-CM^2-SR)			
THICKNESS (cm)	0.1	1.0	10.0	100.0
TEMPERATURE (^{o}K)				
5000	2.12×10^5	1.99×10^6	1.20×10^7	3.20×10^7
10000	4.61×10^8	3.47×10^9	2.81×10^{10}	1.33×10^{11}
15000	4.86×10^{10}	2.06×10^{11}	7.18×10^{11}	9.13×10^{11}
20000	4.40×10^{11}	1.41×10^{12}	2.79×10^{12}	2.89×10^{12}
25000	1.15×10^{12}	4.04×10^{12}	6.90×10^{12}	7.05×10^{12}
30000	1.65×10^{12}	7.82×10^{12}	1.42×10^{13}	1.46×10^{13}
35000	1.92×10^{12}	1.13×10^{13}	2.58×10^{13}	2.70×10^{13}
40000	2.14×10^{12}	1.41×10^{13}	4.12×10^{13}	4.61×10^{13}
50000	2.65×10^{12}	1.90×10^{13}	7.45×10^{13}	1.10×10^{14}
60000	3.36×10^{12}	2.47×10^{13}	1.05×10^{14}	2.07×10^{14}

TABLE B-III

RADIATIVE FLUX AT $\rho = 10^{-6}$ gm/cm^3

	FLUX (ERGS/SEC-CM^2)			
THICKNESS (cm)	0.1	1.0	10.0	100.0
TEMPERATURE (^{o}K)				
5000	1.97×10^4	1.96×10^5	1.89×10^6	1.56×10^7
10000	2.78×10^8	1.75×10^9	1.37×10^{10}	1.00×10^{11}
15000	3.15×10^{10}	1.52×10^{11}	6.55×10^{11}	2.14×10^{12}
20000	1.42×10^{11}	1.72×10^{11}	2.82×10^{12}	7.22×10^{12}
25000	1.85×10^{11}	1.17×10^{12}	5.86×10^{12}	1.57×10^{13}
30000	1.87×10^{11}	1.30×10^{12}	8.15×10^{12}	2.93×10^{13}
35000	1.86×10^{11}	1.37×10^{12}	9.64×10^{12}	4.54×10^{13}
40000	1.88×10^{11}	1.45×10^{12}	1.09×10^{13}	5.98×10^{13}
50000	2.07×10^{11}	1.71×10^{12}	1.38×10^{13}	8.48×10^{13}
60000	2.48×10^{11}	2.12×10^{12}	1.78×10^{13}	1.11×10^{14}

TABLE B-IV

RADIATIVE INTENSITY AT $\rho = 10^{-6}$ gm/cm^3

INTENSITY (ERGS/SEC-CM^2-SR)

THICKNESS (cm)	0.1	1.0	10.0	100.0
TEMPERATURE (°K)				
5000	3.14×10^{3}	3.13×10^{4}	3.11×10^{5}	2.90×10^{6}
10000	5.46×10^{7}	3.21×10^{8}	2.38×10^{9}	1.95×10^{10}
15000	6.35×10^{9}	3.29×10^{10}	1.45×10^{11}	5.64×10^{11}
20000	2.79×10^{10}	1.64×10^{11}	6.76×10^{11}	2.00×10^{12}
25000	3.49×10^{10}	2.27×10^{11}	1.33×10^{12}	4.24×10^{12}
30000	3.44×10^{10}	2.40×10^{11}	1.66×10^{12}	7.67×10^{12}
35000	3.35×10^{10}	2.47×10^{11}	1.84×10^{12}	1.09×10^{13}
40000	3.33×10^{10}	2.55×10^{11}	2.02×10^{12}	1.34×10^{13}
50000	3.60×10^{10}	2.92×10^{11}	2.49×10^{12}	1.79×10^{13}
60000	4.28×10^{10}	3.56×10^{11}	3.16×10^{12}	2.32×10^{13}

TABLE B-V

RADIATIVE FLUX AT $\rho = 10^{-7}$ gm/cm^3

FLUX (ERGS/SEC-CM^2)

THICKNESS (cm)	0.1	1.0	10.0	100.0
TEMPERATURE (°K)				
5000	3.06×10^{2}	3.01×10^{3}	2.99×10^{4}	2.98×10^{5}
10000	3.72×10^{7}	2.01×10^{8}	1.22×10^{9}	9.46×10^{9}
15000	2.27×10^{9}	1.29×10^{10}	7.08×10^{10}	3.21×10^{11}
20000	3.81×10^{9}	2.33×10^{10}	1.47×10^{11}	7.99×10^{11}
25000	3.42×10^{9}	2.39×10^{10}	1.60×10^{11}	1.06×10^{12}
30000	2.95×10^{9}	2.26×10^{10}	1.63×10^{11}	1.15×10^{12}
35000	2.65×10^{9}	2.19×10^{10}	1.66×10^{11}	1.23×10^{12}
40000	2.53×10^{9}	2.20×10^{10}	1.71×10^{11}	1.32×10^{12}
50000	2.70×10^{9}	2.45×10^{10}	1.97×10^{11}	1.61×10^{12}
60000	3.26×10^{9}	2.97×10^{10}	2.43×10^{11}	2.05×10^{12}

TABLE B-VI

RADIATIVE INTENSITY AT $\rho = 10^{-7}$ gm/cm^3

INTENSITY (ERGS/SEC-CM^2-SR)

THICKNESS (cm)	0.1	1.0	10.0	100.0
TEMPERATURE (°K)				
5000	4.94×10^{1}	4.81×10^{2}	4.77×10^{3}	4.76×10^{4}
10000	7.62×10^{6}	3.99×10^{7}	2.26×10^{8}	1.64×10^{9}
15000	4.60×10^{8}	2.52×10^{9}	1.48×10^{10}	6.93×10^{10}
20000	7.31×10^{8}	4.49×10^{9}	2.81×10^{10}	1.73×10^{11}
25000	6.21×10^{8}	4.43×10^{9}	3.00×10^{10}	2.02×10^{11}
30000	5.10×10^{8}	4.07×10^{9}	3.00×10^{10}	2.10×10^{11}
35000	4.44×10^{8}	3.87×10^{9}	3.00×10^{10}	2.19×10^{11}
40000	4.17×10^{8}	3.82×10^{9}	3.05×10^{10}	2.32×10^{11}
50000	4.41×10^{8}	4.16×10^{9}	3.48×10^{10}	2.74×10^{11}
60000	5.32×10^{8}	5.02×10^{9}	4.26×10^{10}	3.44×10^{11}

APPENDIX C

LISTING OF COMPUTER PROGRAM

The numerical computer program is listed on the following pages. The input data consisted of the plasma temperature and density, the beginning and end cuts on the spectral range of frequency, the mass fraction of hydrogen, the number of cuts, ten plasma shock layer thicknesses, and the spectral location of each cut.

The program is written in the language of Fortran IV. It was run on an IBM System/360, model 50 computer.

```
      COMMON/MIMIM/JED,JLN,ASTART
      COMMON/CONST1/XNH,XNP,XNHE1,XNHE2,XNHE3,XNE,PEB,PB,XNH2,XNH2P,XNHM
      COMMON/CONST2/ ELM,PM,HM,HEM,HEM2,HEM3,H2M,H2PM,HMM,PC
      COMMON/CONST3/XK,H,C,RH,RHE,XIH,XIHE1,XIHE2,XDISS,W5,W6
      COMMON/CONST4/SE,CER,AO,C1
      COMMON/PART1/ DE,NMH,NMHE1,NMHE2
      COMMON/PART2/ ZZ1,ZZ2,ZZ3
      COMMON/IONED/JHY,JHE,JHEII,JM,LM,LINE,JEDGE
      COMMON/ONE/VL(2,4,12),WLL(2,4,12),VN(2,6),WLN(2,6),CX(6),CY(6)
      COMMON/ TWO / GX(6),X1,Y1
      COMMON/T3/XNN(2,12),XIIL,XIINTS,XLO,XHE(26),FLX,FLXL
      COMMON/FOUR/LINEHY(2,4,12),ANM(2,4,12),PI
      COMMON/ SIX / WLLH(50),WLNH(5),WLL1(34),WLN1(13),WLL2(50),WLN2(5)
      COMMON/SEVEN/STEM,DHVKT,MAX(2)
      COMMON/TEN/CONSTA,EBC
      COMMON/AVEONE/CUT(120),BK(120),NCUT,TEMPD
      DIMENSION XLO(10)
C
C                   INITIAL INPUT
C
    1 READ (1,2,END=99999) TEMP,RHO,HV1,HV2,DHV,F
      READ(1,5)IW,ISTOP,NCUT,EPS
      READ(1,3)(XLO(M),M=1,10)
C        IF IW EQ 0, DOES NOT WRITE ANY OF THE LONG TABLE
C              HVKT1 IS GREATER THAN FIRST EDGE
C              HVKT1 IS GREATER THAN FIRST LINE
    5 FORMAT(3I4,1E13.6)
    2 FORMAT(5E13.6,F7.3)
    3 FORMAT(10F7.2)
      READ(1,9)(CUT(J),J=1,NCUT)
    9 FORMAT(9F8.4)
      FLX=0.
      XIINTS=0.
      WRITE(3,4)
    4 FORMAT(1H1,20X,10HINPUT DATA/20X,29HTEMP  RHO    HV1    HV2    DHV   F/
     $20X,17HIW ISTOP NCUT EPS/20X,13HXLO * * * XLO)
      WRITE(3,2) TEMP,RHO,HV1,HV2,DHV,F
      WRITE(3,5)IW,ISTOP,NCUT,EPS
      WRITE(3,3)(XLO(M),M=1,10)
      WRITE(3,9)(CUT(J),J=1,NCUT)
C
C                   INITIALIZATION
```

```
BLI=0.0
TEMD=TEMP
TEMPD=TEMP
JEDGE=1
IEND=0
INPUT=-1
PI=3.141593
CER=2.81785E-13
BC=1.013246E+06
AC=5.29172E-09
C=2.997930E+10
SE=4.80286E-10
XK=1.38044E-16
XKEV=8.6164E-05
HVKT1=HV1/(XKEV*TEMP)
HVKT2=HV2/(XKEV*TEMP)
H=6.62517E-27
C1=SE*SE/H
HM=1.6734E-24
RH=109677.6
RHE=109737.3
ELM=9.1055E-28
PM=1.67239E-24
HEM=6.6470E-24
HEM2=6.6460E-24
HEM3=HEM2-ELM
H2M=2.*HM
H2PM=H2M-ELM
HMM=HM+ELM
XDISS=7.16E-12
W5=6.2187E+03
W5=W5*C*H
W6=2.13794E+04
W6=W6*C*H
CONSTA=1.0E+08*C*H/(XK*TEMP)
EBC=2.*(XK*TEMP)**4/(H*(H*C)**2)
CALL COMP9( 0005,TEMP,E,RHO,LABEL,0.0)
JHY=5
IF(NMH.LT.5) JHY=NMH
JHEII=5
IF(NMHE2.LT.5) JHEII=NMHE2
MAX(1)=12
MAX(2)=12
IF(NMH.LT.12) MAX(1)=NMH
IF(NMHE2.LT.12) MAX(2)=NMHE2
ED=DE/1.6021E-12
```

```
      WRITE(3,60) ED,NMH,NMHE1,NMHE2
   60 FORMAT(9X,10HDENERGY EV,5X,3HNMH,5X,5HNMHE1,5X,5HNMHE2/10X,F10.6,5
     1X,I3,6X,I3,6X,I3)
      WRITE(3,53)
   53 FORMAT(25X25H**  FINAL COMPOSITION  **/8X4HTEMP7X2HNE10X2HNP10X2HN
     1H10X2HH29X3HH2P10X2HHM/20X2HHE9X3HHE29X3HHE39X3HPEB10X2HPB/)
      WRITE(3,62)TEMP,XNE,XNP,XNH,XNH2,XNH2P,XNHM,XNHE1,XNHE2,XNHE3,PEB,
     1PB
   62 FORMAT(5X,F10.0,1P6E12.4/15X,1P6E12.4)
      CALL EDGE(TEMP)
      CALL HEBFF(INPUT,V,TEMP,XLK)
      CALL HMBF(INPUT,TEMP,WL,ABSC)
      WRITE(3,600) JHY,JHE,JHEII
  600 FORMAT(20X,6I4)
      RR1=RH*C*H/(XK*TEMP)
      RR2=4.*RR1*RHE/RH
      DO 799 K=1,12
      XNN(1,K)=0.
      XNN(2,K)=0.
      SN=K
      EN1=RR1*(1.-1./SN/SN)
      IF(EN1.GT.60.) GO TO 800
      IF(K.GT.MAX(1)) GO TO 800
      XNN(1,K)=XNH*2.*SN*SN*EXP(-EN1)/ZZ1
  800 EN2=RR2*(1.-1./(SN*SN))
      IF(EN2.GT.60.) GO TO 799
      IF(K.GT.MAX(2)) GO TO 799
      XNN(2,K)=XNHE2*2.*SN*SN*EXP(-EN2)/ZZ3
  799 CONTINUE
      WRITE(3,801)(XNN(1,K),K=1,12)
  801 FORMAT(/20X,28HPOPULATION OF THE HYD LEVELS/6E14.6/6E14.6)
      WRITE(3,802)(XNN(2,K),K=1,12)
  802 FORMAT(/20X,28HPOPULATION OF THE HE2 LEVELS/6E14.6/6E14.6)
      CALL  LYMAN(IZ,J,INPUT,TEMP,F,V,XLK)
      CALL BALMER(IZ,J,INPUT,TEMP,F,V,XLK)
      CALL PASCHN(IZ,J,INPUT,TEMP,F,V,XLK)
      CALL BRACKT(IZ,J,INPUT,TEMP,F,V,XLK)
      IF(F.LT.999) CALL HE1BB(INPUT,TEMP,WL,XLK)
      CALL OPTHIN(TEMP,F)
      CALL DELTWL(INPUT,IEND,EPS,F,HVKT2,A,DELTAS,DELTA)
      A=HVKT1
      IBACK=0
C
C                    MAIN CALCULATION
C
      INPUT=0
      IF(IW.GT.0) WRITE(3,6)IW
    6 FORMAT(/2X,5HIW = ,I6/)
```

```
      DO 878 M=1,10
      XIINTS=0.
      FLX=0
      BLI=0.
      WRITE(3,101)
  101 FORMAT(4X,2HWL,9X,2HEV,8X,1HA,9X,2HTA,9X,2HBB,9X,2HBI,9X,2HDF,
     $9X,2HFT,9X,2HDI,9X,1HI,10X,3HTXL)
      DELTA=(CUT(1)-CUT(2))/(XKEV*TEMP)
      A=HVKT1
      K=1
   51 A=A-DELTA
      TAC=BK(K)
      AA=0.5*(CUT(K)+CUT(K+1))/(XKEV*TEMP)
      CALL BLBOD(AA,BLACK)
      BLACK1=2.*PI*BLACK
      TXL=TAC*XLO(M)
      CALL SPE3(TXL,SE3,ETXL)
      DF=BLACK1*SE3
C       E3 FUNCTION RETURNS(1-EXP(-X)   AS E-XL TO SAVE CUMPUTER TIME
      DI=BLACK*(ETXL)
  201 XIINTS=DELTA*DI+XIINTS
      FLX=DELTA*DF+FLX
      IF(IW.EQ.0) GO TO 79
      WL=CONSTA/A
      EV=A*XKEV*TEMP
   77 WRITE(3,18)WL,EV,A,TAC,BLACK,BLI,DF,FLX,DI,XIINTS,TXL
   18 FORMAT(1X,F10.3,F10.5,9(1PE11.3))
   79 BLACK2=PI*BLACK
C        USE PI*BLACK SINCE ONLY CALCULATING ONE SIDED FLUX  SIG*T**4/2
      BLI=DELTA*BLACK+BLI
      K=K+1
      IF (K.EQ.NCUT) GO TO 114
      DELTA=(CUT(K)-CUT(K+1))/(XKEV*TEMP)
      GO TO 51
C
C                   FINAL OUTPUT
C
  114 WRITE(3,13)XLO(M),FLX
   13 FORMAT(/30X,34HINTEGRATED FLUX (ERGS/(CM**2 SEC))/20X,10HTHICKNESS
     1 ,1PE14.5//20X,10HTOTAL FLUX,1PE14.5)
      TOTAL=1.8048E-05*TEMP**4
      TOTF=TOTAL*PI
      WRITE (3,21) TOTF
   21 FORMAT (/10X,'BLACKBODY FLUX = ',E14.6,' ERG/(SEC/CM2)')
      WRITE(3,19)TOTAL
   19 FORMAT(/10X,18HSIG(T4)  INTENSITY,E14.6,21H ERG/(SEC CM2 STRAD))
      WRITE(3,24) BLI
   24 FORMAT(/10X,24HINTEGRATED BLACKBODY IS ,E14.6)
```

```
      BBMAX=1275 *40000 /TEMP
      WRITE(3,30) BBMAX
   30 FORMAT(20X,29HWL OF BBMAX PER UNIT FREQ. IS,F10.2)
      WRITE(3,20)XLO(M),XIINTS
   20 FORMAT(/30X,38HINTEGRATED INTENSITY ERGS/(CM2 SEC SR)/20X,10HTHICK
     1NESS ,1PE14.5/20X,10HTOTAL INTS,1PE14.5)
  878 CONTINUE
      IF(ISTOP.GT.0) GO TO 1
99999 STOP
      END




      SUBROUTINE ABSCOF(INPUT,TEMP,F,A,BBAC,CAC,TAC,DELTAS,DELTA)
C
C        THIS SUBROUTINE CALCULATES ABSORBTION COEFF. AND DELTA
C
      DIMENSION XKBB(2)
      COMMON/CONST1/XNH,XNP,XNHE1,XNHE2,XNHE3,XNE,PEB,PB,XNH2,XNH2P,XNHM
      COMMON/CONST2/ EM,PM,HM,HEM,HEM2,HEM3,H2M,H2PM,HMM,PC
      COMMON/CONST3/XK,H,C,RH,RHE,XIH,XIHE1,XIHE2,XDISS,W5,W6
      COMMON/PART1/ DE,NMH,NMHE1,NMHE2
      COMMON/IONED/JHY,JHE,JHEII,JM,LM,LINE,JEDGE
      COMMON/ONE/VL(2,4,12),WLL(2,4,12),VN(2,6),WLN(2,6),CX(6),CY(6)
      COMMON/T3/XNN(2,12),XIIL,XIINTS,XLO,XHE(26),FLX,FLXL
      COMMON/SEVEN/STEM,DHVKT,MAX(2)
C
C                    MAIN CALCULATION
C
      V=A*XK*TEMP/H
      WL=1.0E+08*C/V
      XKBB(1)=0.
      XKBB(2)=0.
      XKBB3=0.
      XKHMS=0.
      IZ=0
   20 IZ=IZ+1
      MA=MAX(IZ)
C
C                    CALLS LINES
C
      IF(F.LT..001.AND.IZ.EQ.1) GO TO 505
      IF(MAX(IZ).LT.2) GO TO 505
   99 DO 100 J=2,MA
      XLK=0.
```

```
      CALL LYMAN (IZ,J,INPUT,TEMP,F,V,XLK)
  100 XKBB(IZ)=XKBB(IZ)+XLK
      IF(MAX(IZ).LT.3) GO TO 505
      DO 500 J=3,MA
      XLK=0.
      CALL BALMER(IZ,J,INPUT,TEMP,F,V,XLK)
  500 XKBB(IZ)=XKBB(IZ)+XLK
      IF(MAX(IZ).LT.4) GO TO 505
      DO 502 J=4,MA
      XLK=0.
      CALL PASCHN(IZ,J,INPUT,TEMP,F,V,XLK)
  502 XKBB(IZ)=XKBB(IZ)+XLK
      IF(MAX(IZ).LT.5) GO TO 505
      DO 504 J=5,MA
      XLK=0.
      CALL BRACKT(IZ,J,INPUT,TEMP,F,V,XLK)
  504 XKBB(IZ)=XKBB(IZ)+XLK
  505 IF(IZ.EQ.1.AND.F.LE..999) GO TO 20
      IF(F.LT..999) CALL HE1BB(INPUT,TEMP,WL,XKBB3)
      INPUT=INPUT+1
      BBAC=XKBB(1)+XKBB(2)+XKBB3
C
CC                    CALLS CONTINUUM
C
      XKHC1=0.
      XKHC2=0.
      XKHE1=0.
      IF(F.GE..001) CALL HYBFF(V,TEMP,XKHC1)
      IF(F.LE..999) CALL HE2BFF(V,TEMP,XKHC2)
      IF(F.LE..999) CALL HEBFF(INPUT,V,TEMP,XKHE1)
      CAC=XKHC1*XNN(1,1)*HM+XKHC2*XNN(2,1)*HEM2+XKHE1*XHE(1)*HEM
C
CC                    STIMULATED EMISSION FACTOR
C
      STEM=1.
      IF (A.LT.20.) STEM=1.-EXP(-A)
      IF(F-.001) 50,55,55
   55 CALL HMBF(INPUT,TEMP,WL,XKHM)
      XKHMS=XNE*PEB*PO*XKHM
      CALL H2PBF(TEMP,WL,XKH2)
      TEMD=TEMP
      CALL H2WERN(WL,TEMD,XKWERN)
      CALL H2LYMN(WL,TEMD,XKLYMN)
      CALL H2PHOT(WL,TEMD,XKPHOT)
      BBAC=BBAC+XKWERN+XKLYMN+XKPHOT
      CAC=CAC+XKH2*XNH*XNP
   50 BBAC=BBAC*STEM
      CAC=CAC*STEM+XKHMS
      TAC=CAC+BBAC
      RETURN
      END
```

```
      SUBROUTINE ARLENE(F,ALIN,GA,SL)
C
C        CALCULATES AVERAGE VALUE OF ABSORPTION COEFFICIENT
C
C     ***************************************************
C     **  TAC       HAS UNITS OF INVERSE CM.   ***********
C     **  CONTK     HAS UNITS OF INVERSE CM.   ***********
C     **  BOUNDK    HAS UNITS OF INVERSE CM.   ***********
C     **  AA        HAS UNITS OF HV/KT         ***********
C     **  CUT(J)    HAS UNITS OF EV            ***********
C     **  ALIN(K)   HAS UNITS OF HV/KT         ***********
C     **  EVLIN     HAS UNITS OF EV            ***********
C     **  GA        HAS UNITS OF HV/KT         ***********
C     **  GEV       HAS UNITS OF EV            ***********
C     **  HEV       HAS UNITS OF EV-SEC        ***********
C     **  D1 & D2   HAVE UNITS OF EV           ***********
C     ***************************************************
      COMMON/AVEONE/CUT(120),BK(120),NCUT,TEMP
      COMMON/IONED/JHY,JHE,JHEII,JM,LM,LINF,JEDGE
      COMMON/CONST3/XK,H,C,RH,RHE,XIH,XIHE1,XIHE2,XDISS,W5,W6
      DIMENSION ALIN(120),GA(120),SL(120)
      XKEV=8.6164E-05
      HEV=4.1354E-15
      KS=1
      J=2
      AA=CUT(1)/(XKEV*TEMP)
      INPUT=1
      TEMPD=TEMP
      CALL ABSCOE(INPUT,TEMPD,F,AA,DUM,DUM1,TAC,D5,D6)
   20 CC=TAC
      VVCUT=(CUT(J)+CUT(J-1))/2.
      AA=VVCUT/(XKEV*TEMP)
      CALL ABSCOE(INPUT,TEMPD,F,AA,DUM,DUM1,TAC,D5,D6)
      BG=TAC
      AA=CUT(J)/(XKEV*TEMP)
      CALL ABSCOE(INPUT,TEMPD,F,AA,DUM,DUM1,TAC,D5,D6)
      T=TAC
      CONTKA=0.
      CONTKS=0.
   92 BOUNDK=0.0
      DO 50 K=KS,LM
      KSAVE=K
      EVLIN=ALIN(K)*XKEV*TEMPD
      IF (EVLIN.LT.CUT(J)) GO TO 51
      D1=ALIN(K)*XKEV*TEMPD-CUT(J)
      D2=CUT(J-1)-ALIN(K)*XKEV*TEMPD
      GEV=GA(K)*XKEV*TEMP
      BOUNDK=HEV*SL(K)*(ATAN(D2/GEV)+ATAN(D1/GEV))/
     1(3.141593*(D1+D2))+BOUNDK
   50 CONTINUE
```

```
 51 IF (BOUNDK-3.) 77,77,78
 77 CONTKS=(CC+4.*BG+T)/6.
    GO TO 33
 78 CONTKA=0.5*(T+CC)
 33 BK(J-1)=CONTKS+CONTKA+BOUNDK
    WRITE(3,101)BK(J-1),CUT(J),CUT(J-1)
101 FORMAT(5X,18HAVG. ABS. COEF. IS,E14.6,17H IN INTERVAL FROM,
   $E14.6,3H TO,E14.6,3H EV)
    KS=KSAVE
    J=J+1
    IF(J.LE.NCUT) GO TO 20
    RETURN
    END
```

```
    FUNCTION ASOLVE(B3P,B4P)
    DOUBLE PRECISION B3P,B4P,A,F,ONE,DA
    ONE=1.0
    N=0
    K=0
    A=1.0
    DA=.10
  1 F=(ONE-A)**4*B3P**2-A**4*B4P+.5*(ONE-A)*A*A*B3P*B4P
    K=K+1
    IF(K-12)2,18,18
 18 WRITE(3,19)K,N,A,DA,F,B3P,B4P
 19 FORMAT(2X,17HK.GT.12 IN ASOLVE,2I4,3E12.4,2D12.4)
    STOP
  2 IF(F-0.00000) 3,10,4
  3 A=A-DA
    GO TO 1
  4 A=A+DA
    K=0
    N=N+1
    DA=DA/10.
    A=A-DA
    IF(N.LT.5) GO TO 1
 10 ASOLVE=A
    RETURN
    END
```

```
      SUBROUTINE BALMER(IZ,J,INPUT,TEMP,F,V,XLK)
C        CALLS BALMER LINES
      SWING(QQQQQ1,QQQQQ2)=QQQQQ1*QQQQQ1/(QQQQQ2*QQQQQ2)
      SHAPE(QCCIM,QCCII,QDALF,QALFIM,QALFII)=QCCIM+(QCCII-QCCIM)*(QDALF-
     1QALFIM)/(QALFII-QALFIM)
      COMMON/CONST1/XNH,XNP,XNHE1,XNHE2,XNHE3,XNE,PEB,PR,XNH2,XNH2P,XNHM
      COMMON/CONST2/ ELM,PM,HM,HEM,HEM2,HEM3,H2M,H2PM,HMM,PC
      COMMON/CONST3/XK,H,C,RH,RHE,XIH,XIHE1,XIHE2,XDISS,W5,W6
      COMMON/CONST4/SE,CER,A0,C1
      COMMON/ONE/VL(2,4,12),WLL(2,4,12),VN(2,6),WLN(2,6),CX(6),CY(6)
      COMMON/T3/XNN(2,12),XIIL,XIINTS,XLO,XHE(26),FLX,FLXL
      COMMON/FOUR/LINEHY(2,4,12),ANM(2,4,12),PI
      COMMON/SIXX/HWIDTH(2,4,12),HWH(50),HW1(35),HW2(50)
      COMMON/BLUE/STRENG(2,4,12)
      DIMENSION FNM(10),ALF(4,19),SA(3,3,19),SB(3,3,19),SC(3,3,19)
      DIMENSION SD(3,3,19),S23(19),S24(19),S25(19),S26(19),NL(6)
      IF(INPUT.GE.0) GO TO 10
      READ(1,91)(FNM(I),I=1,10)
   91 FORMAT(6E11.4)
      WRITE (3,6)
    6 FORMAT (/,20X,12HBALMER LINES,/20X,6HFNM(I))
      WRITE (3,7) (FNM(I),I=1,10)
    7 FORMAT (2X,1P10E11.3)
      DO 12 K=1,4
      READ(1,9)(ALF(K,I),I=1,19)
   12 WRITE(3,99)(ALF(K,I),I=1,19)
    9 FORMAT(19F4.3)
   99 FORMAT(19F6.3)
      DO 210 NT=1,3
      DO 211 NN=1,3
      READ(1,19)(SA(NT,NN,I),I=1,19)
      READ(1,19)(SB(NT,NN,I),I=1,19)
      READ(1,19)(SC(NT,NN,I),I=1,19)
  211 READ(1,19)(SD(NT,NN,I),I=1,19)
  210 CONTINUE
   19 FORMAT(10F8.2)
      DO 216 NT=1,3
      DO 216 NN=1,3
  216 WRITE(3,218) (SA(NT,NN,I),I=1,16)
      DO 217 NT=1,3
      DO 217 NN=1,3
  217 WRITE(3,218) (SB(NT,NN,I),I=1,16)
      DO 219 NT=1,3
      DO 219 NN=1,3
  219 WRITE(3,218) (SC(NT,NN,I),I=1,16)
      DO 221 NT=1,3
```

```
      DO 221 NN=1,3
  221 WRITE(3,218) (SD(NT,NN,I),I=1,16)
  218 FORMAT(16F8.3)
      XN=XNE
      CALL GRIEM(TEMP,XN,1.0E+16,1.0E+17,1.0E+18,3,14,SA,S23)
      CALL GRIEM(TEMP,XN,1.0E+15,1.0E+16,1.0E+17,3,19,SB,S24)
      CALL GRIEM(TEMP,XN,1.0E+15,1.0E+16,1.0E+17,3,13,SC,S25)
      CALL GRIEM(TEMP,XN,1.0E+14,1.0E+15,1.0E+16,3,10,SD,S26)
      FO=SE*2.61*XNE**.6667
      CS=SE*SE/(C*ELM)
      NL(3)=14
      NL(4)=19
      NL(5)=13
      NL(6)=10
      N=2
      S=N
      CORR=H/(C*XK*TEMP)
      IZ=1
      IF(IZ.EQ.1.AND.F.LT..001) GO TO 112
  110 IF(IZ.EQ.2.AND.F.GT..999) GO TO 112
      LINEHY(IZ,2,3)=-1
      LINEHY(IZ,2,4)=-1
      LINEHY(IZ,2,5)=-1
      LINEHY(IZ,2,6)=-1
      HWIDTH(IZ,2,3)=FO*VL(IZ,2,3)**2/(PI*S23(1)*1.0E+08)*CORR
      HWIDTH(IZ,2,4)=FO*VL(IZ,2,4)**2/(PI*S24(1)*1.0E+08)*CORR
      HWIDTH(IZ,2,5)=FO*VL(IZ,2,5)**2/(PI*S25(1)*1.0E+08)*CORR
      HWIDTH(IZ,2,6)=FO*VL(IZ,2,6)**2/(PI*S26(1)*1.0E+08)*CORR
      WRITE(3,913) (HWIDTH(IZ,2,II),II=3,6)
  913 FORMAT(2X,38HHALFWIDTHS OF 2-3 TO 2-6 LINES (HV/KT),4E14.6)
      DO 111 NP=3,12
      SP=NP
      NP1=NP-2
      CF=FNM(NP1)
      STRENG(IZ,N,NP)=PI*SE*SE*CF*XNN(IZ,N)/(ELM*C)
C
C     STRENG IS THE LINE STRENGTH IN UNITS OF INVERSE CM-SEC
C
  111 ANM(IZ,N,NP)=8.*((S*PI*VL(IZ,N,NP)*SE)/(SP*C))**2*CF/(ELM*C)
      WRITE(3,169) (STRENG(IZ,2,MM),MM=3,6)
  169 FORMAT(2X,42HLINE STRENGTHS OF 2-3 TO 2-6 LINES (HV/KT),4E14.6)
  112 IZ=IZ+1
      IF(IZ.EQ.2) GO TO 110
      DO 31 J=7,12
      NP=J
      CFNM=FNM(J-2)
   31 CALL HILINE(INPUT,IZ,TEMP,V,N,NP,CFNM,F,XLK)
      GO TO 20
```

```
   10 N=2
      NP=J
      IF(LINEHY(IZ,N,NP).GT.0) GO TO 20
      J1=J-2
      XLK=0.
      IF(J-6) 50,50,100
   50 NMAX=NL(J)
      DALF=1.0E+08*C*ABS(V-VL(IZ,N,NP))/(F0*VL(IZ,N,NP)**2)
      IF(DALF.GT.ALF(J1,NMAX)) GO TO 300
      DO 51 I=1,NMAX
      II=I
      IF(DALF.LT.ALF(J1,I)) GO TO 52
   51 CONTINUE
   52  IM=II-1
      IF(NP.EQ.3) SHAP=SHAPE(S23(IM),S23(II),DALF,ALF(J1,IM),ALF(J1,II))
      IF(NP.EQ.4) SHAP=SHAPE(S24(IM),S24(II),DALF,ALF(J1,IM),ALF(J1,II))
      IF(NP.EQ.5) SHAP=SHAPE(S25(IM),S25(II),DALF,ALF(J1,IM),ALF(J1,II))
      IF(NP.EQ.6) SHAP=SHAPE(S26(IM),S26(II),DALF,ALF(J1,IM),ALF(J1,II))
      GO TO 44
C        WING LINE SHAPES  (GRIEM'S BOOK PP 93)
  300 IF(NP.EQ.3) SHAP=S23(NMAX)*SWING(ALF(J1,NMAX),DALF)
      IF(NP.EQ.4) SHAP=S24(NMAX)*SWING(ALF(J1,NMAX),DALF)
      IF(NP.EQ.5) SHAP=S25(NMAX)*SWING(ALF(J1,NMAX),DALF)
      IF(NP.EQ.6) SHAP=S26(NMAX)*SWING(ALF(J1,NMAX),DALF)
   44 XLK=SHAP*CS*FNM(J1)*XNN(IZ,N)*C*PI*1.0E+08/(F0*VL(IZ,N,NP)**2)
      GO TO 20
  100 CFNM=FNM(J1)
      CALL HILINE(INPUT,IZ,TEMP,V,N,NP,CFNM,F,XLK)
C        XLK IS IN UNITS OF 1/CM
   20 RETURN
      END
```

```
      SUBROUTINE BLBOD (A,B)
C     EBC CONTAINS CONSTANTS TO MAKE B(V)DV = B(A)DA
C        CALCULATES BLACKBODY FUNCTION (B) IN ERGS/(CM**2 SEC STERAD)
      COMMON/TEN/CONSTA,EBC
      F=A
      IF (F-.05) 30,30,20
   20 F=EXP(F)-1.
   30 B=EBC*A*A*A/F
      RETURN
      END
```

```
      SUBROUTINE BRACKT(IZ,J,INPUT,TEMP,F,V,XLK)
C        CALLS BRACKETT  LINES
      COMMON/CONST2/ ELM,PM,HM,HEM,HEM2,HEM3,H2M,H2PM,HMM,PO
      COMMON/CONST3/XK,H,C,RH,RHE,XIH,XIHE1,XIHE2,XDISS,W5,W6
      COMMON/CONST4/SE,CER,AO,C1
      COMMON/ONE/VL(2,4,12),WLL(2,4,12),VN(2,6),WLN(2,6),CX(6),CY(6)
      COMMON/FOUR/LINEHY(2,4,12),ANM(2,4,12),PI
      COMMON/T3/XNN(2,12),XIIL,XIINTS,XLO,XHE(26),FLX,FLXL
      COMMON/BLUE/STRENG(2,4,12)
      DIMENSION FNM(8)
      IF(INPUT.GE.C) GO TO 10
      READ(1,9)(FNM(I),I=1,8)
    9 FORMAT(6E11.4)
      WRITE (3,6)
    6 FORMAT (/,20X,13HBRACKET LINES,/20X,6HFNM(I))
      WRITE (3,7) (FNM(I),I=1,8)
    7 FORMAT (2X,1P8E11.3)
      N=4
      S=N
      DO 112 IZ=1,2
      DO 111 NP=5,12
      SP=NP
      NP1=NP-4
      CF=FNM(NP1)
      STRENG(IZ,N,NP)=PI*SE*SE*CF*XNN(IZ,N)/(ELM*C)
C
C     STRENG IS THE LINE STRENGTH IN UNITS OF INVERSE CM-SEC
C
  111 ANM(IZ,N,NP)=8.*((S*PI*VL(IZ,N,NP)*SE)/(SP*C))**2*CF/(ELM*C)
  112 CONTINUE
      DO 31 J=5,12
      NP=J
      CFNM=FNM(J-4)
   31 CALL HILINE(INPUT,IZ,TEMP,V,N,NP,CFNM,F,XLK)
      GO TO 20
   10 N=4
      NP=J
      IF(LINEHY(IZ,N,NP).GT.C) GO TO 20
      J1=J-4
      CFNM=FNM(J1)
      CALL HILINE(INPUT,IZ,TEMP,V,N,NP,CFNM,F,XLK)
C        XLK IS IN UNITS OF 1/CM
   20 RETURN
      END
```

```
      SUBROUTINE COMP9(EPS,TEMP,F,RHO,LABEL,WDEB)
C     THIS PROGRAM CALCULATES THE COMPOSITION OF A  HYDROGEN AND HELIUM SLAB
      COMMON/SOLV1 / A7,A8,A9,ALF,BETA,GAMMA,XNH2PP,XNHEP
      COMMON/SOLV2/ B4,B5,B6,DELTA,ZETA,ETA
      COMMON/PART1/ DE,NMH,NMHE1,NMHE2
      COMMON/PART2/ ZH,Z1,Z2
      COMMON/CONST3/XK,H,C,RH,RHE,XIH,XIHE1,XIHE2,XDISS,W5,W6
      COMMON/CONST2/ EM,PM,HM,HEM,HEM2,HEM3,H2M,H2PM,HMM,PO
      COMMON/CONST1/XNH,XNP,XNHE1,XNHE2,XNHE3,XNE,PEB,PB,XNH2,XNH2P,XNHM
      DOUBLE PRECISION A7,A8,A9,ALF,BETA,GAMMA,ONE
      DOUBLE PRECISION B4, B5,B6,DELTA,ZETA,ETA
      ISW= 1
      LABEL=C
      ONE=1.00000
      PI=3.1415927
      C1=XK/H
      C2=EM/H
      C3=(6.2831854*C1*C2)**1.5
      TK=TEMP*XK
      XNH2PP=F*RHO/H2M
      XNHEP=0.
      IF(F.GT.1.0E-10) GO TO 48
      XNHEP=RHO/HEM
      GO TO 52
   48 XNHEP=H2M*XNH2PP*(1.-F)/(F*HEM)
   52 F1=C3*(HEM2*TEMP/HEM)**1.5*XK*TEMP
      F2=C3*(HEM3*TEMP/HEM2)**1.5*XK*TEMP
      F3=C3*(PM*TEMP/HM)**1.5*XK*TEMP
      G4=C3*(HM*TEMP/(2.*EM))**1.5*TK
      G5=C3*(HM*TEMP/HMM)**1.5*TK
      G6=C3*(H2PM*TEMP/H2M)**1.5*TK
      DEB1=SQRT(XK*TEMP/(4.*PI))/4.80286E-10
      DEBRAD=DEB1/(SQRT(3.*XNH2PP+XNHEP))
      KOUNT=1
   54 DEBRA1=DEBRAD
      DE=4.80286E-10*4.80286E-10/DEBRAD
      XIH=2.178E-11-DE
      XIHE1=3.938E-11-DE
      XIHE2=8.716E-11-DE*2.
      C4=XIH/XK
      C5=XIHE1/XK
      C6=XIHE2/XK
      ZH =PARTH(TEMP,0)
      Z1 =ZHE1(TEMP,0)
```

```
      Z2 =ZHE2(TEMP,C)
      ZH2=PARH2(TEMP,C)
      ZH2P=PARH2P(TEMP,C)
      A7=2.*Z2*F1*EXP(-C5/TEMP)/Z1
      A8=2.*F2*EXP(-C6/TEMP)/Z2
      A9=2.*F3*EXP(-C4/TEMP)/ZH
      B4=G4*(ZH*EXP(-XDISS/(2.*TK)))**2/ZH2
      B5=2.*G5*EXP(-W5/TK)*ZH
      B6=2.*G6*ZH2P*EXP(-C4/TEMP)*EXP((W6-XDISS)/TK)/ZH2
      CALL SOLVE(ISW,EPS,TEMP,PE,ITT)
      XNE=(2.*ZETA*(ALF-DELTA*(ONE-ALF))+ETA*(ONE-ZETA))*XNH2PP
     1+BETA*(1.+GAMMA)*XNHEP
      XH2=2.*ZETA*XNH2PP
      XNP=ALF*XH2
      XNHM=DELTA*(ONE-ALF)*XH2
      XNH2P=ETA*(ONE-ZETA)*XNH2PP
      XNHE2=BETA*(ONE-GAMMA)*XNHEP
      XNHE3=BETA*GAMMA*XNHEP
      DEBCAL=DEB1/(SQRT(XNE+XNP+XNHE2+4.*XNHE3+XNHM+XNH2P))
      ADEB=ABS(DEBCAL-DEBRA1)/DEBCAL
      IF(ADEB-EPS)56,56,55
   55 DEBRAD=DEBCAL+WDEB*(DEBRA1-DEBCAL)
      KOUNT=KOUNT+1
      IF(KOUNT-20) 57,57,58
   58 ISW=-1
      WRITE(3,90)KOUNT,DEBCAL,DEBRA1,XNE,XNP,XNHM,XNH2P,XNHE2,XNHE3,TEMP
     1,RHO,ADEB,EPS
   90 FORMAT(2X,17HCOMP9 KOUNT.GT.20,I4,1P8E12.4/19X,1P4E12.4)
   57    IF(KOUNT.LE.25) GO TO 54
      LABEL=1
      RETURN
   56 XNH=(ONE-DELTA)*(ONE-ALF)*XH2
      XNH2=(ONE-ETA)*(ONE-ZETA)*XNH2PP
      XNHE1=(ONE-BETA)*XNHEP
      PER=PE/P0
      DP=-(4.80286E-10**3/3.)*SQRT(PI/(XK*TEMP))*(DEB1/DEBCAL)**3
      DPR=-DP/P0
      PR=(XNE+XNP+XNH+XNH2P+XNHM+XNH2+XNHE1+XNHE2+XNHE3)*TK/P0+DPR
      CH=XNE+XNP+XNHE2+XNHE3+XNH+XNHE1+XNH2P+XNH2+XNHM
      CH1=1./(8.*PI*DEBCAL**3)
      IF(CH1.GT.CH) WRITE(3,60)
   60 FORMAT(10X,24HDEBYE THEORY IS NOT GOOD)
      RETURN
      END
```

```
      SUBROUTINE DELTWL(INPUT,IEND,EPS,F,HVKT2,A,DELTAS,DELTA)
C
C        THIS SUBROUTINE CHECKS JUMP OF INTERVAL DELTA AND END CONDITION
C
      COMMON/PART1/ DE,NMH,NMHE1,NMHE2
      COMMON/IONED/JHY,JHE,JHEII,JM,LM,LINE,JEDGE
      COMMON/ONE/VL(2,4,12),WLL(2,4,12),VN(2,6),WLN(2,6),CX(6),CY(6)
      COMMON/ SIX / WLLH(50),WLNH(5),WLL1(34),WLN1(13),WLL2(50),WLN2(5)
      COMMON/SEVEN/STEM,DHVKT,MAX(2)
      COMMON/TEN/CONSTA,EBC
      COMMON/SIXX/GHVKT(2,4,12),HWH(50),HW1(35),HW2(50)
      COMMON/MIMIM/DELMIN,DIN,ICAN,JED,JLN,IBACK,ASTART
      COMMON/HELONE/ NMAX,AHE(34),XNU(34),WLHE(34),IWM(34)
      COMMON/BEC/SLNH(50),SLNHE1(34),SLNHE2(50)
      DIMENSION WE(25),WLIN(120),GA(120),SL(120)
      JLN= 1
C
CCC                  INITIALIZATION
C
      JED=1
C                    SETTING UP THE ARRAY OF IONIZATION EDGES
C
      JM=0
      IF(F-.01) 11,14,14
   11 DO 12 J=1,JHE
      JM=JM+1
   12 WE(JM)=WLN1(J)
      DO 13 J=1,JHEII
      JM=JM+1
   13 WE(JM)=WLN2(J)
      GO TO 20
   14 DO 15 J=1,JHY
      JM=JM+1
   15 WE(JM)=WLNH(J)
      IF(F-.99) 11,11,20
C
CC                   SETTING UP THE ARRAY OF LINES
C
   20 LM=0
      IF(F-.01) 21,26,26
   21 DO 22 J=1,34
      IF(IWM(J).LT.0) GO TO 22
      LM=LM+1
      SL(LM)=SLNHE1(J)
      GA(LM)=HW1(J)
      WLIN(LM)=WLL1(J)
   22 CONTINUE
   23 DO 24 J=1,38
```

```
      IF(WLL2(J).LT.5.) GO TO 24
      LM=LM+1
      SL(LM)=SLNHE2(J)
      GA(LM)=HW2(J)
      WLIN(LM)=WLL2(J)
   24 CONTINUE
   25 GO TO 29
   26 DO 27 J=1,38
      IF(WLLH(J).LT.5.) GO TO 27
      LM=LM+1
      SL(LM)=SLNH(J)
      GA(LM)=HWH(J)
      WLIN(LM)=WLLH(J)
   27 CONTINUE
C
CC                    ORDERING THE IONIZATION EDGES
C
   28 IF(F-.99) 21,21,29
   29 DO 300 I=2,JM
      K=I-1
      J=I
  309 IF(WE(J)-WE(K)) 310,320,320
  310 A=WE(J-1)
      WE(J-1)=WE(J)
      WE(J)=A
  320 IF(K.EQ.1) GO TO 300
      K=K-1
      J=J-1
      GO TO 309
  300 CONTINUE
C
CC                    ORDERING THE LINES
C
      KOU=1
      IF(LM.LT.2) GO TO 401
      DO 400 I=2,LM
      K=I-1
      J=I
  409 IF(WLIN(J)-WLIN(K)) 410,420,420
  410 A=WLIN(J-1)
      WLIN(J-1)=WLIN(J)
      WLIN(J)=A
      B=GA(J-1)
      GA(J-1)=GA(J)
      GA(J)=B
      B=SL(J-1)
      SL(J-1)=SL(J)
      SL(J)=B
```

```
C
C       SL HAS UNITS OF INVERSE CM-SEC
C
  420 IF(K.EQ.1) GO TO 400
      K=K-1
      J=J-1
      GO TO 409
  400 CONTINUE
  401 KOU=KOU+1
      IF (KOU.EQ.2) WRITE (3,1000)
      IF (KOU.EQ.3) WRITE (3,1001)
      WRITE(3,1)(WLIN(J),J=1,LM)
      IF (KOU.EQ.2) WRITE (3,1002)
      IF (KOU.EQ.3) WRITE (3,1003)
 1000 FORMAT (/,' WAVELENGTHS OF EXISTING LINES (ANGSTROMS)')
 1001 FORMAT (/,' HV/KT POSITIONS OF EXISTING LINES')
 1002 FORMAT (/,' WAVELENGTHS OF EXISTING EDGES (ANGSTROMS)')
 1003 FORMAT (/,' HV/KT POSITIONS OF EXISTING EDGES')
      WRITE(3,1)(WE(J),J=1,JM)
    1 FORMAT(10E12.4)
      IF (KOU.GE.3) GO TO 511
      DO 200 J=1,LM
  200 WLIN(J)=CONSTA/WLIN(J)
      DO 201 J=1,JM
  201 WE(J)=CONSTA/WE(J)
      GO TO 401
C       WE AND WLIN ARE NOW IN HV/KT UNITS
  511 CALL ARLENE (F,WLIN,GA,SL)
      RETURN
      END
```

```
      SUBROUTINE EDGE(TEMP)
C        IONIZATION EDGES OF HYDROGEN AND IONIZED HELIUM
      COMMON/PART1/ DE,NMH,NMHE1,NMHE2
      COMMON/CONST3/XK,H,C,RH,RHE,XIH,XIHE1,XIHE2,XDISS,W5,W6
      COMMON/ONE/VL(2,4,12),WLL(2,4,12),VN(2,6),WLN(2,6),CX(6),CY(6)
      COMMON/ TWO / GX(6),X1,Y1
```

```
      COMMON/ SIX / WLLH(50),WLNH(5),WLL1(34),WLN1(13),WLL2(50),WLN2(5)
      DIMENSION AN(2,6),AL(2,4,12),EVN(2,6),EVL(2,4,12)
      X1=(RH*C*H-DE)/(XK*TEMP)
      Y1=(4.*RHE*C*H-2.*DE)/(XK*TEMP)
      AND=XK*TEMP/H
      RHS=X1*AND
      RHES=Y1*AND
      HEV=4.1354E-15
      DO 100 J=1,5
      SN=J
      S2=SN*SN
      CY(J)=Y1/S2
      CX(J)=X1/S2
      GX(J)=2.*RHS/S2
      VN(2,J)=RHES/S2
      VN(1,J)=RHS/S2
      EVN(2,J)=VN(2,J)*HEV
      EVN(1,J)=VN(1,J)*HEV
      WLN(2,J)=C*1.0E+08/VN(2,J)
      WLN(1,J)=C*1.0E+08/VN(1,J)
      AN(2,J)=VN(2,J)/AND
  100 AN(1,J)=VN(1,J)/AND
      CX(6)=X1/36.
      CY(6)=Y1/36.
      VN(1,6)=0.
      VN(2,6)=0.
      DO 98 L=1,2
      DO 98 J=1,4
      DO 98 K=1,12
      EVL(L,J,K)=0.0
      AL(L,J,K)=0.0
      VL(L,J,K)=0.
   98 WLL(L,J,K)=0.
      WRITE(3,6)
    6 FORMAT(/20X,20HHYD IONIZATION EDGES)
      WRITE(3,51)(EVN(1,J),J=1,5)
   51 FORMAT(5X,17HFREQ. EDGES (EV) ,5E14.6)
      WRITE (3,4) (AN(1,J),J=1,5)
    4 FORMAT(5X,17HFREQ. EDGES (A)  ,5E14.6)
      WRITE(3,7)(WLN(1,J),J=1,5)
    7 FORMAT(5X,17HWAVE LENGTH EDGES,5E14.6)
      WRITE(3,8)
    8 FORMAT(/20X,24HHELIUM2 IONIZATION EDGES)
      WRITE(3,51)(EVN(2,J),J=1,5)
      WRITE (3,4) (AN(2,J),J=1,5)
      WRITE(3,7)(WLN(2,J),J=1,5)
      DO 99 J=1,4
```

```
      JJ=J+1
      DO 99 K=JJ,12
      SN=J
      SNP=K
      EX=1./SN/SN-1./SNP/SNP
      VL(1,J,K)=RH*C*EX
      VL(2,J,K)=4.*RHE*C*EX
      EVL(1,J,K)=VL(1,J,K)*HEV
      EVL(2,J,K)=VL(2,J,K)*HEV
      WLL(2,J,K)=C*1.0E+08/VL(2,J,K)
      WLL(1,J,K)=C*1.0E+08/VL(1,J,K)
      AL(1,J,K)=VL(1,J,K)/AND
   99 AL(2,J,K)=VL(2,J,K)/AND
      WRITE(3,5)
    5 FORMAT(/20X16HHYD LINE CENTERS)
      WRITE(3,1)
    1 FORMAT(/8X1H2 0X1H3 0X1H4 0X1H5 0X1H6 0X1H7 0X1H8 0X1H9 9X2H10 9X2H1
     $19X2H12)
      KS=1
  201 WRITE(3,13)
   13 FORMAT(/20X,14HELECTRON VOLTS)
      DO 250 J=1,4
  250 WRITE(3,2)J,(EVL(KS,J,K),K=2,12)
      WRITE(3,18)
   18 FORMAT(/20X,11HHV/KT UNITS)
      DO 200 J=1,4
  200 WRITE (3,2) J,(AL(KS,J,K),K=2,12)
    2 FORMAT(I4,11E11.4)
      WRITE(3,3)
    3 FORMAT(/20X,10HWAVELENGTH)
      DO 101 J=1,4
  101 WRITE(3,2) J,(WLL(KS,J,K),K=2,12)
      WRITE(3,9)
    9 FORMAT(/20X20HHELIUM2 LINE CENTERS)
      KS=KS+1
      IF(KS.EQ.2) GO TO 201
      DO 53 N=1,5
      WLNH(N)=WLN(1,N)
   53 WLN2(N)=WLN(2,N)
      RETURN
      END
```

```
      FUNCTION GAMI(B)
C        THIS DECK CALCULATES THE INCOMPLETE GAMMA FUNCTION(4/3,B)
      GAMI=.75*B**1.3333
      FAC=1.
      FN=1.
      DO 10 N=1,50
      FN=FN*(-1.)
      F1=N
      FAC=FAC*F1
      E1=4./3.+F1
      DGAMI=FN*B**E1/(FAC*E1)
      GAMI=GAMI+DGAMI
      IF(ABS(DGAMI).LT..0001) GO TO 11
   10 CONTINUE
   11 GAMI=.893144-GAMI
      RETURN
      END
```

```
      SUBROUTINE GRIEM(T,XNE,XNE1,XNE2,XNE3,JM,KM,S,S2)
      DIMENSION S(3,3,19),S1(3,19),S2(19)
C          THIS SUBROUTINE INTERPOLATES LINE PROFILES FROM GRIEM
      IF(T-10000.) 5,5,10
    5 NUM=1
    8 DO 6 J=1,JM
      DO 7 K=1,KM
    7 S1(J,K)=S(NUM,J,K)
    6 CONTINUE
      GO TO 50
   10 IF(T-20000.) 11,11,15
   11 DO 12 J=1,JM
      DO 13 K=1,KM
   13 S1(J,K)=S(1,J,K)+(S(2,J,K)-S(1,J,K))*(T-10000.)/10000.
   12 CONTINUE
      GO TO 50
   15 IF(T-40000.) 16,16,20
   16 DO 17 J=1,JM
      DO 18 K=1,KM
   18 S1(J,K)=S(2,J,K)+(S(3,J,K)-S(2,J,K))*(T-20000.)/20000.
   17 CONTINUE
      GO TO 50
   20 NUM=3
      GO TO 8
   50 IF(XNE-XNE1) 55,55,60
```

```
   55 NUM=1
   57 DO 56 K=1,KM
   56 S2(K)=S1(NUM,K)
      GO TO 100
   60 IF(XNE-XNE2) 65,65,70
   65 DO 66 K=1,KM
   66 S2(K)=S1(1,K)+(S1(2,K)-S1(1,K))*(XNE-XNE1)/(XNE2-XNE1)
      GO TO 100
   70 IF(XNE-XNE3) 75,75,80
   75 DO 76 K=1,KM
   76 S2(K)=S1(2,K)+(S1(3,K)-S1(2,K))*(XNE-XNE2)/(XNE3-XNE2)
      GO TO 100
   80 NUM=3
      GO TO 57
  100 RETURN
      END


      SUBROUTINE HEBFF(INPUT,V,TEMP,XKHEC)
C        THIS PROGRAM CALCULATES THE CONTINUOUS ABSORPTION COEF. FOR HEL
C        AND IONIZATION EDGES
      XKHEC=0.
   55 RETURN
      END


      SUBROUTINE HE1BB(INPUT,TEMP,WL,HEBAC)
C        BOUND BOUND ABS. COEF. FOR HELIUM
      HEBAC=0.
  600 RETURN
      END


      SUBROUTINE HE2BFF(V,TEMP,XKHC)
      XKHC=0.
      RETURN
      END
```

```
      SUBROUTINE HILINE(INPUT,IZ,TEMP,V,N,NP,CFNM,F,XLK)
C
CC       THIS DECK CALCULATES THE ABSORPTION COEF. FOR TRANSITIONS FROM
CC       LEVELS 1, 2, 3, 4, TO LEVELS 1 THROUGH 12 OF HYDROGEN AND HELIUM 2
CC         XLKH IS THE ABSORPTION COEFFICIENT IN UNITS OF  1/CM
C
      COMMON/CONST1/XNH,XNP,XNHE1,XNHE2,XNHE3,XNE,PEB,PB,XNH2,XNH2P,XNHM
      COMMON/CONST2/ ELM,PM,HM,HEM,HEM2,HEM3,H2M,H2PM,HMM,PC
      COMMON/CONST3/XK,H,C,RH,RHE,XIH,XIHE1,XIHE2,XDISS,W5,W6
      COMMON/CONST4/SE,CER,A0,C1
      COMMON/IONED/JHY,JHE,JHEII,JM,LM,LINE,JEDGE
      COMMON/PART1/ DE,NMH,NMHE1,NMHE2
      COMMON/ONE/VL(2,4,12),WLL(2,4,12),VN(2,6),WLN(2,6),CX(6),CY(6)
      COMMON/T3/XNN(2,12),XIIL,XIINTS,XLO,XHE(26),FLX,FLXL
      COMMON/FOUR/LINEHY(2,4,12),ANM(2,4,12),PI
      COMMON/SEVEN/STEM,DHVKT,MAX(2)
      COMMON/SIXX/GHVKT(2,4,12),HWH(50),HW1(35),HW2(50)
      COMMON/BLUE/STRENG(2,4,12)
      DIMENSION GV(2,4,12)
      IF(INPUT.GE.0) GO TO 90
      CS=SE*SE/(C*ELM)
      YM1=XNE*SE*SE*(H/(XK*TEMP))**2/(3.*ELM*PI)
      DW=SQRT(8.*PI*ELM/(XK*TEMP))*XNE*(H/(2.*PI*ELM))**2/9.
      DO 52 IZ=1,2
      IF(F.LT..001.AND.IZ.EQ.1) GO TO 49
      IF(F.GT..999.AND.IZ.EQ.2) GO TO 49
      IF(MAX(IZ).LT.NP) GO TO 49
      Z=IZ
      DW1=DW/(Z*Z)
      YM2=YM1/(Z*Z)
      A=N
      A5=A**5
      B=NP
      YM=YM2*B**4
C
CC       APPROXIMATIONS OF THE EXPONENTIAL INTEGRAL
C
      IF(YM-1.) 40,41,41
   40 EI=-ALOG(YM)-.5772+.9999*YM-.2499*YM*YM+.0552*YM**3-.00976*YM**4
      EI=EI+0.001079*YM*YM*YM*YM
      GO TO 50
   41 EI=EXP(-YM)*(YM+2.335+.251/YM)/(YM*YM+3.331*YM+1.682)
   50 GV(IZ,N,NP)=DW1*EI*(A5+B**5)
C
CC       GV IS IN UNITS OF INVERSE SEC
C
      IF(B.GT.6.1) GV(IZ,N,NP)=GV(IZ,N,NP)*6.75/B
      GA=GV(IZ,N,NP)*H/(XK*TEMP)
      GHVKT(IZ,N,NP)=GA
```

```
C
C         GHVKT IS IN UNITS OF HV/KT
C
      GANG=1.0E+08*C*GV(IZ,N,NP)/(VL(IZ,N,NP)**2)
C
C         GANG IS IN UNITS OF ANGSTROMS
C
      WRITE(3,1)IZ,N,NP,YM,EI,GV(IZ,N,NP),GA,GANG,STRENG(IZ,N,NP)
    1 FORMAT(2X,'IZ N NP YM EI GV GA GANG STRENG '3I4,1P6E13.4)
      LINEHY(IZ,N,NP)=-1
      GO TO 52
   49 LINEHY(IZ,N,NP) =1
   52 CONTINUE
      GO TO 110
C                    MAIN CALCULATION
C                    LORENTZ LINE SHAPE IS USED
C
   90 XLK=0.
      IF(LINEHY(IZ,N,NP).GT.0) GO TO 110
      DEM=(GV(IZ,N,NP))**2+(V-VL(IZ,N,NP))**2
      XLK=CS*CFNM*XNN(IZ,N)*GV(IZ,N,NP)/DEM
  110 RETURN
      END



      SUBROUTINE HMBF(INPUT,TEMP,WL,ABSC )
      DIMENSION CK(6,15),A(15),C(15),T(15)
      DATA CK(1,1),CK(1,2),CK(1,3),CK(1,4),CK(1,5),CK(1,6),CK(1,7),CK(1,
     18),CK(1,9),CK(1,10),CK(1,11),CK(1,12),CK(1,13),CK(1,14),CK(1,15) /
     25.34, 4.63, 4.80, 4.90, 4.97, 5.03, 4.99, 4.87, 4.61, 4.31, 4.25,
     34.34, 4.70, 5.15, 3.74  /
      DATA CK(2,1),CK(2,2),CK(2,3),CK(2,4),CK(2,5),CK(2,6),CK(2,7),CK(2,
     18),CK(2,9),CK(2,10),CK(2,11),CK(2,12),CK(2,13),CK(2,14),CK(2,15) /
     25.15, 4.45, 4.60, 4.71, 4.78, 4.84, 4.80, 4.68, 4.46, 4.22, 4.21,
     34.30, 4.65, 5.10, 3.71  /
      DATA CK(3,1),CK(3,2),CK(3,3),CK(3,4),CK(3,5),CK(3,6),CK(3,7),CK(3,
     18),CK(3,9),CK(3,10),CK(3,11),CK(3,12),CK(3,13),CK(3,14),CK(3,15) /
     24.95, 4.24, 4.41, 4.51, 4.58, 4.64, 4.60, 4.49, 4.30, 4.14, 4.16,
     34.25, 4.60, 5.05, 3.64  /
      DATA CK(4,1),CK(4,2),CK(4,3),CK(4,4),CK(4,5),CK(4,6),CK(4,7),CK(4,
     18),CK(4,9),CK(4,10),CK(4,11),CK(4,12),CK(4,13),CK(4,14),CK(4,15) /
     24.73, 4.03, 4.19, 4.26, 4.36, 4.42, 4.39, 4.30, 4.15, 4.05, 4.10,
     34.20, 4.55, 5.00, 3.58  /
      DATA CK(5,1),CK(5,2),CK(5,3),CK(5,4),CK(5,5),CK(5,6),CK(5,7),CK(5,
     18),CK(5,9),CK(5,10),CK(5,11),CK(5,12),CK(5,13),CK(5,14),CK(5,15) /
     24.50, 3.79, 3.96, 4.06, 4.1 , 4.18, 4.16, 4.10, 4.00, 3.97, 4.04,
     34.13, 4.48, 4.93, 3.50  /
```

```
      DATA CK(6,1),CK(6,2),CK(6,3),CK(6,4),CK(6,5),CK(6,6),CK(6,7),CK(6,
     18),CK(6,9),CK(6,10),CK(6,11),CK(6,12),CK(6,13),CK(6,14),CK(6,15) /
     24.24, 3.53, 3.70, 3.80, 3.86, 3.92, 3.92, 3.89, 3.85, 3.87, 3.95,
     34.05, 4.40, 4.84, 3.30  /
      DATA T(1),T(2),T(3),T(4),T(5),T(6)/  5040., 5600., 6300., 7200.,
     1 8400., 10080.  /
      DATA A(1),A(2),A(3),A(4),A(5),A(6),A(7),A(8),A(9),A(10),A(11),A(12
     1),A(13),A(14),A(15) / 2999., 3000., 4000., 5000., 6000., 8000.,
     310000., 12000., 14000.,16000.,18000., 20000.,30000.,50000.,50001./
      IF(INPUT-0) 3,3,20
    3 IF(TEMP-T(6)) 5,5,4
    4 DO 60 I=1,15
   60 C(I)=CK(6,I)
      GO TO 100
    5 IF(TEMP-T(1)) 6,6,10
    6 DO 70 I=1,15
   70 C(I)=CK(1,I)
      GO TO 100
   10 DO 80 I=2,6
      IP=I
      IF(TEMP.LT.T(I)) GO TO 81
   80 CONTINUE
   81 IM=IP-1
      DO 90 I=1,15
   90 C(I)=CK(IM,I)+(CK(IP,I)-CK(IM,I))*(TEMP-T(IM))/(T(IP)-T(IM))
      GO TO 100
   20 IF(WL-50000.) 21,21,31
   21 IF(WL-3000.) 32,22,22
   22 DO 50 I=2,14
      IP=I
      IF(WL.LT.A(I)) GO TO 23
   50 CONTINUE
   23 IM=IP-1
      BK=C(IM)+(C(IP)-C(IM))*(WL-A(IM))/(A(IP)-A(IM))
      GO TO 40
   31 BK=C(15)+2.*ALOG10(WL/1000.)
      GO TO 40
   32 BK=C(1)-2100./WL
   40 ABSC=1.0E-30*10.**BK
C        ABSC IS THE ABSORPTION COEF. PER UNIT PE PER ELECTRON  (IN 1/CM)
C        HAS STIMULATED EMISSION FACTOR IN IT  FROM DARWIN AND FELENBOK PP460.
  100 RETURN
      END
```

```
      SUBROUTINE HYBFF(V,TEMP,XKHC)
C        CONTINUOUS ABSORPTION COEFFICIENT OF HYDROGEN
      COMMON/CONST2/ EM,PM,HM,HEM,HEM2,HEM3,H2M,H2PM,HMM,PO
      COMMON/CONST3/XK,H,C,RH,RHE,XIH,XIHE1,XIHE2,XDISS,W5,W6
      COMMON/CONST4/SE,CER,AO,C1
      COMMON/PART1/ DE,NMH,NMHE1,NMHE2
      COMMON/IONED/JHY,JHE,JHEII,JM,LM,LINE,JEDGE
      COMMON/ONE/VL(2,4,12),WLL(2,4,12),VN(2,6),WLN(2,6),CX(6),CY(6)
      COMMON/ TWO / GX(6),X1,Y1
      PI2=9.869604
      XKBF=0.
      C2=32.*PI2*RH/(5.1963*HM)
      IF(V.LE.VN(1,1)) GO TO 50
      N=1
      GO TO 52
   50 IF(V.GE.VN(1,JHY).AND.JHY.GE.2) GO TO 51
      N=6
      GO TO 52
   51 DO 101 J=2,JHY
      IF(V.LE.VN(1,J)) GO TO 101
      N=J
      GO TO 52
  101 CONTINUE
   52  XKBFP=0.
      XKCC1=C2*EXP(-X1)*(C1/V)**3
      G1=.1728*(V/(RH*C1))**.333
      IF(N.EQ.6.AND.NMH.GE.6) GO TO 53
      IF(N.EQ.6.AND.NMH.LE.5) GO TO 54
      DO 102 J=N,JHY
      SN=J
      GBF=1.-G1*(GX(J)/V-1.)
  102 XKBFP=XKBFP+ EXP(CX(J))*GBF/SN**3
   53 XKBFP=XKBFP+(EXP(CX(6))-1.)/(2.*CX(1))
      XKBF=XKBFP*XKCC1
   54 GFF=1.+G1*(1.+2.*TEMP*XK/(H*V))
      XKFF=XKCC1*GFF/(2.*CX(1))
      XKHC=XKBF+XKFF
      RETURN
      END
```

```
      SUBROUTINE H2PBF(TEMP,WL,APSC)
C         H2P CONTINUUM ABS COEF.  DOES NOT INCLUDE STIMULATED EMIS FACTOR.
C         FROM BOGGESS,  ASTROPHY. JOUR. V129, PP432, 1959.
      DIMENSION C(14),D(14),A(14)
      DATA A(1),A(2),A(3),A(4),A(5),A(6),A(7),A(8),A(9),A(10),A(11),A(12
     1),A(13),A(14) / 304., 500., 1000., 1500., 2000., 2500., 3000., 400
     20., 5000., 6000., 7000., 8000., 9000., 10000. /
      DATA C(1),C(2),C(3),C(4),C(5),C(6),C(7),C(8),C(9),C(10),C(11),C(12
     1),C(13),C(14) / 50., 19.14, 19.69, 20.20, 20.59, 20.91, 21.18, 21.
     263, 21.98, 22.29, 22.54, 22.77, 22.97, 23.16 /
      DATA D(1),D(2),D(3),D(4),D(5),D(6),D(7),D(8),D(9),D(10),D(11),D(12
     1),D(13),D(14) / 0., 13.46, 4.842, 2.877, 2.004, 1.522, 1.222, .865
     2, .665, .538, .450, .386, .338, .300 /
      ABSC=0.
      IF(WL.GT.100000.) GO TO 99
      T=TEMP/10000.
      IF(WL-A(1)) 99,99,10
   10 IF(WL-A(14)) 11,11,80
   11 DO 12 I=2,14
      IP=I
      IF(WL.LT.A(I)) GO TO 13
   12 CONTINUE
   13 IM=IP-1
      DD=D(IM)+(D(IP)-D(IM))*(WL-A(IM))/(A(IP)-A(IM))
      CC=C(IM)+(C(IP)-C(IM))*(WL-A(IM))/(A(IP)-A(IM))
      GO TO 90
   80 CC=C(13)+(C(14)-C(13))*(WL-A(13))/(A(14)-A(13))
      DD=D(13)+(D(14)-D(13))*(WL-A(13))/(A(14)-A(13))
      IF(DD.LE.0.) DD=0.
   90 FP=-CC-DD/T
      E=10.**FP
      WLCM=1.0E-08*WL
      XX=1.4387/(WLCM*TEMP)
      ABSC=E*WLCM**5*(EXP(XX)-1.)/(12.566*11.9050E-06)
C          ABSC = E/(4 PI BB(WLCM)), WHERE BB(WLCM) IS THE PLANCK INTENSITY AT WL
C           ABSC IS THE H2P ABSORPTION COEF(1/CM) PER NH PER NP.
   99 RETURN
      END
```

```
      SUBROUTINE H2LYMN (WL,TEMD,XKLYMN)
C
C     ****  CALCULATES ABSORPTION COEFFICIENT OF LYMAN BAND  ****
C
C     *****  XKLYMN IS ABS. COEF. OF LYMAN BAND  ****
C     ****  CSWL IS THE ABSORPTION CROSS SECTION  ****
C      ****  FNO IS OSCILLATOR LINE STRENGTH (F NUMBER)  ****
      COMMON/CONST1/XNH,XNP,XNHE1,XNHE2,XNHE3,XNE,PEB,PB,XNH2,XNH2P,XNHM
      DIMENSION T(3),W(30),C(3,30),CS(30)
      DATA T(1),T(2),T(3)/  3000.,6000.,10000./
      DATA W(1),W(2),W(3),W(4),W(5),W(6),W(7),W(8),W(9),W(10),W(11),
     1W(12),W(13),W(14),W(15),W(16),W(17),W(18),W(19),W(20)/
     21000.,1100.,1200.,1300.,1400.,1500.,1600.,1700.,1800.,1900.,
     32000.,2100.,2200.,2300.,2340.,2360.,2400.,2500.,2600.,2700.  /
      DATA W(21),W(22),W(23),W(24),W(25),W(26),W(27),W(28),W(29),W(30)/
     12800.,2900.,3000.,3100.,3200.,3300.,3400.,3480.,3500.,3600./
      DATA C(1,1),C(1,2),C(1,3),C(1,4),C(1,5),C(1,6),C(1,7),C(1,8),
     1C(1,9),C(1,10),C(1,11),C(1,12),C(1,13),C(1,14),C(1,15),
     2C(1,16),C(1,17)/  3.5E-19,1.5E-18,2.0E-18,2.5E-18,2.5E-18,2.5E-18,
     32.5E-18,2.5E-18,2.5E-18,2.5E-18,2.5E-18,1.5E-18,3.5E-19,2.5E-20,
     42.5E-20,1.5E-22,1.0E-22  /
      DATA C(1,18),C(1,19),C(1,20),C(1,21),C(1,22),C(1,23),C(1,24),
     1C(1,25),C(1,26),C(1,27),C(1,28),C(1,29),C(1,30)/  2.5E-23,1.0E-23,
     23.0E-24,1.6E-24,7.0E-25,3.0E-25,1.3E-25,6.5E-26,6.0E-26,2.5E-26,
     31.5E-26,1.0E-27,5.0E-28  /
      DATA C(2,1),C(2,2),C(2,3),C(2,4),C(2,5),C(2,6),C(2,7),C(2,8),
     1C(2,9),C(2,10),C(2,11),C(2,12),C(2,13),C(2,14),C(2,15),
     2C(2,16),C(2,17)/  1.5E-19,6.0E-19,1.5E-18,2.0E-18,2.5E-18,2.5E-18,
     32.5E-18,2.5E-18,2.5E-18,2.5E-18,2.5E-18,2.0E-18,1.5E-18,2.2E-19,
     42.0E-19,8.0E-21,7.0E-21  /
      DATA C(2,18),C(2,19),C(2,20),C(2,21),C(2,22),C(2,23),C(2,24),
     1C(2,25),C(2,26),C(2,27),C(2,28),C(2,29),C(2,30)/  4.0E-21,
     22.7E-21,1.7E-21,1.4E-21,1.0E-21,7.0E-22,4.8E-22,3.8E-22,2.0E-22,
     31.2E-22,8.0E-24,1.0E-24,5.0E-25  /
      DATA C(3,1),C(3,2),C(3,3),C(3,4),C(3,5),C(3,6),C(3,7),C(3,8),
     1C(3,9),C(3,10),C(3,11),C(3,12),C(3,13),C(3,14),C(3,15),C(3,16),
     2C(3,17)/  8.0E-20,4.0E-19,1.0E-18,2.0E-18,2.5E-18,2.5E-18,
     32.5E-18,2.5E-18,2.5E-18,2.5E-18,2.5E-18,2.0E-18,1.7E-18,6.0E-19,
```

```
     46.0E-19,3.0E-20,2.8E-20  /
      DATA C(3,18),C(3,19),C(3,20),C(3,21),C(3,22),C(3,23),C(3,24),
     1C(3,25),C(3,26),C(3,27),C(3,28),C(3,29),C(3,30)/  2.2E-20,1.8E-20,
     21.5E-20,1.2E-20,1.0E-20,7.8E-21,5.5E-21,4.0E-21,2.6E-21,1.5E-21,
     31.0E-22,5.5E-24,3.9E-24  /
      FNO=0.2
      IF (WL.LT.1000..AND.WL.GT.3600.) GO TO 999
      IF (TEMD.GE.10000.) GO TO 20
      IF (TEMD.GE.6000.) GO TO 25
      IF (TEMD.GE.3000.) GO TO 30
      IF (TEMD.LT.3000.) GO TO 35
   20 DO 21 J=1,30
      CS(J)=C(3,J)
   21 CONTINUE
      GO TO 100
   25 DO 26 J=1,30
      CS(J)=C(2,J)+(C(3,J)-C(2,J))*(TEMD-T(2))/(T(3)-T(2))
   26 CONTINUE
      GO TO 100
   30 DO 31 J=1,30
      CS(J)=C(1,J)+(C(2,J)-C(1,J))*(TEMD-T(1))/(T(2)-T(1))
   31 CONTINUE
      GO TO 100
   35 DO 36 J=1,30
      CS(J)=C(1,J)
   36 CONTINUE
      GO TO 100
  999 XKLYMN=0.0
      GO TO 888
  100 CSWL=ULJY(WL,W,30,CS)
      XKLYMN=CSWL*XNH2*FNO
  888 RETURN
      END



      SUBROUTINE H2PHOT (WL,TEMD,XKPHOT)
C
CCC   ****  CALCULATES ABSORPTION COEFFICIENT OF PHOTOIONIZATION BAND  ****
CCC
CCC   *****  XKPHOT IS ABS. COEF. OF PHOTOIONIZATION BAND  ****
C     ****  CSWL IS THE ABSORPTION CROSS SECTION  ****
      COMMON/CONST1/XNH,XNP,XNHE1,XNHE2,XNHE3,XNE,PEB,PB,XNH2,XNH2P,XNHM
      DIMENSION T(3),W(8),C(3,8),CS(8)
      DATA T(1),T(2),T(3)/3000.,5000.,7000./
      DATA W(1),W(2),W(3),W(4),W(5),W(6),W(7),W(8)/
     1500.,600.,700.,780.,800.,900.,1000.,1100./
```

```
      DATA C(1,1),C(1,2),C(1,3),C(1,4),C(1,5),C(1,6),C(1,7),C(1,8)/
     1 1.8E-18,3.3E-19,5.0E-18,6.2E-18,2.0E-18,2.0E-21,2.0E-23,2.0E-24/
      DATA C(2,1),C(2,2),C(2,3),C(2,4),C(2,5),C(2,6),C(2,7),C(2,8)/
     1 1.5E-18,2.0E-18,4.0E-18,5.8E-18,1.5E-18,2.4E-20,2.2E-21,4.2E-22/
      DATA C(3,1),C(3,2),C(3,3),C(3,4),C(3,5),C(3,6),C(3,7),C(3,8)/
     1 1.0E-18,1.9E-18,3.6E-18,5.2E-18,1.0E-18,4.5E-20,1.5E-20,5.8E-21/
      IF (WL.LT.500.0.AND.WL.GT.1100.) GO TO 999
      IF(TEMD.GE.7000.) GO TO 20
      IF (TEMD.GE.5000.) GO TO 25
      IF (TEMD.GE.3000.) GO TO 30
      IF(TEMD.LT.3000.) GO TO 35
   20 DO 21 J=1,8
      CS(J)=C(3,J)
   21 CONTINUE
      GO TO 100
   25 DO 26 J=1,8
      CS(J)=C(2,J)+(C(3,J)-C(2,J))*(TEMD-T(2))/(T(3)-T(2))
   26 CONTINUE
      GO TO 100
   30 DO 31 J=1,8
      CS(J)=C(1,J)+(C(2,J)-C(1,J))*(TEMD-T(1))/(T(2)-T(1))
   31 CONTINUE
      GO TO 100
   35 DO 36 J=1,8
      CS(J)=C(1,J)
   36 CONTINUE
      GO TO 100
  999 XKPHOT=0.0
      GO TO 888
  100 CSWL=ULJY(WL,W,8,CS)
      XKPHOT=CSWL*XNH2
  888 RETURN
      END



      SUBROUTINE H2WERN(WL,TEMD,XKWERN)
C
C     ****  CALCULATES ABSORPTION COEFFICIENT OF WERNER BAND  ****
C
C     *****  XKWERN IS ABS. COEF. OF WERNER BAND  ****
C     ****  CSWL IS THE ABSORPTION CROSS SECTION  ****
C      ****  FNO IS OSCILLATOR LINE STRENGTH (F NUMBER)  ****
      COMMON/CONST1/XNH,XNP,XNHE1,XNHE2,XNHE3,XNE,PEB,PB,XNH2,XNH2P,XNHM
      DIMENSION T(3),W(13),C(3,13),CS(13)
      DATA T(1),T(2),T(3)/3000.,6000.,9000./
      DATA W(1),W(2),W(3),W(4),W(5),W(6),W(7),W(8),W(9),W(10),W(11),
     1W(12),W(13)/ 800.,900.,1000.,1050.,1100.,1150.,1200.,1250.,1300.,
     21350.,1400.,1450.,1500./
```

```
      DATA C(1,1),C(1,2),C(1,3),C(1,4),C(1,5),C(1,6),C(1,7),C(1,8),
     1C(1,9),C(1,10),C(1,11),C(1,12),C(1,13)/  4.2E-18,4.0E-17,
     28.0E-18,8.0E-19,6.0E-20,8.0E-22,1.0E-23,1.5E-25,2.0E-27,2.5E-29,
     33.0E-31,4.5E-33,6.0E-35/
      DATA C(2,1),C(2,2),C(2,3),C(2,4),C(2,5),C(2,6),C(2,7),C(2,8),
     1C(2,9),C(2,10),C(2,11),C(2,12),C(2,13)/  5.0E-18,3.8E-17,1.2E-17,
     24.0E-18,1.0E-18,1.5E-19,1.5E-20,3.0E-21,3.0E-23,3.0E-26,3.0E-29,
     33.0E-32,3.0E-35/
      DATA C(3,1),C(3,2),C(3,3),C(3,4),C(3,5),C(3,6),C(3,7),C(3,8),
     1C(3,9),C(3,10),C(3,11),C(3,12),C(3,13)/  4.2E-18,2.1E-17,1.2E-17,
     24.3E-18,2.0E-18,4.5E-19,1.5E-19,5.0E-20,2.1E-20,6.0E-21,2.0E-21,
     33.0E-22,1.0E-23/
      FNO=0.4
      IF (WL.LT.800.0.AND.WL.GT.1500.) GO TO 999
      IF(TEMD.GE.9000.) GO TO 20
      IF (TEMD.GE.6000.) GO TO 25
      IF (TEMD.GE.3000.) GO TO 30
      IF (TEMD.LT.3000.) GO TO 35
   20 DO 21 J=1,13
      CS(J)=C(3,J)
   21 CONTINUE
      GO TO 100
   25 DO 26 J=1,13
      CS(J)=C(2,J)+(C(3,J)-C(2,J))*(TEMD-T(2))/(T(3)-T(2))
   26 CONTINUE
      GO TO 100
   30 DO 31 J=1,13
      CS(J)=C(1,J)+(C(2,J)-C(1,J))*(TEMD-T(1))/(T(2)-T(1))
   31 CONTINUE
      GO TO 100
   35 DO 36 J=1,13
      CS(J)=C(1,J)
   36 CONTINUE
      GO TO 100
  999 XKWERN=0.0
      GO TO 888
  100 CSWL=ULJY(WL,W,13,CS)
      XKWERN=CSWL*XNH2*FNO
  888 RETURN
      END
```

```
      SUBROUTINE LYMAN(IZ,J,INPUT,TEMP,F,V,XLK)
C        CALLS LYMAN LINES
      SWING(QQQQQ1,QQQQQ2)=QQQQQ1*QQQQQ1/(QQQQQ2*QQQQQ2)
      SHAPE(Q0OIM,Q0OII,QDALF,QALFIM,QALFII)=Q0OIM+(Q0OII-Q0OIM)*(QDALF-
     1QALFIM)/(QALFII-QALFIM)
      COMMON/CONST1/XNH,XNP,XNHE1,XNHE2,XNHE3,XNE,PEB,PB,XNH2,XNH2P,XNHM
      COMMON/CONST2/ ELM,PM,HM,HEM,HEM2,HEM3,H2M,H2PM,HMM,PC
      COMMON/CONST3/XK,H,C,RH,RHE,XIH,XIHE1,XIHE2,XDISS,W5,W6
      COMMON/CONST4/SE,CER,A0,C1
      COMMON/ONE/VL(2,4,12),WLL(2,4,12),VN(2,6),WLN(2,6),CX(6),CY(6)
      COMMON/T3/XNN(2,12),XIIL,XIINTS,XLO,XHE(26),FLX,FLXL
      COMMON/FOUR/LINEHY(2,4,12),ANM(2,4,12),PI
      COMMON/SIXX/HWIDTH(2,4,12),HWH(50),HW1(35),HW2(50)
      COMMON/BLUE/STRENG(2,4,12)
      DIMENSION FNM(11),ALF(2,17),SA(3,3,19),SB(3,3,19),S12(19),S13(19)
      IF(INPUT.GE.0) GO TO 10
      READ(1,8)(FNM(I),I=1,11)
    8 FORMAT(6E11.4)
      READ(1,9)(ALF(1,I),I=1,17)
      READ(1,9)(ALF(2,I),I=1,17)
    9 FORMAT(17F4.0)
      WRITE (3,6)
    6 FORMAT (/,20X,11HLYMAN LINES,/20X,6HFNM(I))
      WRITE (3,7) (FNM(I),I=1,11)
    7 FORMAT (2X,1P11E11.3)
      WRITE(3,9)(ALF(1,I),I=1,17)
      WRITE(3,9)(ALF(2,I),I=1,17)
      DO 300 I1=1,2
      DO 300 I2=1,4
      DO 300 I3=1,12
      STRENG(2,4,12)=0.
      HWIDTH(I1,I2,I3)=0.
  300 LINEHY(I1,I2,I3)=1
      DO 200 NT=1,3
      DO 210 NN=1,3
      READ(1,19)(SA(NT,NN,I),I=1,17)
  210 READ(1,19)(SB(NT,NN,I),I=1,17)
  200 CONTINUE
      DO 23 NT=1,3
      DO 24 NN=1,3
   24 WRITE(3,18) (SA(NT,NN,I),I=1,17)
   23 CONTINUE
      DO 25 NT=1,3
      DO 26 NN=1,3
   26 WRITE(3,18)(SB(NT,NN,I),I=1,16)
   25 CONTINUE
   19 FORMAT(10F8.0)
```

```
   18 FORMAT(4X,17F7.2)
      DO 40 I=1,17
      ALF(1,I)=ALF(1,I)*.0001
   40 ALF(2,I)=ALF(2,I)*.0001
      XN=XNE
      CALL GRIEM(TEMP,XN,1.0E+17,1.0E+18,1.0E+19,3,17,SA,S12)
      CALL GRIEM(TEMP,XN,1.0E+16,1.0E+17,1.0E+18,3,16,SB,S13)
      FO=2.61*SE*XNE**.6667
      CS=SE*SE/(C*ELM)
      N=1
      S=N
      CORR=H/(C*XK*TEMP)
      IZ=1
      IF(IZ.EQ.1.AND.F.LT..001) GO TO 112
  110 IF(IZ.EQ.2.AND.F.GT..999) GO TO 112
      LINEHY(IZ,1,2)=-1
      LINEHY(IZ,1,3)=-1
      HWIDTH(IZ,1,2)=FO*VL(IZ,1,2)**2/(PI*S12(1)*1.0E+08)*CORR
      HWIDTH(IZ,1,3)=FO*VL(IZ,1,3)**2/(PI*S13(1)*1.0E+08)*CORR
      WRITE(3,913) HWIDTH(IZ,1,2),HWIDTH(IZ,1,3)
  913 FORMAT(2X,37HHALFWIDTHS OF LA AND LB LINES (HV/KT),2E14.6)
      DO 111 NP=2,12
      SP=NP
      NP1=NP-1
      CF=FNM(NP1)
      STRENG(IZ,N,NP)=PI*SE*SE*CF*XNN(IZ,N)/(ELM*C)
C
C     STRENG IS THE LINE STRENGTH IN UNITS OF INVERSE CM-SEC
C
  111 ANM(IZ,N,NP)=8.*((S*PI*VL(IZ,N,NP)*SE)/(SP*C))**2*CF/(ELM*C)
      WRITE(3,369) STRENG(IZ,1,2),STRENG(IZ,1,3)
  369 FORMAT(2X,41HLINE STRENGTHS OF LA AND LB LINES (HV/KT),2E14.6)
  112 IZ=IZ+1
      IF(IZ.EQ.2) GO TO 110
      DO 31 J=4,12
      NP=J
      CFNM=FNM(J-1)
   31 CALL HILINE(INPUT,IZ,TEMP,V,N,NP,CFNM,F,XLK)
      GO TO 20
   10 N=1
      NP=J
      XLK=0.
      IF(LINEHY(IZ,N,NP).GT.0) GO TO 20
      J1=J-1
      IF(J-3) 50,75,100
   50 NMAX=17
   49 DALF=1.0E+08*C*ABS(V-VL(IZ,N,NP))/(FO*VL(IZ,N,NP)**2)
      IF(DALF.GT.ALF(J1,NMAX)) GO TO 333
      DO 51 I=1,NMAX
      II=I
```

```
      IF(DALF.LT.ALF(J1 ,I)) GO TO 52
   51 CONTINUE
   52 IM=II-1
      IF(J.EQ.2) SHAP=SHAPE(S12(IM),S12(II),DALF,ALF(J1,IM),ALF(J1,II))
      IF(J.EQ.3) SHAP=SHAPE(S13(IM),S13(II),DALF,ALF(J1,IM),ALF(J1,II))
      GO TO 44
C        WING LINE SHAPES  (GRIEM'S BOOK PP 93)
  333 IF(J.EQ.2) SHAP=S12(NMAX    )*SWING(ALF(J1,NMAX),DALF)
      IF(J.EQ.3) SHAP=S13(NMAX    )*SWING(ALF(J1,NMAX),DALF)
   44 XLK=SHAP*CS*FNM(J1)*XNN(IZ,N)*C*PI*1.0E+08/(F0*VL(IZ,N,NP)**2)
C       DIFINATIONS OF DALF, XLK FROM LASHER, WILSON, AND GRIEF LOCKHEED REPORT
      GO TO 20
   75 NMAX=16
      GO TO 49
  100 CFNM=FNM(J1)
      CALL HILINE(INPUT,IZ,TEMP,V,N,NP,CFNM,F,XLK)
C        XLK IS IN UNITS OF 1/CM
   20 RETURN
      END



      SUBROUTINE OPTHIN(TEMP,F)
      COMMON/CONST2/ ELM,PM,HM,HEM,HEM2,HEM3,H2M,H2PM,HMM,PO
      COMMON/CONST3/XK,H,C,RH,RHE,XIH,XIHE1,XIHE2,XDISS,W5,W6
      COMMON/CONST4/SE,CER,A0,C1
      COMMON/T3/XNN(2,12),XIIL,XIINTS,XLO,XHE(26),FLX,FLXL
      COMMON/ONE/VL(2,4,12),WLL(2,4,12),VN(2,6),WLN(2,6),CX(6),CY(6)
      COMMON/ SIX / WLLH(50),WLNH(5),WLL1(34),WLN1(13),WLL2(50),WLN2(5)
      COMMON/SIXX/GHVKT(2,4,12),HWH(50),HW1(35),HW2(50)
      COMMON/HELONE/ NMAX,AHE(34),XNU(34),WLHE(34),IWM(34)
      COMMON/FOUR/LINEHY(2,4,12),ANM(2,4,12),PI
      COMMON/BEC/SLNH(50),SLNHE1(34),SLNHE2(50)
      COMMON/BLUE/STRENG(2,4,12)
      INPUT=1
      IZ=1
C
C        SETS UP LINES FOR ORDERING IN DELTWL
C
      DO 52 N=1,50
      HWH(N)=0.
      HW2(N)=0.
      SLNH(50)=0.
      SLNHE2(50)=0.
      WLLH(N)=0.
   52 WLL2(N)=0.
      N=0
      DO 50 K=1,4
      DO 50 JJ=1,12
```

```
      J=13-JJ
      IF(WLL(1,K,J).LE.2.) GO TO 50
      IF(LINEHY(1,K,J).GT.0) GO TO 50
      N=N+1
      WLLH(N)=WLL(1,K,J)
      SLNH(N)=STRENG(1,K,J)
      HWH(N)=GHVKT(1,K,J)
   50 CONTINUE
      N=0
      DO 51 K=1,4
      DO 51 JJ=1,12
      J=13-JJ
      IF(WLL(2,K,J).LE.2.) GO TO 51
      IF(LINEHY(2,K,J).GT.0) GO TO 51
      N=N+1
      HW2(N)=GHVKT(2,K,J)
      SLNHE2(N)=STRENG(2,K,J)
      WLL2(N)=WLL(2,K,J)
   51 CONTINUE
      DO 62 NX=1,4
   62 WRITE(3,61)(LINEHY(1,NX,JX),JX=1,12),(LINEHY(2,NX,JX),JX=1,12)
   61 FORMAT(12I4,10X,12I4)
  999 RETURN
      END



      SUBROUTINE PASCHN(IZ,J,INPUT,TEMP,F,V,XLK)
C        CALLS RITZ PASCHEN LINES
      COMMON/CONST2/ ELM,PM,HM,HEM,HEM2,HEM3,H2M,H2PM,HMM,PC
      COMMON/CONST3/XK,H,C,RH,RHE,XIH,XIHE1,XIHE2,XDISS,W5,W6
      COMMON/CONST4/SE,CER,A0,C1
      COMMON/ONE/VL(2,4,12),WLL(2,4,12),VN(2,6),WLN(2,6),CX(6),CY(6)
      COMMON/FOUR/LINEHY(2,4,12),ANM(2,4,12),PI
      COMMON/T3/XNN(2,12),XIIL,XIINTS,XLO,XHE(26),FLX,FLXL
      COMMON/BLUE/STRENG(2,4,12)
      DIMENSION ENM(9)
      IF(INPUT.GE.0) GO TO 10
      READ(1,9)(ENM(I),I=1,9)
    9 FORMAT(6E11.4)
      WRITE (3,6)
    6 FORMAT (/,20X,18HRITZ PASCHEN LINES,/20X,6HENM(I))
      WRITE (3,7) (ENM(I),I=1,9)
    7 FORMAT (2X,1P9E11.3)
      N=3
      S=N
      DO 112 IZ=1,2
      DO 111 NP=4,12
```

```
      SP=NP
      NP1=NP-3
      CF=FNM(NP1)
      STRENG(IZ,N,NP)=PI*SE*SE*CF*XNN(IZ,N)/(ELM*C)
C
C     STRENG IS THE LINE STRENGTH IN UNITS OF INVERSE CM-SEC
C
  111 ANM(IZ,N,NP)=8.*((S*PI*VL(IZ,N,NP)*SE)/(SP*C))**2*CF/(ELM*C)
  112 CONTINUE
      DO 31 J=4,12
      NP=J
      CFNM=FNM(J-3)
   31 CALL HILINE(INPUT,IZ,TEMP,V,N,NP,CFNM,F,XLK)
      GO TO 20
   10 N=3
      NP=J
      IF(LINEHY(IZ,N,NP).GT.0) GO TO 20
      J1=J-3
      CFNM=FNM(J1)
      CALL HILINE(INPUT,IZ,TEMP,V,N,NP,CFNM,F,XLK)
C        XLK IS IN UNITS OF 1/CM
   20 RETURN
      END



      FUNCTION PARH2(T,L)
C        CALCULATION OF THE MOLECULAR HYDROGEN INTERNAL PARTITION FUNCTION
C        ( FROM ROSENBAUM AND LEVITT  NASA TN D 1107)
C
      DIMENSION A(4,5)
C        TEMP FROM 5000  TO 10000
      DATA A(1,1),A(1,2),A(1,3),A(1,4),A(1,5) / -6.54683, .881995E-02,
     1-.388423E-06, .165857E-09, -.544799E-14/
C        TEMP FROM 10000  TO 20000
      DATA A(2,1),A(2,2),A(2,3),A(2,4),A(2,5) / -4.80441, .309313E-02 ,
     1.113739E-05, .226904E-10,  -.835477E-15/
C        TEMP FROM 20000  TO 50000
      DATA A(3,1),A(3,2),A(3,3),A(3,4),A(3,5) / -117.836, .0126636 ,
     1 .135294E-05, -.161543E-10, .768922E-16 /
C        TEMP FROM 50000  TO 100000
      DATA A(4,1),A(4,2),A(4,3),A(4,4),A(4,5) / -683.782 , .0547547,
     1 .150914E-06, -.608597E-12, .586301E-18 /
      IF(T-10000.) 10,11,11
   10 N=1
      GO TO 16
   11 IF(T-20000.) 12,12,13
   12 N=2
      GO TO 16
```

```
   13 IF(T-50000.) 14,14,15
   14 N=3
      GO TO 16
   15 N=4
   16 IF(L.GT.0) GO TO 20
      Z=A(N,1)
      DO 100 J=2,5
      K=J-1
  100 Z=Z+A(N,J)*T**K
      GO TO 200
   20 Z=A(N,2)
      DO 101 J=3,5
      K=J-2
  101 Z=Z+(J-1)*A(N,J)*T**K
  200 PARH2=Z
      RETURN
      END



      FUNCTION PARH2P(T,L)
C        CALCULATION OF THE INTERNAL PARTITION FUNCTION OF H2P ION
C          (FROM PATCH AND MCBRIDE   NASA  TN D 4523)
C
      DIMENSION A(4,5)
C        TEMP FROM 4900  TO 10000
      DATA A(1,1),A(1,2),A(1,3),A(1,4),A(1,5) / 33.1155, -.749475E-02,
     1 .846179E-05, .172222E-08, -.991997E-13 /
C        TEMP FROM 10000  TO 20000
      DATA A(2,1),A(2,2),A(2,3),A(2,4),A(2,5) / -.115436E+04, .224826,
     1 .628029E-05, -.183934E-09,   -.550228E-15 /
C        TEMP FROM 20000  TO 50000
      DATA A(3,1),A(3,2),A(3,3),A(3,4),A(3,5) / -.396794E+04, .654921,
     1 -.164701E-04, .253177E-09, -.171716E-14 /
C        TEMP FROM 50000  TO 56000
      DATA A(4,1),A(4,2),A(4,3),A(4,4),A(4,5) / .313008E+04,  .0981358,
     1 .765602E-06, -.534710E-11, -.967768E-16 /
C         LINEAR FROM 56000 TO 100000  (Q(100000)  EQUALS  10**4)
      IF(T-56000.) 9,9,50
   50 IF(L.GT.0) GO TO 55
      Z=8042.+.01958*T
      GO TO 200
   55 Z=.01958
      GO TO 200
    9 IF(T-10000.) 10,10,11
   10 N=1
      GO TO 16
   11 IF(T-20000.) 12,12,13
```

```
   12 N=2
      GO TO 16
   13 IF(T-50000.) 14,14,15
   14 N=3
      GO TO 16
   15 N=4
   16 IF(L.GT.0) GO TO 20
      Z=A(N,1)
      DO 100 J=2,5
      K=J-1
  100 Z=Z+A(N,J)*T**K
      GO TO 200
   20 Z=A(N,2)
      DO 101 J=3,5
      K=J-2
  101 Z=Z+(J-1)*A(N,J)*T**K
  200 PARH2P=Z
      RETURN
      END
```

```
      FUNCTION PARTH(T,L)
C        HYDROGEN PARTITION FUNCTION
C        THE LTH MOMENT
      COMMON/PART1/ DE,NMH,NMHE1,NMHE2
      XK=1.38044E-16
      Z=0.
      IF(L.EQ.0) Z=1.
      R=2.178E-11/(XK*T)
      XNH=SQRT(2.178E-11/DE)
      NMH=XNH
      IF(NMH-2) 71, 30, 30
   30 DO 50 J=2,NMH
      XJ=J
      G=XJ*XJ
      E=R*(1.-1./G)
      IF(E-60.) 50, 50, 71
   50 Z=Z+E**L*G*EXP(-E)
   71 PARTH=2.*Z
      RETURN
      END
```

```
      SUBROUTINE SOLVE(ISW,EPS,TEMP,PE,ITT)
C        SOLVES SAHA EQUATIONS FOR COMPOSITION
      COMMON/CONST1/XNH,XNP,XNHE1,XNHE2,XNHE3,XNE,PER,PB,XNH2,XNH2P,XNHM
      COMMON/CONST2/ EM,PM,HM,HEM,HEM2,HEM3,H2M,H2PM,HMM,PC
      COMMON/CONST3/XK,H,C,RH,RHE,XIH,XIHE1,XIHE2,XDISS,W5,W6
      COMMON/SOLV1/ A7,A8,A9,ALF,BETA,GAMMA,XNH2PP,XNHEP
      COMMON / SOLV2/ B4, B5,B6,DELTA,ZETA,ETA
      DOUBLE PRECISION B4, B5,B6,DELTA,ZETA,ETA,ZSOLVE
      DOUBLE PRECISION A7,A8,A9,ALF,BETA,GAMMA,ONE,A7P,A9P
      DOUBLE PRECISION A(30),B(30),G(30),P(30)
      DOUBLE PRECISION D(30),Z(30),E(30),X,B4P,B6P
      DOUBLE PRECISION DSQRT
      ITT=1
      ONE=1.000000
      XK=1.38044E-16
      HP=XNH2PP*XK*TEMP
      HEP=XNHEP*TEMP*XK
      IF(XNH2PP.LT.1.) GO TO 50
C        PURE HYDROGEN
      A9P=A9/HP
      B4P=B4/HP
      B6P=B6/HP
      J=1
      A(1)=ASOLVE(A9P,B4P)
      Z(1)=(ONE-A(1))*A9P/(2.*A(1)*A(1))
      P(1)=2.*Z(1)*A(1)*HP
      D(1)=P(1)/(B5+P(1))
      E(1)=B6/(B6+P(1))
      IF(ISW.LT.0) WRITE(3,30) J,P(1),E(J),D(1),A(1),Z(1)
      IF(XNHEP.GT.1.) GO TO 55
      DO 99 J=2,30
      ITT=J
      JJ=J-1
      P(J)=(2.*Z(JJ)*(A(JJ)-D(JJ)*(ONE-A(JJ)))+E(JJ)*(ONE-Z(JJ)))*HP
      IF(J.GT.3) P(J)=(P(J)+P(JJ))/2.
      E(J)=B6/(B6+P(J))
      D(J)=P(J)/(B5+P(J))
      A(J)=A9*(ONE-D(J))/(P(J)+A9*(ONE-D(J)))
      IF(A(J).LT.D(J)) WRITE(3,31)A(J),D(J)
   31 FORMAT(10X12HA(J).LT.D(J),2D14.6)
      IF(A(J).LT.D(J)) A(J)=D(J)
      IF(E(J).GT.ONE) WRITE(3,4321) E(J)
 4321 FORMAT(20X,12HE(J).GT.1.00, D14.6)
      IF(E(J).GT.ONE) E(J)=ONE
      X=B4P*(ONE-E(J))/(4.*(ONE-D(J))**2*(ONE-A(J))**2)
      Z(J)=ZSOLVE(X)
      IF(ISW.LT.0.OR.J.GT.25) WRITE(3,30)J,P(J),E(J),D(J),A(J),Z(J),X
   30 FORMAT(2X,I6,6D14.6)
      IF(ABS(SNGL((P(J)-P(JJ))/P(J))).LT.EPS) GO TO 60
```

```
   99 CONTINUE
      IF(XNHEP.LT.1.) GO TO 60
C        HYDROGEN AND HELIUM
   55 A7P=A7/HEP
      B(1)=ZSOLVE(A7P)
      P(1)=(2.*Z(1)*(A(1)-D(1)*(ONE-A(1)))+E(1)*(ONE-Z(1)))*HP+B(1)*HEP
      G(1)=A8/(P(1)+A8)
      IF(ISW.LT.0) WRITE(3,1) J,P(J),E(J),D(J),A(J),Z(J),G(J),B(J)
      DO 100 J=2,30
      ITT=J
      JJ=J-1
      P(J)=(2.*Z(JJ)*(A(JJ)-D(JJ)*(ONE-A(JJ)))+E(JJ)*(ONE-Z(JJ)))*HP
      P(J)=P(J)+B(JJ)*(ONE+G(JJ))*HEP
      IF(J.GT.3) P(J)=(P(J)+P(JJ))/2.
      E(J)=B6/(B6+P(J))
      D(J)=P(J)/(B5+P(J))
      A(J)=A9*(ONE-D(J))/(P(J)+A9*(ONE-D(J)))
      IF(P(J).LE.0.) WRITE(3,1)J,P(J),E(J),D(J),A(J),X,Z(J),G(J),B(J)
      IF(E(J).GT.ONE) WRITE(3,4321) E(J)
      IF(E(J).GT.ONE) E(J)=ONE
      X=B4P*(ONE-E(J))/(4.*(ONE-D(J))**2*(ONE-A(J))**2)
      Z(J)=ZSOLVE(X)
      G(J)=A8/(P(J)+A8)
      B(J)=A7/((ONE-G(J))*P(J)+A7)
      IF(ISW.LT.0.OR.J.GT.25)WRITE(3,1)J,P(J),E(J),D(J),A(J),X,Z(J),G(J)
     1,B(J)
    1 FORMAT(2X,I6,8D14.6)
      IF(ABS(SNGL((P(J)-P(J-1))/P(J))).LT.EPS) GO TO 70
      IF(G(J).LT..05) P(J)=(P(J)+P(J-1))/2.
  100 CONTINUE
      WRITE(3,2)J
    2 FORMAT(//10X,4HJ = ,I6,10X,23HNO CONVERGENCE IN SOLVE//)
      GO TO 70
C        PURE HELIUM
   50 A7P=A7/HEP
      B(1)=ZSOLVE(A7P)
      P(1)=B(1)*HEP
      J=1
      IF(ISW.LT.0)WRITE(3,3)J,B(1),P(1),A7,A8
      DO 101 J=2,30
      ITT=J
      G(J)=A8/(P(J-1)+A8)
      B(J)=A7/(P(J-1)*(ONE-G(J))+A7)
      P(J)=B(J)*(ONE+G(J))*HEP
      IF(ISW.LT.0.OR.J.GT.25) WRITE(3,3) J,B(J),G(J),P(J)
      IF(ABS(SNGL((P(J)-P(J-1))/P(J))).LT.EPS) GO TO 80
      IF(G(J).LT..05) P(J)=(P(J)+P(J-1))/2.
  101 CONTINUE
```

```
      WRITE(3,2)J
      GO TO 70
    2 FORMAT(4X,74J B G P,16,4D14.6)
   60 ALF=A(J)
      PE=P(J)
      ETA=F(J)
      DELTA=D(J)
      ZETA=Z(J)
      BETA=0.
      GAMMA=0.
      GO TO 90
   70 ALF=A(J)
      DELTA=D(J)
      ETA=F(J)
      ZETA=Z(J)
      BETA=B(J)
      GAMMA=G(J)
      PE=P(J)
      GO TO 90
   80 ALF=0.
      BETA=B(J)
      GAMMA=G(J)
      PE=P(J)
      ETA=0.
      ZETA=0.
      DELTA=0.
   90 RETURN
      END


      SUBROUTINE SPE3(Z,SE3,E)
      DATA A1,A2,A3,A4/8.57333,18.0590,8.63476,0.267774/
      DATA B1,B2,B3,B4/9.57332,25.6330,21.0997,3.95850/
      DATA C1,C2,C3,C4,C5,C6/ -.577215,  .9999919, -.2499106,
     1        5.51968E-02, -9.76004E-03, 1.07860E-03/
C     THIS FUNCTION CALCULATES 0.5-E3(Z) AND ALSO RETURNS 1-EXP(-Z) AS E
      SE3=0.5
      E=1.0
      IF (Z.GE.10.0) GO TO 30
    9 IF(Z-.0001) 10,10,3
   10 E=Z
      SE3=Z
      GO TO 30
    3 Z2=Z*Z
      G=EXP(-Z)
      EG=G/Z
      Z3=Z2*Z
```

```
      IF (Z-1.0) 50,50,100
   50 E1=-ALOG(Z)+C1+C2*Z+C3*Z2+C4*Z3+C5*Z2*Z2+C6*Z2*Z3
      GO TO 200
  100 Z4=Z2*Z2
      E1=E0*(Z4+A1*Z3+A2*Z2+A3*Z+A4)/(Z4+B1*Z3+B2*Z2+B3*Z+B4)
  200 E2=G-Z*E1
      E=1.0-G
      SE3=0.5*(1.0-(G-Z*E2))
   30 RETURN
      END
```

```
      FUNCTION ULJY(X,XPOINT,NPOINT,YPOINT)
      DIMENSION XPOINT(30),YPOINT(30)
C
C        THIS FUNCTION FITS A STRAIGHT LINE BETWEEN POINTS X(J) ANDX(J+1)
C        AND EVALUATES THE VALUE OF Y AT THE POINT X.
C        XPOINT MUST BE POSITIVE AND INCREASE WITH NPOINT
C
      ULJY=0.
      IF(X.LT.XPOINT(1)) GO TO 100
      IF(X.GT.XPOINT(NPOINT)) GO TO 100
      IF(X.EQ.XPOINT(1)) GO TO 99
      DO 50 J=2,NPOINT
      K=J-1
      L=J
      IF(X.LE.XPOINT(J)) GO TO 90
   50 CONTINUE
   90 ULJY=(YPOINT(K)-YPOINT(L))*(X-XPOINT(K))/(XPOINT(K)-XPOINT(L))
      ULJY=ULJY+YPOINT(K)
      GO TO 100
   99 ULJY=YPOINT(1)
  100 RETURN
      END
```

```
      FUNCTION ZHE1(T,L)
C     PARTITION FUNCTION FOR NATURAL HELIUM
C          LTH MOMENT OF THE PARTITION FUNCTION
      COMMON/PART1/ DE,NMH,NMHE1,NMHE2
      DIMENSION W(25),G(25),R(25)
      H=6.62517E-27
      XK=1.38044E-16
      C=2.99793E+10
C **** PRINCIPAL QUANTUM NUMBER IS 1
C **** W(N=1) =0 AND IS TAKEN CARE OF BY SETTING Z = 1 INITALLY
C **** PRINCIPAL QUANTUM NUMBER IS 2
      W(1)=159850.32
      W(2)=166271.70
      W(3)=169081.50
      W(4)=171129.15
C **** PRINCIPAL QUANTUM NUMBER IS 3
      W(5)=186000.
C **** PRINCIPAL QUANTUM NUMBER IS 4
      W(6)=191444.
C **** PRINCIPAL QUANTUM NUMBER IS 5
      W(7)=193915.
C **** PRINCIPAL QUANTUM NUMBER IS 6
      W(8)=195255.
C **** PRINCIPAL QUANTUM NUMBER IS 7
      W(9)=196065.
C **** PRINCIPAL QUANTUM NUMBER IS 8
      W(10)=196590.
C **** PRINCIPAL QUANTUM NUMBER IS 9
      W(11)=196950.
C **** PRINCIPAL QUANTUM NUMBER IS 10
      W(12)=197208.
C **** PRINCIPAL QUANTUM NUMBER IS 11
      W(13)=197400.
      W(14)=197543.
      W(15)=197655.
      W(16)=197745.
      W(17)=197817.
      W(18)=197876.
      W(19)=197925.
      W(20)=197967.
      W(21)=197800.
      W(22)=198031.
      W(23)=198056.
      W(24)=198077.
      G(1)=3.
      G(2)=1.
      G(3)=9.
      G(4)=3.
      DO 10 J=5,24
      XJ=J-2
```

```
   10 G(J)=(2.*XJ)**2
      Z=0.
      IF(L.EQ.0) Z=1.
      WM=(3.938E-11-DE)/(C*H)
      XN=SQRT(2.178E-11/DE)
      NMHE1=XN
      DO 11 J=1,24
      IF(W(J).GT.WM) GO TO 12
      R(J)=H*C*W(J)/(XK*T)
      IF(R(J).GT.60.) GO TO 20
   11 Z=Z+G(J)*(R(J)**L)*EXP(-R(J))
   12 IF(J.GT.4) NMHE1=J-2
      IF(J.LE.4) NMHE1=2
   20 ZHE1=Z
      RETURN
      END


      FUNCTION ZHE2(T,L)
C     PARTITION FUNCTION FOR POSITIVE HELIUM ION
C          LTH MOMENT OF THE PARTITION FUNCTION
      COMMON/PART1/ DE,NMH,NMHE1,NMHE2
      XK=1.38044E-16
      R=8.716E-11/(XK*T)
      Z=0.
      IF(L.EQ.0) Z=1.
      XZ=SQRT(8.712E-11/(2.*DE))
      NMHE2=XZ
      IF(NMHE2.LT.2) GO TO 51
      DO 50 J=2,NMHE2
      X=J
      G=X*X
      E=R*(1.-1./G)
      IF(E.GT.60.) GO TO 51
   50 Z=Z+G*E**L*EXP(-E)
   51 ZHE2=2.*Z
      RETURN
      END


      FUNCTION ZSOLVE(X)
      DOUBLE PRECISION ZSOLVE,X,A,DSQRT
      IF(X-.001) 10,20,20
   10 A=DSQRT(X)*(1.+X/8.-X*X/128.)-X/2.
      GO TO 100
   20 IF(X-1000.) 30,30,40
   30 A=X*(DSQRT(1.+4./X)-1.)/2.
      GO TO 100
   40 A=1.-1./X
  100 ZSOLVE=A
      RETURN
      END
```